

**CHONDRO PROGENITOR CELL RESPONSE
TO
SPECIFICALLY MODIFIED SUBSTRATE
INTERFACES**

Inauguraldissertation

zur
Erlangung der Würde eines Doktors der Philosophie
vorgelegt der
Philosophisch-Naturwissenschaftlichen Fakultät
der Universität Basel

von

DANIEL VONWIL
aus Horw (LU)

Basel (Schweiz), 2010

Genehmigt von der Philosophisch Naturwissenschaftlichen

Fakultät auf Antrag von:

Prof. Dr. U. Aebi (Fakultätsverantwortlicher & Dissertationsleiter)

Prof. Dr. W. Meier (Korreferent)

Basel, den 27.04.2010

Dekan Prof. Dr. E. Parlow

Summary

Current visions in cartilage repair aim at moving from fibrocartilaginous to a more hyaline like repair tissue by combining autologous cells of different origins (*in situ* recruited or *in vitro* precultivated) with repair supporting biomaterials. The role of a chondro-supportive biomaterial within a cartilage defect is seen to support infiltration/recruitment of chondroprogenitor cells (CPC), accelerate their chondrogenic differentiation and to protect/modulate the newly formed tissue.

Overall, this thesis aimed at studying whether modification of selected substrate interface properties allows for modulating chondroprogenitor cell phenotype & function under expansion or differentiation conditions *in vitro*. The goal was to contribute to the definition of material characteristics which could be implemented in the design of biomaterials in order to improve current matrix assisted cartilage repair strategies and outcomes.

Substrate composition & architecture (Chapter I) were found to modulate the chondrogenic differentiation of mesenchymal stem cells (MSC). Using a di block copolymer model substrate (Polyactive®) with a more hydrophobic composition better supported MSC chondrogenesis, than a more hydrophilic composition. Moreover, a

highly interconnected 3D fibre deposited scaffold architecture allowed for the formation of larger MSC aggregates and was found to considerably better support MSC chondrogenesis than compression molded scaffolds.

Restricting cell/substrate interaction specifically to an RGD-containing peptide ligand (Chapter II) modulated the de-differentiation of proliferating HAC and their subsequent capacity to form cartilaginous matrix. This demonstrated the advantage of small ECM fragments in combination with protein resistant materials to control cell/surface interaction. An important finding was the better maintenance of the HAC chondrocytic phenotype during expansion. It suggests, that an RGD-restricted substrate has the potential to improve the outcome of matrix assisted *in situ* cartilage repair, which initially requires recruited/infiltrated CPC to proliferate, while keeping/inducing their capacity to form cartilaginous matrix.

Substrate elasticity allowed for modulating the chondrogenic commitment of HAC (Chapter III). The finding, that a soft substrate (0.3kPa) better supported the chondrogenic phenotype of HAC than i.e. a stiffer substrate (75kPa) suggests this parameter to be promising for modulating the outcome of matrix assisted cartilage repair.

Overall, this thesis demonstrates that substrate properties hold substantial potential to modulate CPC behaviour, which could be exploited to improve materials employed in matrix assisted cartilage repair. Yet, although differentially supporting CPC chondrogenesis, none of the substrates was *per se* chondro-inductive (see chapter I and III) but required for additional, exogenic stimuli as for e.g. transforming growth factor beta (TGF). Thus, modulatory substrate properties as i.e. architecture, composition, ligand presentation and stiffness should be combined with the instructive capacity of soluble stimuli to exploit the full potential of biomaterials in cartilage repair.

Acknowledgements

I WISH TO THANK TO:

...**Ueli Aebi** for having supported my wish to do a PhD in Tissue Engineering and for sharing his rich treasure of experience in science with me.

...**Michael Heberer** for his faith in me and for having provided the platform from which I could drill for scientific treasures.

...**Ivan Martin**, for his unbroken positive attitude towards my “off-the-group-focus” research topic, his openness, and his memorable, incredible small anecdotes.

...**Daniel Gygax** for evoking my interest for Tissue Engineering and for sharing with me his passion for research and education.

...**Andrea Barbero**, my most direct and most heavily involved supervisor for his continuous support. Once more Grille Mazie!

...**Simon Ströbel** for having accepted me as his novice in Tissue Engineering, for the countless discussions which ended with the phrase (we will see....) and for having grown close to me as a dear friend.

...**Martin Schuler** for his valuable inputs to the RGD manuscript and the great lunch time meetings... in case I did not miss it ;-).

...my master students **Géraldine Guex, Olivia Haupt** and **Andreas Trüssel** for their contributions to my work, the countless discussions of possible and sometimes impossible ideas as well as for their great companionship.

...**Peter Fischer, Varvara Mitropoulos** from the ETHZ, **Matthias Lütolf** and **Samy Gobaa** from the EPFL Lausanne for their help with the rotational reholocicay.

...**Jens Riedle** from CellCoTec for helpful discussions and inputs.

...our lab technicians **Francine Wolf** and **Sandra Feliciano** for their “firm motherly spirit” which reaches into the farthest corners of the lab. I do not want to imagine the lab without you.

...the **lab crowd** in general (including in my incomprehensive list: my beautiful neighbour Bea; the “Epizentrum” Elia; Adam with the typical Swiss nickname “Adamkri”; Sinan the “Swiss Discovery Channel” in person; Paul the “Wizard of Excel”; Arnaud the “Schümlipflümli”; Rosy-Uta-Anna-Chitra the “Yogis”; Princess Silvia; “JF TF” now at UK; Andrea, the “Universal Library of Medicine and Science”; the “Lab Divas” Nunzia, Clém and Chiara; David the “Calm Story Teller”; Alessandra the “Gelati Vendor”, Sylvie the “Great”, Arne the “Doctor” and of course our “paper tigers” Caro and Anke) for the splendid weddings, barbecues, yoga sessions, the incredible theme parties and all the other unforgettable events. I will miss you guys!

...the company **F. Hoffmann-La Roche AG**, for the solid chemistry laboratory training, the unforgettable, lineage committing exchange year in Rochester (MN, USA) and for their unconditional financial support of my studies in chemistry and nanosciences. Special thanks to:

- ...**Erich Schmidlin**, the master of intuitive chemistry for his unbroken support, friendship and for being my role model as a gentle man.
- ...**Roland Schürmann** and **Uwe Klinkhammer** for having opened my eyes to see that there is chemistry beyond the “Repetitorium für Organische Chemie”.
- ...**Bernhard Menzi** for the special training period in his lab.
- ...**Henri Hoffmann, Franz Frei, Georg Trickes** and **Alois Kunz** for their passion to help young adults grow.

...**David Carish** from the Rochester Community and Technical College for having sparked my fire for the marvellous world of the human biology.

...my dear Friend **Míc**, for his inspiring, enriching and deep friendship.

...**my Parents** and my godmother **Rita** for their love and for unconditionally backing me up on my adventurous paths.

...and to my Venus on earth, **Lara**, for her love!

Table of Contents

TABLE OF CONTENTS	- 1 -
ABBREVIATIONS.....	- 4 -
GENERAL INTRODUCTION	- 6 -
<i>Cartilage.....</i>	<i>- 6 -</i>
Major Types of Cartilage.....	- 6 -
Composition and Structure of Articular Cartilage.....	- 8 -
<i>Mechanical environment in mature cartilage.....</i>	<i>- 12 -</i>
<i>Cartilage Developmpt.....</i>	<i>- 13 -</i>
<i>Soluble Growth Factors Involved in Cartilage Development</i>	<i>- 15 -</i>
<i>Articular Cartilage Defects and Self Repair</i>	<i>- 16 -</i>
<i>Articular Cartilage Defect Treatments.....</i>	<i>- 18 -</i>
Arthroscopic repair procedures.....	- 18 -
Osteochondral Transfer	- 19 -
Cell Based Cartilage Repair Techniques	- 19 -
Based on chondrocytes	- 19 -
Based on bone marrow stromal cells	- 20 -
Ex vivo procedure.....	- 20 -
MSC mobilized by microfracturing.....	- 21 -
Chondro Progenitor Cells	- 22 -
MSC.....	- 22 -
Expanded De-differentiated Chondrocytes.....	- 23 -
Designed Biomaterials to Control Cell Function	- 24 -
i) Architecture	- 24 -
ii) Ligand Presentation.....	- 25 -
iii) Mechanical Properties.....	- 26 -
Need for Characterizing Parameters for Chondro-Supportive Biomaterials	- 28 -
CHAPTER I	- 34 -
SUBSTRATE COMPOSITION & ARCHITECTURE MODULATES	
CHONDROGENESIS OF HUMAN MESENCHYMAL STEM CELLS.....	- 34 -
INTRODUCTION	- 35 -
STUDY 1	- 37 -
<i>Aim.....</i>	<i>- 37 -</i>
Scaffold Fabrication.....	- 38 -
Cell Isolation and Expansion.....	- 39 -
Cell Seeding and Culture on Three Dimensional Scaffolds	- 40 -

Biochemical Analysis	- 40 -
Cell Seeding Efficiency and Retention.....	- 41 -
Histological and Immunohistochemical Analysis	- 41 -
Gene Expression Analysis	- 42 -
<i>Results</i>	- 43 -
<i>Discussion</i>	- 47 -
<i>Outlook</i>	- 49 -
STUDY 2	- 50 -
<i>Aim</i>	- 50 -
<i>Methods</i>	- 51 -
Scaffold Fabrication.....	- 51 -
MSC Isolation and Expansion	- 51 -
Optimization of in vitro Culture Conditions.....	- 51 -
Chondrocyte Seeding and Culture on Three Dimensional Scaffolds	- 54 -
<i>Results</i>	- 56 -
<i>Discussion</i>	- 59 -
CONCLUSION STUDY I & II	- 61 -
CHAPTER II.....	- 62 -
RGD-PEPTIDE RESTRICTED INTERACTIONS WITH A PROTEIN RESISTANT SUBSTRATE ARE SUFFICIENT FOR HUMAN ARTICULAR CHONDROCYTE ADHESION, GROWTH & MAINTENANCE OF CARTILAGE FORMING CAPACITY	- 62 -
ABSTRACT	- 63 -
INTRODUCTION	- 64 -
METHODS	- 67 -
<i>Polymer Synthesis and Characterization</i>	- 67 -
<i>Surface Modification for Cell Culture</i>	- 69 -
<i>Cell isolation and Expansion</i>	- 69 -
<i>Cell Attachment & Proliferation</i>	- 70 -
<i>Cell Morphology</i>	- 71 -
<i>Initial Cell Spreading, Kinetic & Motility</i>	- 72 -
<i>Chondrogenic Assay</i>	- 72 -
<i>Gene Expression Analysis</i>	- 73 -
<i>Biochemical Analysis</i>	- 74 -
<i>Histological and Immunohistochemical Analysis</i>	- 74 -
<i>Statistical Analysis</i>	- 74 -
RESULTS	- 75 -
<i>Substrate Characterization</i>	- 75 -
<i>HAC attachment, Spreading Kinetics & Proliferation</i>	- 75 -
<i>HAC Morphology & Motility During Cell Expansion</i>	- 78 -
<i>HAC De-Differentiation During Cell Expansion</i>	- 80 -
<i>HAC Re-Differentiation in Pellet Culture</i>	- 81 -
DISCUSSION	- 83 -
CONCLUSION	- 87 -
CHAPTER III.....	- 88 -

SUBSTRATE ELASTICITY MODULATES TGF BETA STIMULATED RE-DIFFERENTIATION OF EXPANDED HUMAN ARTICULAR CHONDROCYTES	- 88 -
ABSTRACT	- 89 -
INTRODUCTION	- 91 -
<i>Substrate Preparation.....</i>	<i>- 95 -</i>
<i>Substrate Characterization by Rotational Rheometry.....</i>	<i>- 96 -</i>
<i>Cell Culture</i>	<i>- 97 -</i>
<i>Cell Culture</i>	<i>- 98 -</i>
<i>Chondrogenic Re-differentiation culture.....</i>	<i>- 98 -</i>
<i>Attachment & Proliferation</i>	<i>- 99 -</i>
<i>Cell morphology</i>	<i>- 100 -</i>
<i>Fluorescence Labelling, Acquisition and Analysis.....</i>	<i>- 100 -</i>
<i>Gene Expression Analysis.....</i>	<i>- 101 -</i>
RESULTS	- 103 -
<i>Substrate Characterization.....</i>	<i>- 103 -</i>
<i>HAC Attachment and Proliferation</i>	<i>- 105 -</i>
<i>HAC Morphology.....</i>	<i>- 106 -</i>
<i>HAC Actin Cytoskeleton and Focal Adhesions</i>	<i>- 108 -</i>
<i>Sox-9 Expression</i>	<i>- 110 -</i>
<i>Gene Expression</i>	<i>- 113 -</i>
<i>Type II Collagen Protein Expression</i>	<i>- 114 -</i>
DISCUSSION.....	- 117 -
<i>Attachment & Proliferation</i>	<i>- 117 -</i>
<i>Morphology & Sox9 Expression.....</i>	<i>- 118 -</i>
<i>Chondrodifferentiation</i>	<i>- 119 -</i>
<i>Mechanisms of Mechanotransduction</i>	<i>- 121 -</i>
OUTLOOK	- 122 -
CONCLUSION	- 124 -
MAIN CONCLUSION	- 125 -
MAIN OUTLOOK	- 127 -
REFERENCES	- 129 -
CURRICULUM VITAE	- 149 -

Abbreviations

AA	Acrylamide; monomer
ACI	Autologous chondrocyte implantation
APS	Amonium persulfate
BIS	N,N'-methylenbisacrylamide, crosslinker
CM	Compression molded scaffold acrchitecture
CPC	Chondroprogenitor Cells (i.e. MSC and expanded/de-diff. HAC)
DMEM	Dulbecco's modified Eagle's medium
DMSO	Dimethylsulfoxide
DNA	Deoxyribonucleic acid
dNTP	Deoxyribonucleosid triphosphates
DTT	Dithiothreitol
CDNA	Copy DNA
CI	Type I Collagen
CM	Complete medium
<i>E</i>	Young's modulus
ECM	Extracellular Matrix
EDTA	Ethylenediaminetetraacetic acid
F-actin	Filamentous actin
FBS	Fœtal bovine serum
FG	Fibrin Glue
FGF-2	Fibroblastic growth factor-2
FN	Fibronectin
GAG	Glycosaminoglycans
<i>G</i>	Dynamic shear modulus
<i>G'</i>	Shear storage modulus
<i>G''</i>	Shear loss modulus
HAC	Human articular Chondrocytes
HEPES	4-(2-hydroxyethyl)-1-piperazineethanesulfonic acid
MACI	Matrix assisted autologous chondrocyte implantation
MRNA	Messenger RNA
MSC	Mesenchymal stem cells
NC	Nasal chondrocytes
MW	Molecular weight
N_0	Initial number
N_1	Final number
<i>p</i>	Perimeter

PA	Poly acrylamide
PBS	Phosphate buffered saline
PBT	Poly butylene terephthalate
PCR	Polymerase chain reaction
PDGF-BB	Platelet-derived growth factor
PEG	Poly ethyleneglycol
PEGT	Poly ethylene glycol terephthalate
RGD	Peptide sequence Arg-Gly-Asp; cell adhesion motif in FN
RNA	Ribonucleic acid
rRNA	Ribosomal RNA
SEM	Scanning electron microscopy
SFM	Serum free medium
Sox-9	Transcription factor Sox-9
TCPS	Tissue culture treated plastic (gas plasma treated poly styrene)
TGF	Transforming growth factor beta
TGF β -1	Transforming growth factor beta 1
TGF β -3	Transforming growth factor beta 3
TMED	Tetramethylethylenediamine
UV	Ultra violet light 350nm
ν	Poisson ratio
w%	Weight percent (g/g)
w/	With
w/o	Without
ϕ	Shape factor phi
μ CT	Micro computed tomography
3DF	Three dimensional fibre deposited scaffold architecture

General Introduction

Cartilage

Major Types of Cartilage

Cartilage is a specialized avascular connective tissue comprising of only one single type of cell called chondrocyte which is sparsely populated in a collagen and proteoglycan rich hydrated extracellular matrix (ECM). Based on the biochemical composition and structure of the ECM, the mechanical properties and structural characteristics of the tissue, three major types of cartilage (elastic cartilage, fibrous cartilage and hyaline cartilage) can be distinguished:

i) Elastic cartilage is found in the pinna of the ear, in the walls of the auditory and eustachian canals and tubes, as well as in the larynx and in the epiglottis. This type of cartilage with a more elastic property maintains tube-like structures permanently open and provides intermediate mechanical stability. Elastic cartilage mostly consists of type II collagen matrix elements and elastic fiber bundles (elastin) which manifest in

aligned fiber structures. This structural composition provides a tissue which is stiff yet elastic.

ii) Fibrocartilage is most prominently found in areas which require greater tensile strength and support such as i.e. between intervertebral discs and at sites of tendons or ligaments connected to bone tissue. Typically, fibrocartilage is found at locations which are under considerable mechanical stress (i.e. tendon and ligaments) but still provides properties which allow flexible body movement. Accordingly, fibrocartilage mainly consists of type I collagen fibers which are aligned in thick fiber bundles and chondrocytes arranged in parallel rows between these fibers. The fibrous type of cartilage is usually associated with a dense connective tissue, namely the hyaline type cartilage which defines the third type of cartilage (1)

iii) Hyaline type cartilage is the most abundant type of cartilage and is found in the nose, Larynx, trachea, bronchi, in the ventral ends of the ribs, and at the articular ends of the long bones. Characterized by the arrangement of the chondrocytes in multicellular stacks which prominently produce a type II collagen and a proteoglycan rich matrix, the hyaline type of cartilage provides the flexible support in nose and ribs but can also sustain mechanical load during body motion as shown at the surface of articular joints. This hyaline type of cartilage is lining as a thin layer of deformable, load bearing tissue at the bony ends of diarthrodial joints and is more specifically called articular cartilage (1).

Composition and Structure of Articular Cartilage

The primary function of articular cartilage is the absorption and distribution of forces, generated during joint loading and to provide a lubricating tissue surface which prevents the abrading and degradation of the joint and the subchondral bone structure during joint motion. Indeed, the articular type of hyaline cartilage has to bear and tolerate enormous physical stress and load during its entire lifetime.

At first glance, articular cartilage may appear to be a relatively primitive tissue, which simply consists of chondrocytes entrapped in hydrated extracellular. However, in order to maintain its mechanical function and integration, this tissue reveals a unique, highly defined structural organization that can be subdivided into two domains, the i) cartilage zonation and ii) the organization of the extracellular matrix:

i) The structure and composition of the entire articular cartilage tissue varies according to the distance from the tissue surface and reflects its functional role. Four different zones arranged as layers horizontally to the tissue surface can be distinguished and are characterized according to the extracellular matrix composition and cellular morphology (see Fig. 1).

In the *superficial zone* the layer of tissue is composed of flattened ellipsoid-shaped chondrocytes and a high concentration of thin collagen fibers arranged in parallel to the articular surface (2). In this layer the pericellular matrix structure mentioned below can not be found. The thin layer of cells is covered with an acellular sheet of collagen fibers (*lamina splendens*) which functions as a protective barrier

between the synovial fluid and the cartilage tissue and controls the in- and egress of larger size molecules (3). Its rather low permeability regulates the diffusion transport of nutrients and oxygen to the underlying cartilage structures. Only within this zone chondrocytes synthesize and secrete the superficial zone protein lubricin (4;5) responsible to reduce surface friction during joint motion. The specific arrangement of the collagen fibrils which lay in parallel to the joint surface, provides a high mechanical stability of the tissue layer and mainly contributes to the tensile stiffness and strength of articular cartilage (6-9).

Below the superficial zone is the *midzone* where cell density is lower. It displays more typical morphologic features of a hyaline cartilage with spherical/rounded cells and an extensive extracellular matrix rich in the proteoglycan aggrecan. The collagen fibers are synthesized at a lower quantity but show larger diameter fibrils which are aligned obliquely or randomly to the articular surface and describe an intermediate structure between the superficial zone and the adjacent deep zone.

In the *deep zone*, the chondrocytes have a round morphology and are arranged in cell columns perpendicular to the cartilage surface. The extracellular matrix contains a high content of glycosaminoglycans and large diameter collagen fibers which form arcades perpendicular to the joint surface (10).

The partially *calcified zone* defines the boundary of cartilage tissue to the subchondral bone. This rather thin layer of calcified cartilage with intermediate mechanical properties functions as a buffer between the cartilage and bone tissue. The cells have a smaller volume and are partially surrounded by calcified cartilage

matrix. The chondrocyte in this zone usually persist in a hypertrophic cell stage which correlates with the expression of collagen type X. Finally this boundary provides an optimal integration to the subchondral bone tissue and prevents vascular invasion.

ii) In addition to the zonal segregation, the matrix surrounding the chondrocytes of articular cartilage varies in its organization and can be divided in three compartments, such as the pericellular region adjacent to the cell body, the territorial region enveloping the pericellular matrix, and the interterritorial compartment which defines the space between these cellular regions (see Fig. 1) (1).

The *pericellular region* which is rich in proteoglycan, decorin, aggrecan, collagen type VI, and cell membrane associated molecules like anchorin and decorin (11-13) defines a narrow rim of a filamentous matrix network which fulfills the functions of the interlink between the chondrocyte cell body and the territorial matrix structure.

The *territorial region* describes an envelop surrounding the cells or cluster of cells with their pericellular matrix. Thin collagen fibrils (most prominently collagen type II) bind to the pericellular matrix and form a basket like structure which protects the cell from damage during loading and deformation of the cartilage tissue. Moreover these structures may also contribute to transmit mechanical signals to the chondrocytes during joint-loading (14;15).

The *interterritorial region* confines the most volume of the articular cartilage tissue and contains intermolecular cross linked collagen fibrils (collagen type II),

non collagen proteins and aggregates of glycoproteins (16). This extracellular matrix composition provides the tissue with its functional characteristic to absorb mechanical load.

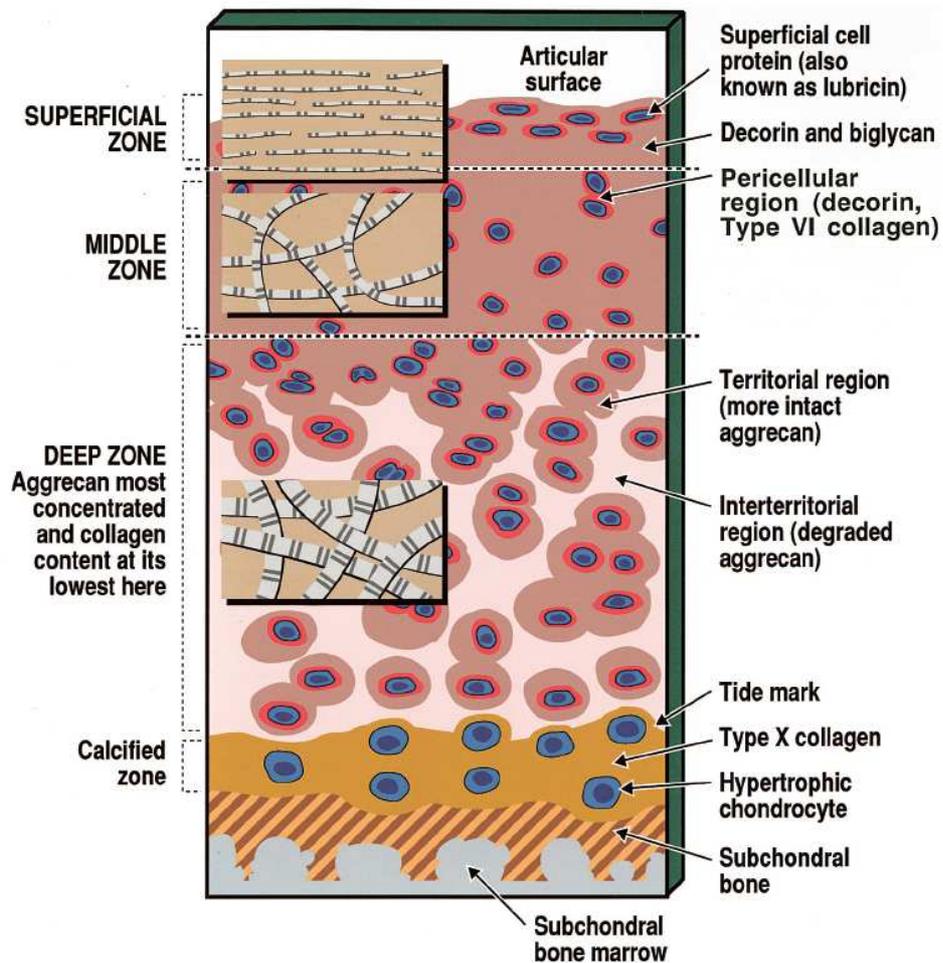


Fig. 1 Schematic drawing of articular cartilage composition and structure. Articular cartilage can be divided into four different zones (superficial, mid, deep and calcified) which each has a characteristic composition and structure (inserts show organization and relative diameters of collagen macrofibrils in different zones). Reproduced from Poole *et al.* 2001(17).

Mechanical environment in mature cartilage

Chondrocytes and cartilage tissue during joint motion are exposed to body weight load which creates a rigorous mechanical environment for articular cartilage tissue such as direct compression, shear, and hydrostatic pressure. The function of articular cartilage to undergo tissue deformation is dependent on the specific arrangement of macromolecules in the extracellular matrix. Especially the organization of collagen fibers into a three dimensional arranged collagen network can balance the swelling pressure of the proteoglycan-water “gel” (18;19). Cartilage is considered as a viscoelastic material composed of three principal phases: a solid phase composed of a dense, collagen fibrillar network and charged proteoglycan aggregates, a fluid phase of water and an ion phase with ionic species for neutralizing the charged matrix components (20;21). Under physiological condition these three phases define an equilibrium where the extension of the proteoglycan-water gel volume is restricted by the firm collagen frame (22). The bound water in the cartilage tissue and finally the mechanical properties of the cartilage tissue are influenced by the interaction of water with the large, negatively charged proteoglycan aggregates (23). The negatively charged proteoglycans mostly driven by chondroitin sulphate residues are balanced by a high concentration of cations dissolved in the cartilage tissue (24).

In summary, the mechanical function of articular cartilage tissue bases on the matrix structure surrounding each single cell, the arrangement of the extracellular matrix fibres within the single zonal compartment and the proportional composition of the different extracellular matrix components.

Cartilage Development

Articular cartilage as a part of the limb skeleton develops in a well defined and controlled multistep differentiation process of cells from the mesenchymal origin (25-27). The establishment of the cartilage structure follows precise and distinct patterns of cell differentiation and cell rearrangement driven by environmental factors such as cell-cell and cell matrix interaction, growth factor and morphogen mediated signaling (28;29) as well as defined biomechanical conditions (30).

The steps of development are divided into distinct phases (see Fig. 2). Initially phase mesenchymal precursor cells migrate from the lateral mesoderm towards the presumptive skeletogenic site and determine the cartilage anlagen (31). Following, the epithelial-mesenchymal interactions results in the mesenchymal condensation. The pre-chondrogenic condensation is a prerequisite for the future establishment of the limb skeleton (32) and is associated with an increased cell to cell contact which facilitate the intercellular communication and the transfer of small molecules between the cells (33). It has been shown that such a high cell density is required to allow chondrogenic development (34) and that the level of cell condensation correlates with the stage of chondrogenic development (35;36). Additionally, cell-matrix interactions appeared to play an important role in mesenchymal condensation (37). For example the integrin mediated binding of chondrocytes to collagen, has been shown to be essential for chondrocyte survival (38;39). Next, the overt differentiation of immature pre-chondrocytes into fully committed chondrocytes is manifested by an increased cell proliferation and by the up-regulation of cartilage specific matrix components like collagen type II α 1, IX and XI and aggrecan. In the final commitment of the chondrogenic

phenotype the cells reduce their proliferative activity and maintain the functional integrity of the mature cartilage tissue (25-27).

The initial function of the cartilage during embryonic development is to give stability to the embryo and serve as a template for myogenesis and later for neurogenesis. Most of the embryonic cartilage is replaced by bone during a process called the endochondral ossification (40;41).

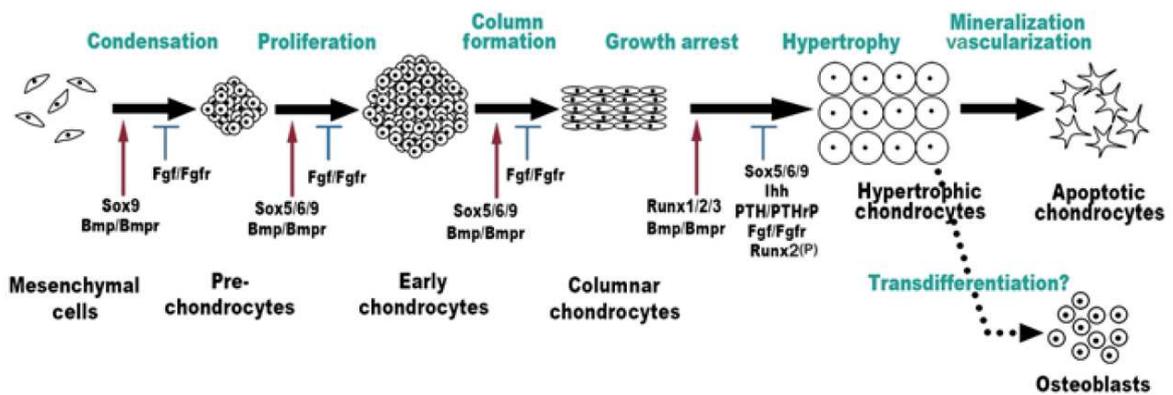


Fig. 2 Schematic representation of the multistep process of chondrogenesis in the developing limb bud. Undifferentiated mesenchymal cells derived from the lateral plate mesoderm aggregate to form condensations, which prefigure the future skeletal pattern. These cells differentiate into chondrocytes to undergo a series of differentiation processes including proliferation, hypertrophy and cell death. Proliferating chondrocytes are eventually arranged into parallel columns and subsequently exit the cell cycle to convert into hypertrophic chondrocytes. Following the onset of hypertrophy, chondrocytes direct mineralization and vascular invasion. On vascularization, osteoblasts are transported by blood vessels into the cartilage, producing bone matrix using the residual cartilage template as a scaffold. Concomitantly, hypertrophic chondrocytes undergo programmed cell death and are replaced by the bone matrix. Reproduced from Shimizu *et al.* 2007 (42).

During the endochondral ossification, the chondrocytes progress to the hypertrophic phenotype, which is characterized by a massive enlargement of the cell, the onset of the expression of type X collagen (43), an increased expression and activity of the alkaline phosphatase and the carbonic anhydrase and a reduction in the synthesis of the type II collagens and proteoglycan. Protease inhibitors which prevent vascular invasion are also reduced. Vascularization of the tissue takes place, and most or all of the hypertrophic chondrocytes undergo apoptosis followed by their replacement by osteoblasts which in turn will deposit bone matrix in the free lacunae. At the cell level, the entire endochondral ossification process can be seen as a sequential progression of the three chondrocytic phenotypes: the committed mesenchymal cell, the differentiated chondrocyte and the hypertrophic chondrocytes (44).

Within these developmental processes growth promoting factors act on the cell and contribute to establish a mature cartilage tissue.

Soluble Growth Factors Involved in Cartilage Development

Within the multi step cell differentiation process a number of growth factors and morphogens are involved and essential during chondrocyte maturation and cartilage tissue formation. The most prominent growth factors belong to the transforming growth factor (TGF- β) superfamily which are responsible for chondrocyte proliferation (TGF- β 1), terminal differentiation (TGF- β 3; bone morphogenic protein; BMP) (45) or to promote cell-cell interaction in the early stage of chondrogenesis (BMP) (46). The insulin like growth factor 1 (IGF-1) which belongs to the IGF family of peptide hormones (including insulin) regulates many cellular functions during cartilage maturation such as induction of

chondrocyte differentiation (47) and proliferation (48). In mature cartilage IGF-1 promotes and maintains the anabolic synthesis of proteoglycan and type II collagen (49) and inhibits the nitric oxide-induced de-differentiation of articular chondrocytes (50). Furthermore members of the fibroblast growth factor (FGF) family of morphogenes influence processes correlated with cell division and chondrocyte proliferation and have been shown to promote chondrocyte proliferation in a human growth plate ex vivo culture system (51).

Finally, only the combinatorial action of these growth and morphogenic factors specifically expressed in selective tissue areas in different developmental phases and at defined concentrations establishes the precise structure of the articular cartilage tissue.

Articular Cartilage Defects and Self Repair

Articular cartilage lesions, caused by trauma, osteochondritis dissecans or as a result of instability or abnormal loading are a common cause of disability, often associated with pain, reduction of joint mobility and loss of function and can ultimately lead to osteoarthritis. Articular cartilage has a very limited intrinsic healing capacity, related to the absence of vascularization and the presence of few and very specialized cells with low mitotic activity. According to the size of cartilage tissue damage in the cartilage surface, several grades of tissue injury can be distinguished which lead to different healing response (52-54).

In the case of partial thickness defects, the classical self-repair of injured cartilage tissue goes through conserved mechanisms of cell and tissue necrosis followed by the proliferation of surviving chondrocytes adjacent to the site of the lesion. Although these cells aggregate in clusters and demonstrate a temporary increased type II collagen synthesis, in long term the formed tissue shows a loss of hyaline like cartilage characteristics. Thus, these chondral lesions remain almost unchanged and can proceed towards osteoarthritic diseases (55).

In the case of full thickness defects, the lesion penetrates to the subchondral bone part gaining access to the cells that reside in the bone marrow space including the mesenchymal stem cells located therein. The repair response elicited by this type of defect results in the formation of a fibrocartilaginous tissue in the defect void. Anyhow, the decreased deposition of extracellular matrix components and the formed tissue with fibro-cartilage structures lack the strength, the mechanical properties and duration of the original articular cartilage tissue as it has been demonstrated in longer time follow-up studies (56;57).

In comparison to native cartilage, the repair tissue generated by spontaneous self healing commonly shows limitations in regard to its composition and mechanical durability (see tab. 1) The discrepancy between native cartilage and repair tissue increases the probability of tissue and joint degeneration (58) and thus spurred the the development of articular cartilage defect treatments.

Table 1: Cellular, biochemical and mechanical characteristics of hyaline cartilage and fibrocartilage (59)

	Hyaline cartilage	Fibrocartilage
Cell morphology	Superficial zone: fibroblastic Middle/deep zones: round/ellipsoid	Mix population of round and fibroblastic cell within the tissue
Cell organization	Middle/deep zones: cells in columns	Cells not organized in columns
Cellularity (% of total volume)	2-5%	>10%
Total Collagen (% dry weight)	67-86%	60-70%
Collagen type II (% of total collagen)	95%	< 20%
Collagen type I (% of total collagen)	< 5%	> 80%
Total GAG (% dry weight)	20-40%	2-4%
Compression moduli (MPa)	0.1-0.4	> 1
Tensile moduli (MPa)	< 5	50-200

Articular Cartilage Defect Treatments

The different strategies to treat cartilage defects vary from more conservative approaches, like physiotherapeutic measures or application of pharmaceuticals (i.e. corticosteroids, hyaluronic acid and growth factors) towards more invasive (i.e. surgical) procedures.

Arthroscopic repair procedures

Arthroscopic *lavage* and *debridement* are often used to alleviate joint pain. Lavage involves irrigation of the joint during arthroscopy, while debridement is the removal of the damaged tissue from the joint. Both of these procedures are routinely used to alleviate joint pain however do not induce repair of articular cartilage (60;61).

Osteochondral Transfer

Osteochondral transplantation of autogenic and allogeneic tissue has been widely used to treat predominantly large osteochondral defects. Allogeneic material derived from cadaveric donors and it is indicated for large post traumatic defects of joints. Beaver et al. (62) reported satisfactory long-term results with these grafts, but the logistic of implanting a fresh allograft and the risk of transmitting infection reduce the indication for this procedure only to severe cases. Instead, autologous osteochondral graft implantation, involves the removal of cylindrical plugs of osteochondral tissue from non load bearing regions of the articular cartilage and their implantation into the prepared full depth defect with press-fit fixation. This procedure is indicated in osteochondral defects of 3 to 5 cm² in young patient. It provides the re-establishing of a functional cartilage surface which can absorb body weight load but has limitation in terms of poor tissue integration within the adjacent native cartilage tissue. Furthermore, the surgical intervention damages intact host tissue and might enhance the donor site morbidity (63;64).

Even though such invasive procedures hold promise and showed acceptable results in some cases the outcome of these procedures shows generally limitations in terms of quality and reproducibility (65).

Cell Based Cartilage Repair Techniques

Based on chondrocytes

The first requirement of chondrocyte based cartilage repair techniques is the excision of a small biopsy of healthy cartilage from the patient for cell isolation and expansion. The use of growth factors allows a higher cell proliferation rate (66) which reduces culture time

required to obtain sufficient cell numbers. Tissue engineering of cartilaginous grafts is a challenging technique since dedifferentiation of chondrocytes, occurring during expansion (67-69), has to be reversed by culturing cells in substrates supporting a spherical morphology, such as polymer gels (70-72) or porous polymer scaffolds (73-75). The combination of all these steps clearly indicates that this technique is far from being an intraoperative procedure and is time and money consuming.

Based on bone marrow stromal cells

Bone marrow is a highly complex and organized tissue where several types of differentiated cells coexist with immature cells namely hematopoietic stem cells (HSC) which can self-renew and differentiate into all the mature peripheral blood types, and mesenchymal stem cells or marrow stromal cells (MSC) that serve as long-lasting precursors from bone marrow, bone, cartilage, and connective tissues (76-78)

Ex vivo procedure

Bone marrow mesenchymal stem cells (MSC) can easily be isolated by their adhesion to plastic, and grown *in vitro*. Monolayer expanded MSC have been shown to have the ability to differentiate *in vitro* into several mesenchymal tissue cells including chondrocytes, osteoblast, adipocytes and tenocytes when plated in appropriated environments (79). In particular, chondrogenesis of MSC occurs when these cells are cultured in three-dimensional aggregates (“pellets”) (80-82) or cultured on porous polymers in the presence of Transforming Growth Factor beta (TGF β)(83).

MSC mobilized by microfracturing

Defects of articular cartilage that penetrate the subchondral bone elicit an intrinsic fibrocartilaginous repair process. Mesenchymal stem cells from the bone marrow have been proposed to be involved in this regenerative process. Treatment of cartilage defect by microfracture (84) results in the formation of a fibrocartilaginous tissue which does not exhibit the same functional and mechanical properties that native hyaline cartilage (85). The main differences between hyaline and fibrocartilage are summarized in table 1.

Recently, Kramer et al (86) showed that MSC from bone marrow migrate to a cartilage defect after microfracturing the subchondral bone and that these cells when guided *in vivo* to a collagen I/III membrane at the site of the defect were capable to differentiate *in vitro* into chondrogenic cell type under specific culture conditions. These findings show that while the treatment by microfracturing leads to fibrocartilaginous tissue formation, the cells originated from bone marrow have the capacity to generate cartilaginous tissue *in vitro* when placed cultured under appropriate conditions.

In an attempt to enhance the filling of articular cartilage defect with functional repair tissue, collagen matrices have been used in conjunction with microfracture (procedure called autologous matrix-induced chondrogenesis, AMIC) in dog and sheep models (87-89). After studying the *in vitro* chondrogenic differentiation of sheep MSC in a collagen matrix (90) Dorotka *et al.* (91) studied whether the implantation of such a matrix, supplemented or not with autologous chondrocytes would facilitate cartilage repair after microfracturing. However, the implantation of the collagen matrix did not enhance the quality of repair observed after microfracturing unlike the matrix which was cell seeded. In a canine model, Breinan *et al.* (92) investigated the effect of treating a cartilage defect

by microfracturing in combination with a type II collagen scaffold and demonstrated that after 15 weeks, implantation of the matrix increased the amount of tissue filling in the defect but the tissue was predominantly fibrous in nature.

These findings suggest that current materials lack chondroinductive and/or mechanical properties to properly stimulate the production of hyaline cartilage by the infiltrating progenitor cells.

Chondro Progenitor Cells

Both mesenchymal stem cells (MSC) and expanded/de-differentiated human articular chondrocytes (HAC) are known to undergo chondrogenic differentiation or re-differentiation respectively, when cultured under chondrogenic conditions. From this perspective, both MSC and HAC can be considered as chondro progenitor cells.

MSC

Reservoirs of stem cells can be found throughout several tissues of the adult body and are thought to contribute to tissue regeneration upon trauma, disease or aging. Bone marrow i.e. contains mesenchymal stem cells, which can be isolated by adhesion to tissue culture plastic. When exposed to various growth factors, these adherent cells are capable of differentiating into connective tissue lineages including adipocytes, osteoblasts as well as chondrocytes (93). Chondrogenesis of

MSC can be induced by culturing them as aggregates in chemically defined medium containing insulin, dexamethasone, ascorbic acid and transforming growth factor beta (94).

Expanded De-differentiated Chondrocytes

During expansion in monolayer, human articular chondrocytes (HAC) are known to undergo rapid de-differentiation (95;96). De-differentiation of chondrocytes manifests by cell morphological transition from round to fibroblast-like, the loss of large proteoglycans (e.g. aggrecan) and type II collagen production (97;98), and the switch to synthesis of type I collagen, fibronectin (FN), and small noncartilaginous proteoglycans (98;99).

The use of specific factors during monolayer expansion of HAC has been shown to accelerate the process of de-differentiation but induces HAC to acquire a differentiation plasticity which is similar to that of MSC (100). Culturing aggregates (suspension or pellet culture) of expanded/de-differentiated HAC in a medium containing the strong chondrogenic stimulus TGF β -3, allows for re-induction of chondrogenic differentiation (101;102). Thus, expanded/de-differentiated HAC are not only of clinical relevance but, owing to their plasticity, also serve as a potent model to investigate processes involving fate commitment and the maintenance of mesenchymal progenitor cells.

Designed Biomaterials to Control Cell Function

Generally, a biomaterial is any material, natural or synthetic, that comprises whole or part of a living structure or biomedical device which performs, augments, or replaces a natural function. Natural materials can provide a physical environment which influences cell function (103;104), but often suffer from high lot-to-lot variability, potential pathogens (105), and the risk to elicit an immune response upon implantation due to xenogenic protein components (106;107). In contrast to natural materials, synthetic materials offer the potential for improved control, repeatability, safety and scalability. Moreover, synthetic materials can be specifically designed on different length scales (molecular, cellular and macroscopic) and thereby allow to assemble targeted, physiological environments for controlling cell function (108).

In recent years it has been recognized that biomaterials have to be tailored for each specific therapeutic application. Among the most important material properties to be controlled are: i) architecture, ii) ligand presentation as well as iii) mechanical properties (see Fig. 3) (108).

i) Architecture

The architectural organization of a biomaterial can be defined on different length scales ranging from nano- to millimetre. In the nano- to micrometer range, parameters like ligand presentation, cell-material interactions, force transmission, molecular diffusion and cell-cell interactions are governed (109-114). At larger scales, the material architecture determines bulk mechanical properties, possible cell seeding methods, cell migration and molecular diffusion (i.e. nutrient/waste

exchange) (115-118). Additionally, biomaterials can either be organized as two dimensional (2D) or three dimensional (3D) environments:

- In traditional 2D culture systems, signalling and diffusion are inherently asymmetric. Still, such culturing platforms allow for simple observation of cell-material interaction, and can be straightforwardly produced (109;113;119).
- For 3D scaffolds and regenerative implants, three predominant architectures have been used: porous solids, nanofibres and hydrogels. *Microporous 3D solids* with cell porosities greater than the cell diameter (115;117;118;120) may effectively signal as 2D surface (108). *Nanofibrous* scaffolds present a 3D nanostructured topology that resembles the fibrillar ECM proteins *in vivo* (121-123), whereas *hydrogels* simulate the hydrated structural aspect of native ECM (96;124-127).

ii) Ligand Presentation

Ligands modulate the cell phenotype in a manner dependent on their identity (i.e. specificity) (128-131) mode of presentation and density (132-135). Synthetic peptide ligands are often used in place of large proteins or protein fragments because of their stability and ease of synthesis, isolation, and conjugation to materials (136-141).

The ligands must be conjugated to the material for proper presentation (e.g. surface immobilization, polymer modification, or creation of ligand macromers).

Peptide and protein ligands are typically conjugated to materials or material building blocks via primary amines (the amino terminus or lysines) or sulfhydryl groups (cysteines). In addition, spacer arm length and chemistry can in general be tuned to alter ligand availability and activity. Furthermore, the secondary and tertiary structures of native macromolecules frequently present ligands in a specific spatial conformation that promotes binding to receptors (142).

iii) Mechanical Properties

Apart from controlling ligand identity, density and presentation, which determine biomaterial/cell interaction(108), substrate mechanical properties have emerged as important, insoluble, mechanical cues. The mechanical properties of biomaterials are mainly determined by its composition, water content, and structure, which affect inter- and intramolecular forces as well as stress distribution. Common methods of altering the mechanical properties of biomaterials include modulating molecular composition and connectivity, thermal processing and creating reinforced porous composites (108).

Adhesion ligands, which bind to integrins and other cell surface receptors, serve as mechanical transducers between the external material and the internal cytoskeleton of the cell, allowing cells to sense and respond to the stiffness of their substrates(108). Indeed, substrate mechanical properties have been shown to influence the phenotype of several members of the mesenchymal lineage, including fibroblasts(143;144), myoblasts(145;146) and osteoblasts(110).

Moreover mesenchymal stem cells (MSC) have been found to specify lineage and to commit to phenotypes with extreme sensitivity to tissue level elasticity. Soft substrates which mimic brain were neurogenic, stiffer substrates that mimic muscle were myogenic and comparatively stiffer substrates that mimic collagenous bone, proofed to be osteogenic (109).

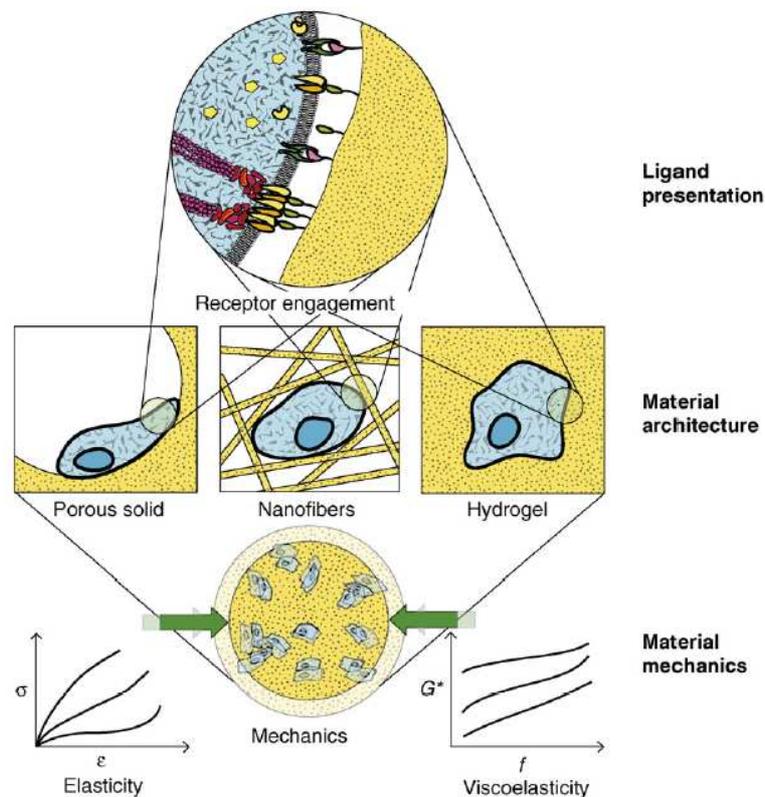


Fig. 3 Design parameters for engineering synthetic stem cell materials. (a) Ligand identity, density, and presentation from the material surface dictate interactions with cell surface receptors to alter cytoskeletal linkages and intracellular signaling pathways. (b) Receptor–ligand interactions are further modulated by material architectures, which provide a two-dimensional (e.g. flat surfaces, microporous solids) or three-dimensional (e.g. nanofibers, hydrogels) micro-environment for cellular engagement. (c) Also, the elastic and viscoelastic properties of the material determine the interplay between cell and material mechanics. Graphs schematically depict mechanical properties: elastic properties via a stress (σ)–strain (ϵ) plot and viscoelastic properties via a complex modulus (G^*)–frequency (f) plot. Reproduced from Saha *et al.* (2007) Designing Synthetic materials to Control Stem Cell Phenotype (147).

Need for Characterizing Parameters for Chondro-Supportive Biomaterials

Up to now there is no common agreement on what specific properties a substrate (i.e. a scaffold) should provide to autologous chondro progenitor (expanded/de-differentiated HAC or MSC) cells in order for them to form hyaline rather than fibrous cartilaginous matrix. Consequently, there is a clear need for defining biomaterial parameters from a biological perspective. Thus, this thesis is dedicated to studying the influence of specific tuneable controllable substrate characteristics 1) surface chemistry & architecture 2) cell adhesion ligand type 3) substrate stiffness on the potential of human chondro progenitor cells to exert their expected function.

Thesis Outline

Clinical Relevance of Biomaterial Supported Cartilage Repair

Since cartilage has a very limited capacity for self repair (148), standard treatments in attempt to overcome this limitation include the technique of microfracturing. This involves debridement of the damaged cartilage and drilling into the subchondral bone to allow for mesenchymal stem cells to invade and deposit cartilaginous matrix. However, the formed repair tissue is fibrous in nature, generally degrades after about half to one year post-surgery and thus the problems return for up to 90% of the patients (149;150).

Current visions in cartilage repair aim at moving from fibrocartilaginous to a more hyaline like repair tissue by combining autologous cells of different origins (*in situ* recruited or *in vitro* precultivated) with repair supporting biomaterials (151). The role of a chondro-supportive biomaterial within a cartilage defect is seen to support infiltration/recruitment of chondroprogenitor cells, accelerate their chondrogenic differentiation and to protect/modulate the newly formed tissue (152).

Thus, the ultimate goal is to improve current clinical outcome from fibrous tissue towards hyaline-like cartilage by assisting cell based and micro fracturing stimulated repair with supportive biomaterials.

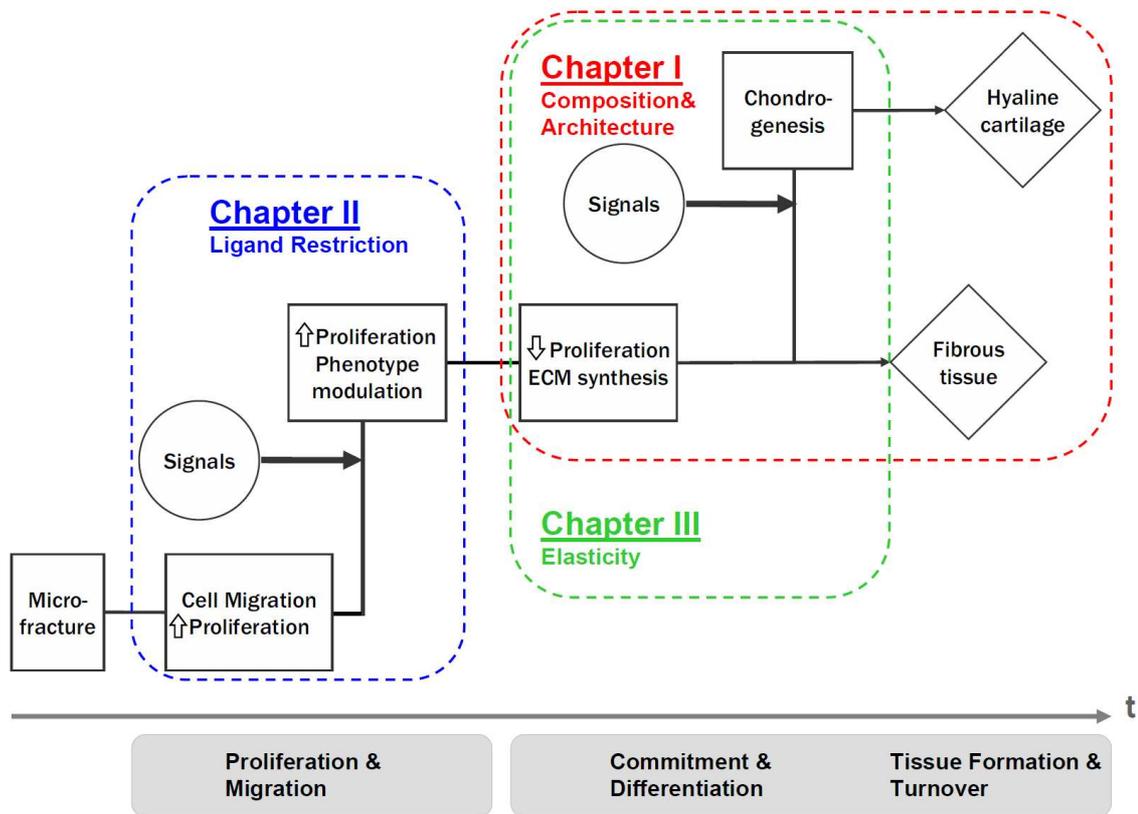


Fig. 1 Schematic view of cartilage repair/regeneration sequence following micro fracturing (adapted from a stepwise model system for limb regeneration by Endo *et al.* 2004 (153)). As indicated by the grey boxes (below the time axis), the repair process has been grouped into two main phases consisting of i) proliferation and ii) differentiation from which *in vitro* conditions were inferred for testing the response of condroprogenitor cells (CPC) to specifically modified substrate interfaces. Boxes with dashed lines delimit the boundary of each chapter and indicate the type of substrate property addressed therein. Chapter I aimed at modulating CPC chondrogenic differentiation through modification of substrate composition & architecture. Chapter II aimed at modulating the phenotype of proliferating CPC by exclusively restricting their interaction with the substrate to an RGD containing peptide ligand. Chapter III aimed at modulating CPC behaviour during differentiation by modifying the substrate elasticity.

General Aim

Overall, this thesis aimed at studying whether modification of selected substrate interface properties allows for modulating chondroprogenitor cell phenotype & function under expansion or differentiation conditions *in vitro*. The goal was to contribute to the definition of material characteristics which could be implemented in the design of biomaterials in order to improve current matrix assisted cartilage repair strategies and outcomes.

Specific Aims and Models

This thesis is divided into three chapters. Each chapter employed its own model substrates to modulate CPC (MSC or expanded/de-differentiated HAC respectively) behaviour and had its specific aims as described below (also see Fig. 1):

- **Chapter I**

Scaffold Composition & Architecture Modulates Chondrogenesis of Human Mesenchymal Stem Cells

Aim: Test, whether chondrogenesis of expanded bone marrow derived mesenchymal stem cells (MSC) can be instructed/modulated by controlled modification of substrate composition and architecture.

Model: Poly (ethylene glycol)-terephthalate-poly(buthylene)-terephthalate block copolymer scaffolds (PolyActive®) of two contrasting compositions (low or high poly (ethylene glycol) content: resulting in different wettability) and two architectures generated by compression moulding (CM) or three dimensional fibre

deposition (3DF) with similar porosity and mechanical properties, but different interconnecting pore architectures were used. MSC seeded on the corresponding substrate were cultured under differentiation conditions +/- transforming growth factor beta 1 (TGF).

- **Chapter II**

An RGD-Restricted Substrate Interface Allows for Expansion and Subsequent Redifferentiation of Human Articular Chondrocytes

Aim: Test, whether an RGD restricted substrate interface allows for human articular chondrocytes (HAC) growth, modulates their proliferation associated de-differentiation and/or their post-expansion chondrogenic capacity.

Model: HAC interaction with the substrate was restricted to RGD by modifying tissue culture treated polystyrene (TCPS) with a poly-(ethylene glycol) (PEG) based copolymer system that renders the surface resistant to protein adsorption while at the same time presenting the bioactive peptide ligand GCRGYGRGDSPPG (*RGD*). In an *in vitro* comparison, HAC were cultured on *RGD* and the standard substrate TCPS under expansion conditions. The chondrogenic capacity of the expanded cells was subsequently tested in pellet culture under differentiation conditions.

- **Chapter III**

Effect of Matrix Elasticity on the Re-differentiation Capacity of Expanded Human Articular Chondrocytes

Aim: Test, whether substrate elasticity modulates the chondrogenic commitment of expanded human articular chondrocytes (HAC).

Model: Providing an environment for differentiation, expanded/de-differentiated HAC were cultured on type I collagen functionalized poly acrylamide (PA) substrates of contrasting stiffness (0.3, 21 and 75kPa, tissue culture treated plastic (TCPS) as infinitely stiff control).



Chapter I

SUBSTRATE COMPOSITION & ARCHITECTURE MODULATES CHONDROGENESIS OF HUMAN MESENCHYMAL STEM CELLS

INTRODUCTION

Using two contrasting compositions of Poly (ethylene glycol)-terephthalate-poly(buthylene)-terephthalate block copolymer scaffolds (PolyActive®; see Fig. 1), it was previously demonstrated that the re-differentiation capacity and cartilaginous matrix deposition of expanded human nasal chondrocytes (NC) could be modulated (117). In specific, the authors demonstrated that a hydrophilic (1000 PEG 70:30) as compared to a more hydrophobic (300 PEG 55:45) composition more strongly induced the chondro-re-differentiation of NC (in absence of exogenous chondrostimuli, as i.e. TGF β to the culture medium). This chondroinductive effect has mainly been attributed to an increase in the vitronectin/fibronectin adsorption ratio from serum by the more hydrophilic substrate (113).

As in recent years human bone marrow derived mesenchymal stem cells (MSC) have been receiving increasing attention for regenerative medicine (152), we wanted to assess, whether the chondroinductive effect of the hydrophilic Polyactive® on NC also applies for expanded MSC. Thus, expanded MSC were cultured on PolyActive® scaffolds of different compositions under conditions published for NC (117). After four weeks of culture in DMEM complete medium, the MSC/scaffold constructs were histologically and biochemically analyzed for deposition of cartilaginous matrix.

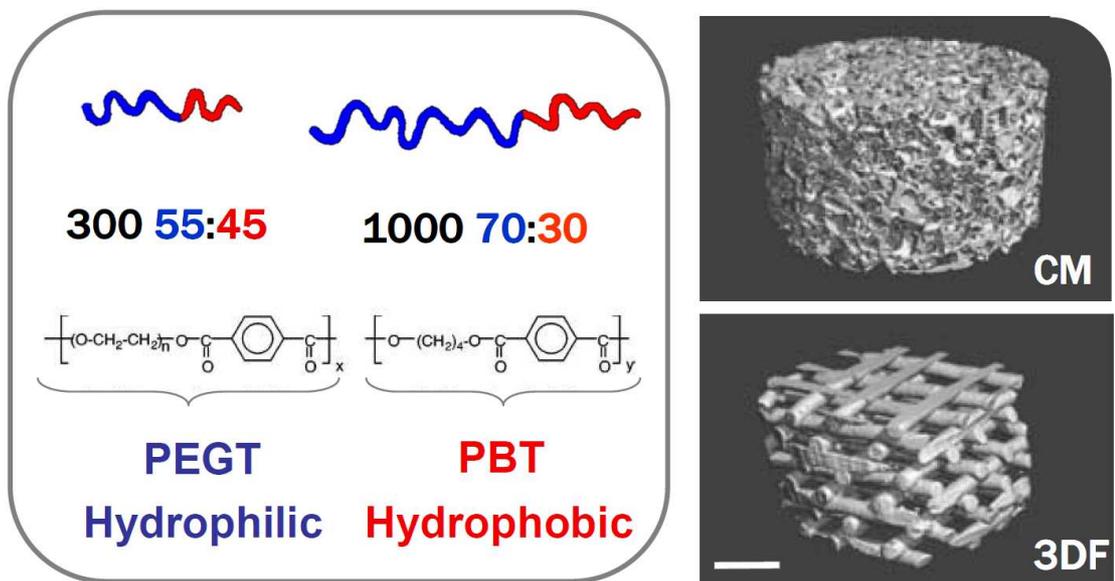


Fig. 1 Composition and architecture of Polyactive® model substrate used throughout chapter one. Left panel shows a schematic drawing of the two different di block copolymers with a composition denoted as a/ b:c, where a represents the poly ethylene (PEG) molecular weight (g/mol) and b and c represent the weight percentage (wt%) of the poly (ethylene glycol) terephthalate (PEGT; hydrophilic) and the poly (butylene terephthalate) (PBT; hydrophobic) respectively. For simplicity, substrate composition 300 PEG 55:45 (hydrophobic) and 1000 PEG 70:30 (hydrophilic) are denoted as 300 and 1000 respectively. Right panels show three dimensional reconstructions of compression molded (CM) and 3D fiber deposited (3DF) architecture scaffolds from micro computed tomography (μ CT) scans as adapted from (117). Scale bar represents 1mm. Compositions and architecture were selected based on previous work indicating their suitability for chondrocyte culture and cartilaginous matrix formation (117).

STUDY 1

Aim

It was investigated, whether chondrogenesis of expanded MSC can be instructed/modulated by controlled modifications of substrate composition and architecture. As a model system, poly(ethylene glycol)-terephthalate-poly(buthylene)-terephthalate block copolymer substrates (PolyActive®) from two contrasting compositions (low or high PEG content, resulting in different wettability) were used. From these two compositions, scaffold architectures of similar porosity, but different interconnecting pore architectures were employed.

Methods

Scaffold Fabrication

PEGT/PBT copolymers were obtained from CellCoTec (Bilthoven, The Netherlands). 3D scaffolds made from 300 PEG 55:45 (300) and 1000 PEG 70:30 (1000) compositions (Fig. 1) were produced using either a compression molding (CM) and particle leaching technique (120) or a 3DF deposition technique (115;118). Briefly, CM scaffolds were prepared by mixing PEGT/PBT granules with sodium chloride grains (75% by volume), sieved to obtain particles ranging in size from 400 to 600 μm . After CM under heat and pressure, the polymerized PEGT/PBT block was then immersed in demineralized water for 48 h to remove the sodium chloride, and dried under reduced pressure in a vacuum oven. Porous 3DF scaffolds were constructed by successively layering a 0–901 pattern of molten PEGT/PBT fibers from a $\text{\O}250\mu\text{m}$ nozzle onto a computer controlled x^2y^2z table. Fibers within each layer were spaced 1.0mm apart, but were offset (staggered) by 0.5mm between layers to optimize the “visible” surface available for cell seeding. Square blocks of $30\times30\times4\text{mm}^3$ were produced with a consistent pore size, 100% interconnecting pore volume and a porosity of 56%. Cylindrical scaffolds, 2-3mm in height, 4.7mm diameter, were cored from the bulk of porous CM and 3DF blocks prior to cell seeding. Previous thermal analysis studies have demonstrated that CM and 3DF processing techniques do not result in changes of PEG MW or PEGT/PBT composition (118). Therefore, any differences seen in this study between architectures of CM and 3DF scaffolds should not be related to differences in scaffold composition. Due to enhanced instruction of chondrogenesis in de-differentiated chondrocytes on the 1000 chemistry (117), the variation of architecture (CM/3DF) was restricted to this composition.

Cell Isolation and Expansion

Bone marrow derived mesenchymal stem cells (MSC) were obtained as described previously (154). In brief, one bone marrow aspirate was obtained during a routine orthopaedic surgical procedure involving exposure of the iliac crest, after informed consent. A marrow aspirate (20 ml volumes) was harvested from a healthy donor (female, 34 years) using a bone marrow biopsy needle inserted through the cortical bone; the aspirate was immediately transferred into a plastic tube containing 15,000 IU heparin.

Bone marrow nucleated cells were counted after staining with Crystal Violet 0.01% in phosphate-buffered saline (PBS, both from Sigma-Aldrich, Switzerland) and plated at a density of 1×10^5 cells/cm² in alpha minimal essential medium containing 4.5 mg/ml D-glucose, 0.1 mM non-essential amino acids, 1 mM sodium pyruvate, 10 mM HEPES buffer, 100 U/ml penicillin, 100 µg/ml streptomycin, and 0.29 mg/ml L-glutamine, supplemented with 10% FBS (all from Gibco, UK; αMEM complete) supplemented with 5 ng/ml fibroblast growth factor-2 (R&D Systems, Wiesbaden, D) to enhance proliferation and enrich the pluripotent MSC population (155). MSC were cultured in a humidified 37°C/5% CO₂ incubator with medium changes twice a week. MSC were selected on the basis of adhesion and proliferation on the plastic substrate. Upon reaching subconfluency, MSC were detached using 0.05% trypsin/0.53 mM EDTA (GIBCO-BRL, CH) and replated at a density of 3'000 cells/cm² (passage 1, p1). Reaching confluency (p2), MSC were detached and seeded onto scaffolds as described below.

Cell Seeding and Culture on Three Dimensional Scaffolds

Cylindrical scaffolds were prewetted with 70% ethanol, thoroughly rinsed with autoclaved milliQ water, soaked in Dulbecco's modified Eagle's medium (DMEM) containing 4.5 mg/ml D-glucose, 0.1 mM non-essential amino acids, 1 mM sodium pyruvate, 10 mM HEPES buffer, 100 U/ml penicillin, 100 µg/ml streptomycin, and 0.29 mg/ml L-glutamine, 10% FBS (all from Gibco, UK; DMEM complete) and blotted dry on a sterile paper. Expanded MSC (p2; 2.5 Mio./scaffold) were allowed to clott in DMEM complete CM for 20 min. prior to statically seeding them onto scaffolds placed in dishes coated with a thin film of 1% agarose. Seeding volume/scaffold was adjusted to 30µl for the CM 300, 50µl for the CM 1000 and 37µl for the 1000 3DF to compensate for the differential swelling inherent to the corresponding combination of composition and architecture. Constructs were placed in dishes coated with a thin film of 1% agarose and statically cultured in 2ml DMEM complete supplemented with 10 mg/ml insulin and 0.1mM ascorbic acid, either without or with 10ng/ml TGFβ-3 (TGF), with medium changes twice a week. TGF is a strong chondrostimulus (94;156) and was included in the culture medium as a contingency measure, in case the scaffold *per se* would not be chondro- instructive/inductive for MSC. After four weeks of culture, constructs were harvested and processed for gene expression as well as for histological and biochemical analysis.

Biochemical Analysis

Constructs cultured for four weeks were digested with protease K (0.5 ml of 1 mg/ml protease K in 50 mM Tris with 1 mM EDTA, 1 mM iodoacetamide, and 10 µg/ml pepstatin-A) for 15 hours at 56°C (157). The glycosaminoglycan (GAG) content was

measured spectrophotometrically using dimethylmethylene blue (158), with chondroitin sulfate as a standard, and normalized to the DNA amount, measured spectrofluorometrically using the CyQUANT Kit (Molecular Probes, Eugene, OR), with calf thymus DNA as a standard. GAG contents are reported as $\mu\text{g GAG} / \mu\text{g DNA}$.

Cell Seeding Efficiency and Retention

The number of cells was estimated by measuring the amount of DNA in protease K digested constructs (as described in biochemical analysis). Cell seeding efficiency was determined 24 hours after seeding (initial) and expressed as percentage of seeded cells (aliquots of 2.5 Mio. MSC from the cell suspension used for seeding onto the scaffolds corresponding to 100%). Cell retention was estimated by measuring the amount of DNA present in the constructs at the end of four weeks of culture and comparing it to the initial amount of DNA.

Histological and Immunohistochemical Analysis

Constructs cultured for four weeks were fixed in 4% formalin for 24 h, embedded in paraffin, cross-sectioned (12 μm thick), and stained with Safranin O for sulphated GAG (100). Sections were also processed for immunohistochemistry to visualize type II collagen (II-II6B3, Hybridoma Bank, University of Iowa, USA), as previously described (159).

Structural integrity of the scaffold was better maintained on the 300 compared to the 1000 composition. For the latter, sections could be retrieved only where tissue formation had occurred. Otherwise, only small fractures of the constructs could be captured (Fig. 2C). For the 3DF 1000 (Fig. 2E&F), the scaffold material was completely lost, leaving behind

white holes. Scaffold loss was an inevitable artefact introduced during the mounting of histological sections (low adhesion and swelling inherent to the 1000 composition).

Gene Expression Analysis

RNA was extracted from tissue constructs using 250 µl Trizol (Life Technologies, Basel, CH) according to the manufacturer's instructions. Extracted RNA was treated with DNase following the instructions of the Rneasy Kit (Ambion, Austin TX). cDNA was generated from total RNA using reverse-transcriptase Stratascript (Stratagene) in the presence of dNTP and DTT. Real-time PCR reactions were performed and monitored using the ABI prism 7700 Sequence Detection System and the Sequence Detector V program (Perkin-Elmer Applied Biosystems). cDNA samples were analyzed for type I & II collagen and for the housekeeping gene (18S ribosomal RNA), using previously described sequences of primers and probes (100). Each cDNA sample was assessed in duplicate and the collagen mRNA expression levels were normalized to the corresponding 18S rRNA levels.

Results

One day after seeding expanded MSC onto the scaffolds, the constructs with CM architecture revealed a higher seeding efficiency on the 300 ($74\pm 2\%$) compared to the 1000 ($62\pm 2\%$) composition as determined by the amount of DNA. For the 1000 composition, a change in scaffold geometry from CM to 3DF enhanced the seeding efficiency ($72\pm 3\%$). The presence of TGF did not change the seeding efficiency ($<7\pm 5\%$ vs. (-) TGF) and the fraction of cells released to the medium was always below $17\pm 3\%$. After four weeks of static culture, the retention of MSC on the PolyActive® scaffolds was estimated by measuring the amount of DNA present in the constructs (Fig. 3A). Generally, the CM scaffolds maintained their initial DNA level throughout the four weeks of culture, and there was even a slight increase ($11\pm 9\%$) in DNA on the 300 composition. On the 3DF architecture in contrast, the final DNA level nearly dropped to half ($57\pm 5\%$) of the initial level. Overall, MSC retention on PolyActive® did not seem to be affected by the presence of TGF in the culture medium.

Constructs cultured for 4 weeks were formalin fixed, paraffin embedded and stained for glycosaminoglycans (GAG) with safranin O (Fig. 2). Despite for the CM 1000 where little to no tissue could be retrieved, MSC were able to deposit matrix in all conditions. In absence of TGF (Fig. 2A, C, E) formed tissue was predominantly fibrotic, showed no GAG deposition and even became necrotic in parts (Fig. 2E, upper left corner of inset detail view). In presence of TGF, GAG deposition was faintly more visible on the 300 (Fig. 3B) than on the 1000 (Fig. 3D) composition with CM architecture. Strongest GAG

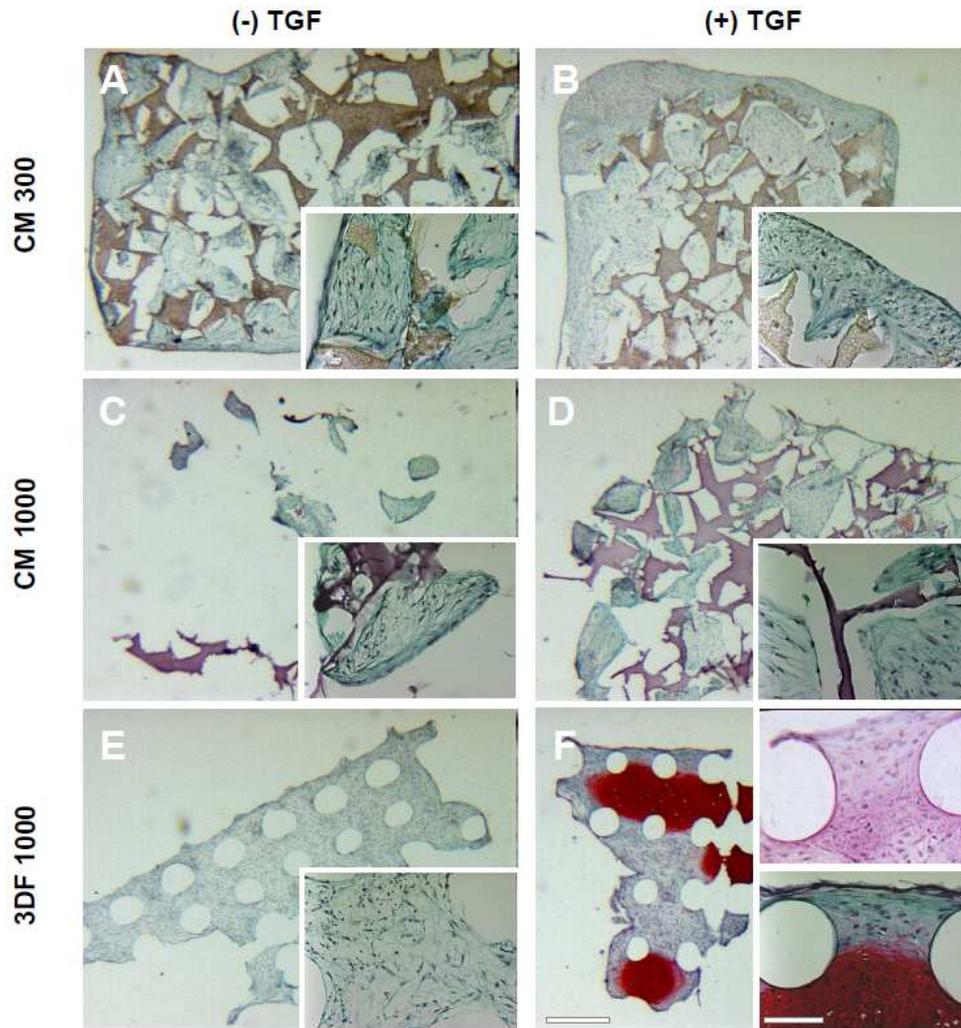


Fig. 2 Light microscopy images of safranin O stained (red: glycosaminoglycans, GAG), representative histological cross-sections of MSC cultured on PolyActive® for four weeks without (A, C, E) or with (B, D, F) chondrogenic stimulus TGF. Small insets show higher power magnifications of large sections shown in corresponding large panel. In F, the upper insert shows a type II collagen stained section consecutive to that stained with safranin O (directly below). Polyactive® composition were 300 PEG 55:45 (300; A&B) and 1000 PEG 70:30 (1000; C-F) in either compression molded (CM; A-D) or 3D fiber deposited (3DF; E&F) architecture. Structural integrity of the scaffold was better maintained for the 300 (brown structures) compared to the 1000 (violet structures) composition. For the latter, sections could be retrieved only where tissue formation had occurred as i.e. for C, only small fractures of the constructs could be captured. In E&F the scaffold material was completely lost, leaving behind white holes. Scaffold loss was an inevitable artifact introduced during the mounting of histological sections (low adhesion and swelling inherent to the 1000 composition). Despite strong focal GAG staining on the 3DF 1000 (F), deposited tissue in A-E was mostly fibrotic, showed little to no GAG accumulation and in E (upper left corner on inset) even displayed necrotic portions. Scale bars: 400 μm (large panels), 100 μm (insets).

staining and presence of rounded cells was detected on the 3DF 1000 in presence of TGF (Fig. 2F). Only for this condition, collagen type II could be detected by immunohistochemistry (Fig. 2F upper inset).

Quantitative, biochemical analysis of accumulated GAG (Fig. 3B) matched with the histological findings. The marginal amounts of GAG/DNA deposited in the absence of TGF were increased by 2 to 4-fold in presence of TGF, reaching the highest value on 3DF1000.

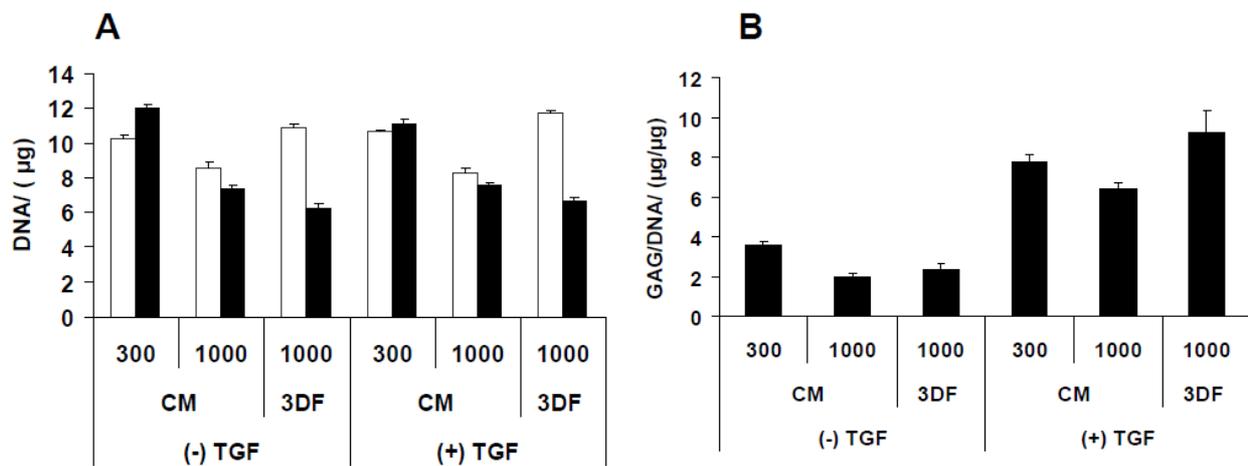


Fig. 3 MSC retention and glycosaminoglycan (GAG) accumulation after 4 weeks of culture on Polyactive® scaffolds without or with chondrogenic stimulus TGF. Panel A displays the initial amount of DNA (white bars) and that found after four weeks (black bars) of culture. Despite the marginal increase in DNA on the 300 PEG 55:45 (300) composition, the compression moulded (CM) scaffolds in general maintained their initial DNA level throughout the culture period. On the 3D fiber deposited (3DF) scaffolds in contrast, initial DNA levels were almost halved ($57\pm5\%$). The presence of TGF did not change this pattern. Panel B shows the amount of accumulated GAG (normalized vs. Amount of DNA at the end of culture) as determined biochemically. The addition of TGF raised the basal levels of GAG/DNA by 2 to 4-fold. The highest GAG/DNA value was reached by the 3DF 1000 while comparing the CM architecture only, the 300 tended towards higher GAG/DNA than the 1000 composition. Error bars represent the standard deviation. Comparing the CM architecture only, the 300 tended towards higher values than the 1000 composition.

Expression levels of mRNA (Fig. 4) revealed more drastic differences than revealed by the accumulation of cartilaginous matrix but followed the same trends/patterns. Type I collagen mRNA (indicator of fibrocartilage) expression was always expressed more strongly than type II collagen (indicator of hyaline cartilage). Most drastic were the mRNA expression changes introduced by adding TGF, which in average raised type I collagen ~300-fold and type II collagen by several orders of magnitude ($4.5E+6$). In presence of TGF, highest type II collagen mRNA expression was found on the 3DF 1000 which was four orders of magnitude higher than that found on CM of the same chemistry. Comparing the CM architecture only, type II collagen mRNA was more than 40 times higher on the 300 than it was on the 1000.

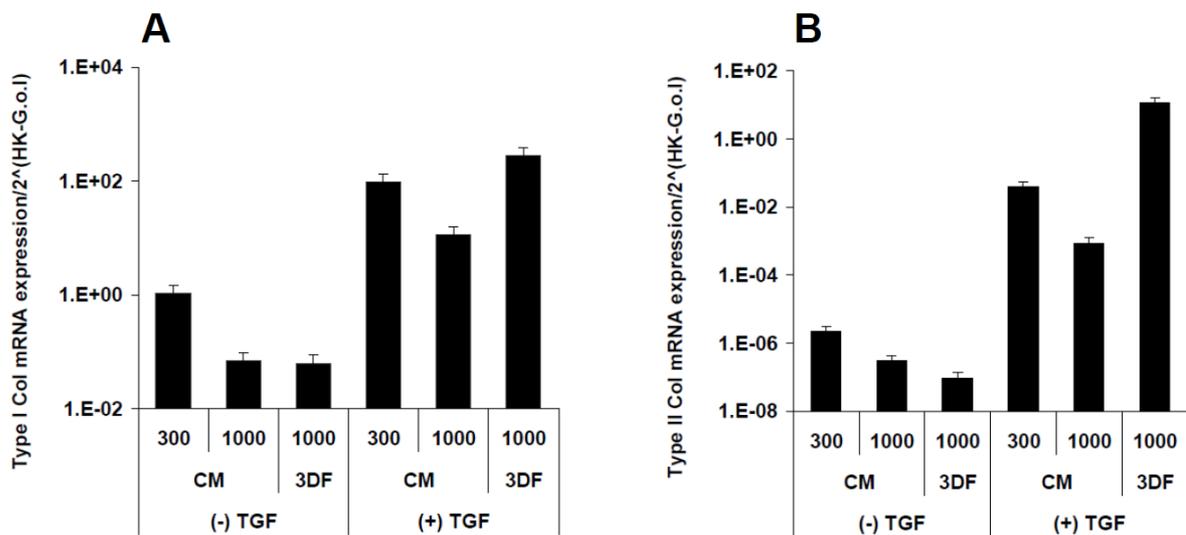


Fig. 4 Type I & II collagen mRNA expression of MSC cultured for four weeks on Polyactive® scaffolds without or with TGF. Genes of interest (G.o.I) were normalized vs. housekeeping gene (HK) 18S. Panel A: type I collagen, panel B: type II collagen. Error bars indicate standard deviation.

Discussion

Using two contrasting compositions and architectures, scaffolds made of PolyActive® were *per se* not able to induce chondrogenesis in MSC. However, in presence of exogenic chondrogenic stimulus TGF, chondrogenesis could be observed which tended to be better supported by the more hydrophobic 300 composition and was further enhanced by changing the scaffold architecture from CM to 3DF. These findings indicate, that controlling scaffold composition and architecture is important to support, but *per se* not sufficient to instruct/induce chondrogenesis in MSC.

Marginal proliferation in any of the conditions excludes the possibility that chondrogenesis was indirectly regulated through differential cell proliferation. Although initially cell seeding efficiency was comparable in all the conditions, a marked loss of cells from 3DF 1000 scaffolds over four weeks of culture reveals a low affinity of MSC for this combination of composition and architecture and prompts for very careful liquid handling during medium changes. Since histological sections indicate that this cell loss did not lead to an obvious decrease in local cell density (1000 composition; 3DF vs. CM) this unlikely affected chondrogenesis of the retained/remaining MSC.

In contrast to the findings with nasal chondrocytes (117), none of the PolyActive® compositions and architecture compositions *per se* allowed for chondrogenesis in MSC. However, supplementing the culture medium with TGF stimulated chondrogenesis in MSC and revealed this process to be slightly modulated by scaffold composition and more strongly by its architecture. Although selectively adsorbed serum proteins (113;160) on the scaffold surface has been reported to instruct human chondrocyte re-differentiation (117), this stimulus alone does not seem to suffice for instructing chondrogenic

differentiation in less committed cells as i.e. MSC. In this light, it appears more appropriate to consider the applied scaffold materials chondro-supportive, instead of chondro-instructive. Also, further investigations on the influence of PolyActive® composition and architecture on MSC differentiation should be performed in presence of a chondrogenic stimulus. A common approach to induce chondrogenesis in MSC, is supplementing the culture medium with a strong differentiation stimulus as i.e. TGFβ (94;156). As an alternative to, exogenous soluble differentiation stimuli, MSC could be exposed to paracrine signals present in an osteochondral microenvironment (161). To this end, a recently introduced ectopic *in vivo* mouse model for human cartilage repair could offer an experimental solution (162). Therein, a MSC/scaffold construct could be placed in a defined osteochondral defect (disk from human femour head explants) and cultured subcutaneously in a nude mouse.

In presence of TGF, chondrogenesis of MSC always followed the same trend which was 3DF 1000 > CM 300 > CM 1000. Thus both, scaffold composition and architecture appeared to modulate MSC chondro-differentiation. That the 300 composition better supported chondrogenesis, contradicts previous reports for nasal chondrocytes (NC) which showed superior chondrogenic differentiation on the 1000 (117). Yet, despite the plasticity of expanded NC (unpublished results), MSC are presumably more progenitor-like. Thus, they could be more sensitive to passing through developmental checkpoints as i.e. cellular condensation to enter chondrogenic differentiation. Therefore, MSC could profit from higher fibronectin (FN) concentration present on the 300 than on the 1000, since FN plays a crucial role in aggregation of cells into mesenchymal condensations (163). In the developing limb bud, cellular condensation is a key step for chondrogenesis of mesenchymal cells as it allows for the appropriate microenvironment through

homotypic cell-cell interactions (for review see (164)). In contrast to MSC, to de-differentiated chondrocytes (as i.e. NC), which already have already passed through condensation once, FN likely provides a different stimulus as i.e. spreading (117), which is known to interfere with re-differentiation (165). While this explanation is quite speculative, there is no doubt that that NC (neuro ectoderm) and MSC (mesoderm) are of quite different germ layer origin and thus likely react to the same stimulus in a different manner.

The higher degree of chondrogenic differentiation mediated by the 3DF architecture (comparing 1000 composition only) is in line with findings for human nasal chondrocytes (117). Lower structural complexity and bigger average pore size of the 3DF facilitate diffusion rate of nutrients and gases as well as waste removal and likely contribute to this effect (116). Moreover, the low affinity of MSC for the 1000 composition combined with the low structural complexity of the 3DF architecture (i.e. high interconnectivity of the pores) could facilitate MSC condensation into larger aggregates.

Outlook

Due to its superior performance, follow-up investigations of substrate chemistry influence on MSC chondrogenesis could be restricted to the 3DF architecture. However, this should be preceded by an optimization of the cell culture protocol in order to prevent cell loss. Under optimized *in vitro* conditions, the effect of substrate chemistry should be reassessed with MSC from another donor, to test the robustness of the observed effect.

STUDY 2

Aim

It was investigated, whether chondrogenesis of expanded MSC can be instructed/modulated by controlled modifications of scaffold composition under optimized *in vitro* conditions. As a model system, poly(ethylene glycol)-terephthalate-poly(buthylene)-terephthalate block copolymer scaffolds (PolyActive®) with 3D fiber deposited (3DF) architecture of two contrasting compositions (low or high PEG content, resulting in different wettability) were used.

Methods

Scaffold Fabrication

See study 1. Compared to the compression molded (CM), the 3D fibre deposited (3DF) scaffolds better supported chondrogenesis of MSC. Thus, in this study scaffold architecture was focussed on 3DF.

MSC Isolation and Expansion

For this study, a bone marrow aspirate (20 ml volume) from a healthy donor (male, 44 years) was used. MSC were isolated and expanded as described in study 1.

Optimization of in vitro Culture Conditions

Based on the findings of the previous study, the *in vitro* culture conditions were optimized for this study. In particular, i) medium composition and ii) cell retention were optimized as follows:

- i) The composition of chondrogenic differentiation medium which was adapted from that previously used for nasal chondrocytes, resulted in limited chondrogenesis of MSC (see study 1). Since foetal bovine serum suppressed TGF β -1 induced chondrogenesis in synoviocytes pellet culture (166) a serum free medium chondrogenic medium (102) was tested as an alternative to the previously used serum containing medium (DMEM complete; see study 1). The chondrogenesis of MSC in presence or absence of serum was investigated in

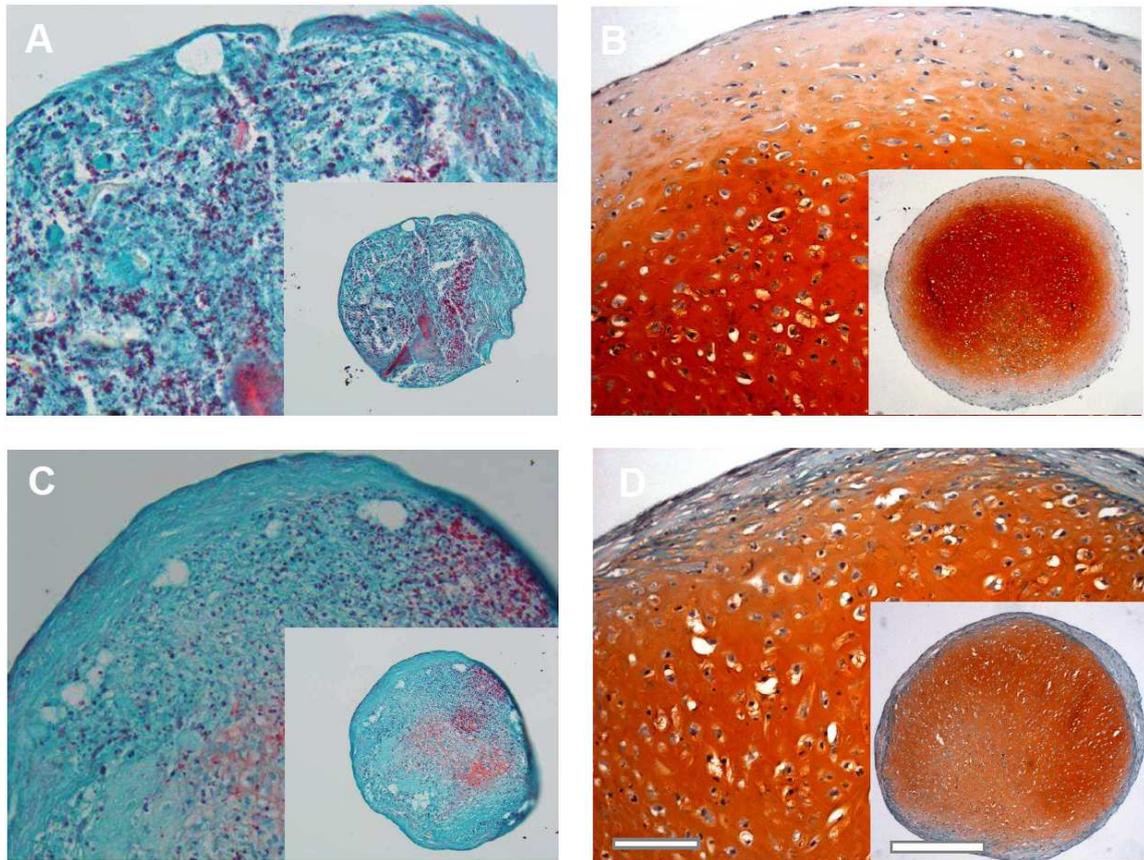


Fig. 5 Light microscopy images of Safranin O stained (red: glycosaminoglycans, GAG), representative histological pellet cross-sections. To test whether chondrogenesis of MSC could be improved using a serum free medium, MSC were cultured as pellets in either (A) 10% serum containing DMEM complete medium as applied for study 1, or (B) serum free medium (SFM), or to isolate the effect of serum in (C) SFM supplemented with 10% serum. To stimulate chondrogenesis, all media contained 0.1 mM ascorbic acid, 10 mg/ml insulin and 10 ng/ml transforming growth factor beta 1 (TGF). MSC aggregated with fibrin glue (D) were also cultured in SFM chondrogenic medium. This was done to isolate the effect of fibrin glue on the chondrogenesis of MSC as it was included in this study to improve MSC retention on the 3D fiber deposited scaffolds. Scale bars: 100 μ m (large panels), 400 μ m (small panels).

pellet culture (see Fig. 5A&B). In brief, aliquots of 5×10^5 MSC/0.5ml were centrifuged at 250 g for 5 min. in 1.5 ml polypropylene conical tubes (Saarstedt, Nümbrecht, Germany) to form spherical pellets. These pellets were cultured either in serum containing DMEM complete (see previous study), or in a chemically defined, serum-free medium (SFM), which consists of DMEM containing 4.5 mg/ml D-glucose, 0.1 mM non-essential amino acids, 1 mM sodium pyruvate, 10 mM HEPES buffer, 100 U/ml penicillin, 100 μ g/ml streptomycin, and 0.29 mg/ml L-glutamine (all Gibco, UK). To isolate the effect of serum, SFM was supplemented with 10% FBS. Additionally, all media were supplemented with the chondrogenic factors ITS⁺ (10 μ g/ml insulin, 5.5 mg/ml transferrin, 5 ng/ml selenium, 0.5 mg/ml bovine serum albumin, 4.7 mg/ml linoleic acid), 1.25 mg/ml human serum albumin, 0.1 mM ascorbic acid 2-phosphate and 10^{-7} M dexamethasone (all Sigma Chemical, USA) and 10 ng/ml TGF- β 1 (R&D, UK). Pellets were cultured for 4 weeks at 37°C / 5% CO₂, with medium changes twice per week.

Light microscopy images of safranin O stained representative histological pellet sections revealed that not only the SFM medium improved the chondrogenesis in MSC but also that serum had a negative effect thereon and even led to necrosis (see Fig. 5C).

ii) As on the 3DF scaffold with the 1000 composition almost half of the initially seeded MSC were lost throughout the culture period, low concentration fibrin glue (FG; TISSEEL® kit, Baxter, Vienna, Austria, dilution 1:16) was used to improve cell retention. Fibrin glue consists of a fibrinogen aprotinin solution (contains Factor XIII), which coagulates when combined with thrombin and calcium

chloride. Taking advantage of FG mediated coagulation, homogenous cell distribution and quantitative seeding efficiency was achieved on 1000 3DF scaffolds (data not shown). To test whether FG interferes with chondrogenesis, FG entrapped MSC were cultured in chondrogenic differentiation medium (see Fig. 5D). For this, aliquots of 5×10^5 MSC/0.5ml were centrifuged at 250 g for 5 min. in 1.5 ml polypropylene conical tubes (Saarstedt, Nümbrecht, Germany). The pellet was resuspended with 52 μ l of 7 mg/ml fibrinogen solution (contains aprotinin as a protease inhibiting FG stabilizer) and the cell suspension transferred to a conical polypropylene tube containing 10 μ l of 31 U/ml thrombin in solution (in 40 mM CaCl_2) where the mixture was allowed to clot. FG entrapped MSC cultured in SFM supplemented with chondrogenic factors (as described above) for four weeks of culture (Fig. 5D) were comparable to conventional pellets (see Fig. 5B) in their accumulation of GAG. As FG was not found to interfere with MSC chondrogenesis, FG was applied in this study to optimize MSC retention on the 3DF scaffolds as described below.

Chondrocyte Seeding and Culture on Three Dimensional Scaffolds

Cylindrical scaffolds were prewetted with 70% ethanol and thoroughly rinsed with autoclaved milliQ water. Prewetted scaffolds were soaked in DMEM complete for 1 hour. This allowed for differential adsorption of serum proteins on the two contrasting compositions, and has been described to be responsible for their difference in modulating chondrocyte redifferentiation (113). Subsequently, the scaffolds were blotted dry on a sterile paper, loaded with a corresponding volume (300: 25 μ l; 1000: 55 μ l) of 31 U/ml

thrombin in 40 mM CaCl₂ solution and placed in an agarose coated 12 well plate for 5 min. before blotting dry again. Holding the scaffold with forceps, P2 expanded MSC (2.5 Mio/scaffold) in the corresponding volume (300: 25 µl; 1000: 55 µl) of 7 mg/ml fibrinogen (in the supplied aprotinin solution) were seeded onto the scaffolds. Seeding volume/scaffold was adjusted to compensate for the differential swelling inherent to the corresponding composition. The cell loaded construct was placed on top of 10 µl 31 U/ml thrombin solution (in 40 mM CaCl₂) in an agarose coated 12 well plate and allowed to stand for 2 min. prior to adding the corresponding medium. Constructs were statically cultured in 2ml of either DMEM complete or SFM supplemented with 10 mg/ml insulin, 0.1mM ascorbic acid and 10ng/ml TGFβ-3 (TGF) for 4 weeks, with culture medium changes twice a week. After harvesting, constructs were processed for histological and, biochemical or gene expression analysis.

Biochemical analysis, cell seeding efficiency & retention, histological & immunohistochemical analysis: see study 1.

Results

One day after seeding expanded MSC onto the scaffolds using fibrin glue (FG), seeding was found to be quantitative and comparable on both scaffold chemistries. With $96\pm 10\%$ for the 300 and $104\pm 11\%$ for the 1000 composition, the seeding efficiency was more than 20% higher than that achieved previously without FG on 3DF 1000 (see study 1).

After four weeks of static culture, the retention of MSC on the PolyActive® scaffolds was estimated by measuring the amount of DNA present in the constructs (Fig. 7A). There was a slight loss of DNA on the 300 composition which tended to be stronger in presence of serum (DMEM complete; $19\pm 10\%$) than in serum free medium (SFM; $11\pm 5\%$). On the 1000 in contrast, the final amounts of DNA were increased and tended to be higher in the absence of serum ($27\pm 13\%$) than in DMEM complete ($8\pm 4\%$).

Constructs cultured for 4 weeks were formalin fixed, paraffin embedded and stained for glycosaminoglycans (GAG) with safranin O (Fig. 6). In all conditions, MSC were able to deposit matrix, which in presence of serum was predominantly fibrotic and showed no GAG deposition (Fig. 6A&C). All constructs were encapsulated by several layers of cells with flattened morphology. This capsule was denser/thicker where serum was present and thinnest for the 300 composition in absence of serum. Some core regions seem to have become necrotic as they contain a dense aggregation of nuclei (Fig. 6 lower left panels in A & B; blue dots). In absence of serum, GAG staining was faint on the 1000, clearly stronger on the 300 and for both compositions most intense just beneath the construct periphery. On the 300, the staining additionally reached into the core regions of the construct.

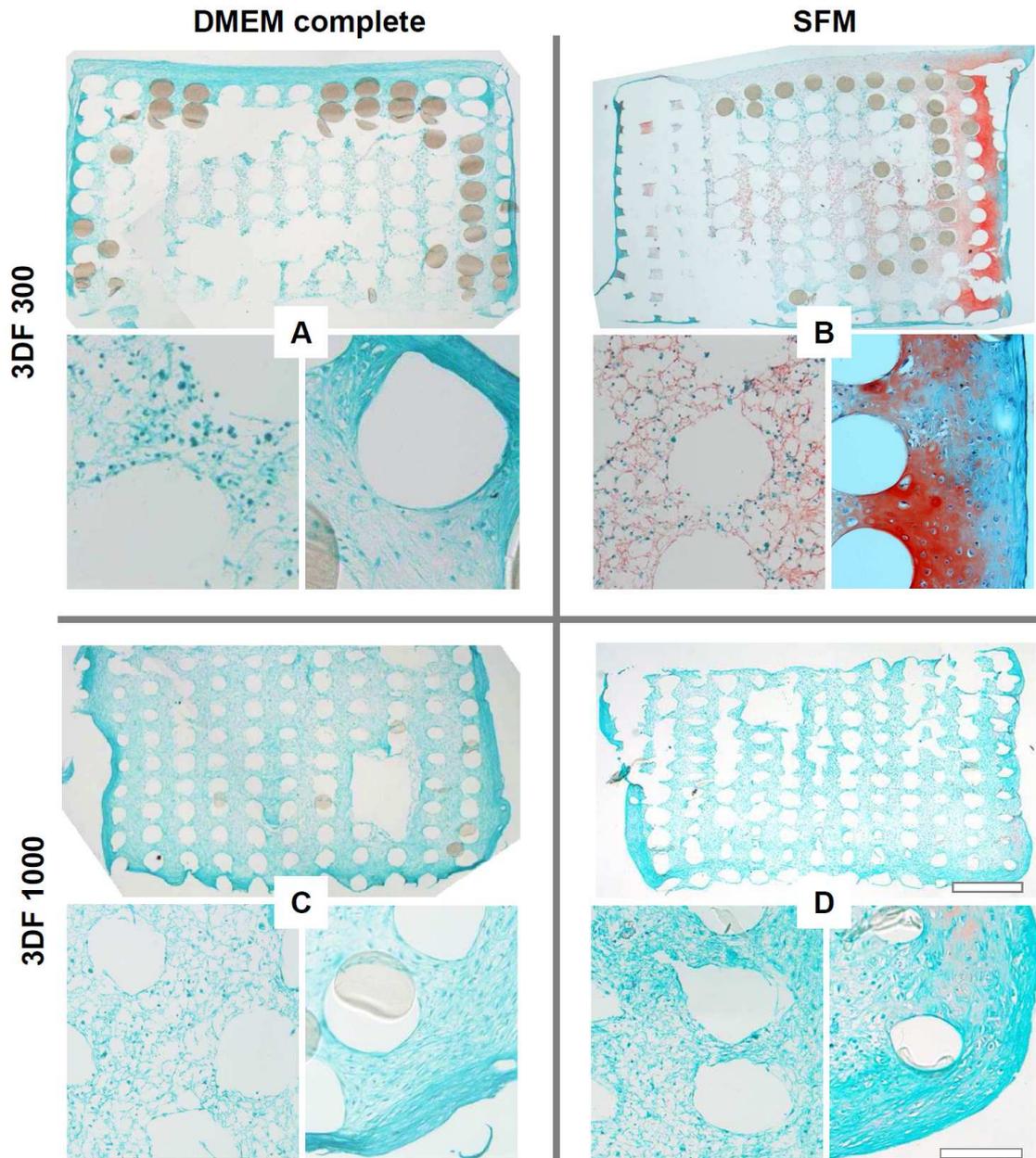


Fig. 6 Light microscopy images of Safranin O stained (red: glycosaminoglycans, GAG), representative histological cross-sections. MSC cultured on PolyActive® for four weeks in either serum containing (DMEM complete: A, C) or serum free (SFMCh: B, D) medium supplemented with chondrogenic factors including 10 ng/ml TGF. Polyactive® architecture was 3D fiber deposited (3DF) with a composition of 300 PEG 55:45 (300; A&B) and 1000 PEG 70:30 (1000; C, D). Small panels (left: core region, right: periphery) show higher power magnifications of corresponding overview panel. Structural integrity of the scaffold (round, brown structures) was better maintained for the 300 compared to the 1000 composition. Scaffold loss was an inevitable artefact introduced during the mounting of histological sections (low adhesion and swelling inherent to the 1000 composition). Fibrin glue improved tissue integrity and allowed for preparing entire histological cross-sections. In all conditions, MSC were able to deposit matrix, which in presence of serum was predominantly fibrotic and showed no GAG deposition (A&C). All constructs

were encapsulated by several layers of cells with flattened morphology. This capsule was denser/thicker where serum was present and thinnest for the 300 composition in absence of serum. Some core regions seem to have become necrotic as they contain a dense aggregation of nuclei (lower left panels in A & B; blue dots). In absence of serum, GAG staining was faint on the 1000, clearly stronger on the 300 and for both compositions most intense just beneath the construct periphery. On the 300, the staining additionally reached into the core regions of the construct. Scale bars: 800 μm (large panels), 200 μm (small panels).

Quantitative, biochemical analysis of accumulated GAG (Fig. 7) matched with the histological findings. In presence of serum, GAG deposition remained marginal and was only slightly higher on the 300 (28%) than on the 1000 composition. Compared to DMEM complete, SFM allowed for increased GAG accumulation (300: 2.5x; 1000: 1.4x) and was 2.3x higher on the 300 than on the 1000 composition. Constructs with the 300 composition reached approximately 70% of the GAG/DNA level found in pellet controls (data not shown).

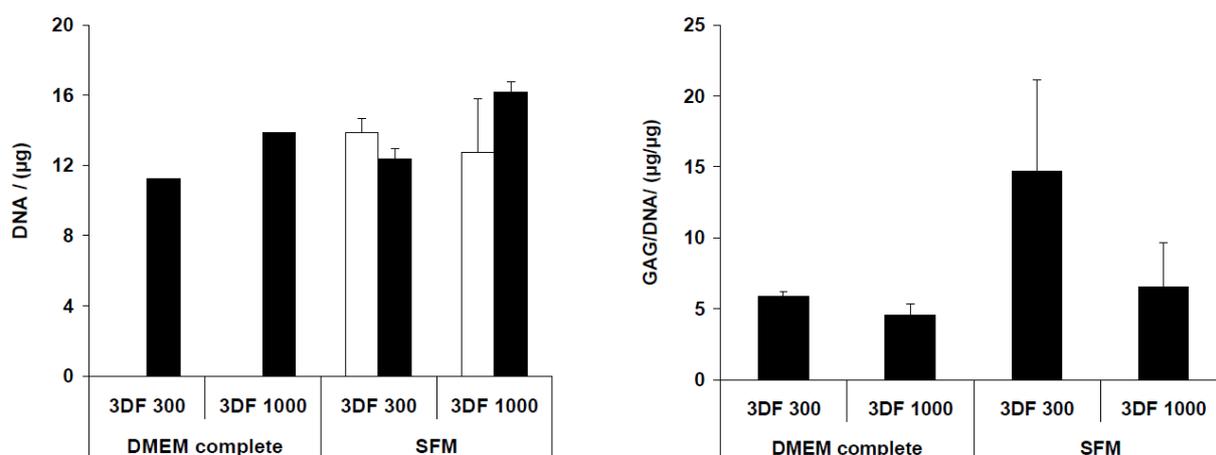


Fig. 7 MSC retention and glycosaminoglycan (GAG) accumulation over 4 weeks of culture on Polyactive® scaffolds in presence of (DMEM complete) or without serum (SFM). Panel A displays the initial amount of DNA (white bars). Measurements were only done for constructs in SFM, as they are not thought to be affected by medium composition in short term (24 hours). Black bars show the amount of DNA found after four weeks of culture. All conditions maintained their initial DNA levels or even permitted for an moderate increase (<27%) throughout the culture period. The average increase was higher in SFM than in presence of serum. Panel B shows the amount of accumulated GAG (normalized vs. the amount of DNA at the end of culture) as determined biochemically. In presence of serum, GAG deposition remained marginal and was only slightly higher on the 300 (28%) than on the 1000 composition. In contrast to DMEM complete however, SFM allowed for increased GAG accumulation (300: 2.5x; 1000: 1.4x) which was 2.3x higher on the 300 than on the 1000 composition. Error bars represent the standard deviation.

Discussion

Using two contrastingly different compositions, scaffolds made of PolyActive® did not support chondrogenesis in MSC if serum was present in the chondrogenic medium. In absence of serum however, chondrogenesis could be observed and tended to be better supported by the more hydrophobic 300 composition. This finding indicates, that controlling scaffold composition can be employed to support chondrogenesis in MSC, but strongly depends on additional soluble instructive/inductive stimuli like i.e. TGF.

For both substrate compositions, fibrin glue modified seeding allowed for quantitative seeding efficiency and cell retention, while changing to a serum free chondrogenic medium allowed for improved MSC chondrogenesis.

An adverse effect of serum on MSC chondrogenesis was evident in both pellets (Fig. 5C) as well as in constructs (Fig. 6). This observation is in line with previous findings in which serum has been found to suppress TGF induced chondrogenesis in synoviocyte pellet culture (166). Although, constructs were cultured in serum free medium, prior to cell seeding substrates were soaked in serum containing medium. This should have allowed for composition inherent, differential serum protein adsorption which has formerly been argued to be the key to the differential support of chondrogenic differentiation on Polyactive® substrates of contrasting chemical composition (113). Fibrin glue (FG) could potentially mask this proteinaceous interface and thus was applied at a diluted concentration. However, under comparable culture conditions as applied in this study, chondrocytes were capable to degrade even higher concentrated FG after two to three days (167). Similar behaviour may be expected from MSC due to their ability to secrete fibrinolytic enzymes which facilitate the degradation of fibrin clots (168). Thus, although FG may have delayed MSC/substrate-interface interaction it unlikely has been able to ultimately mask it. This view also finds support by the fact that although FG was present in this study, the trends for the substrate composition observed in study 1 could be reproduced.

CONCLUSION STUDY I & II

Taken together, in both studies substrate composition & architecture was found to modulate the chondrogenic differentiation of MSC. That the di block copolymer model substrate (Polyactive®) with a more hydrophobic composition better supported MSC chondrogenesis, is likely associated with differential protein adsorption (from serum containing medium). However such proteinaceous interfaces are rather complex with regard to protein composition and conformation thereon. This conceals the specific cues responsible for mediating the observed effects and thus strongly prompts for reducing the substrate interface complexity in subsequent investigations of chondroprogenitor cell-substrate interactions.

Chapter II

RGD-PEPTIDE RESTRICTED
INTERACTIONS WITH A
PROTEIN RESISTANT
SUBSTRATE ARE SUFFICIENT
FOR HUMAN ARTICULAR
CHONDROCYTE ADHESION,
GROWTH & MAINTENANCE OF
CARTILAGE
FORMING CAPACITY

ABSTRACT

This study aimed at testing whether an RGD-restricted substrate interface is sufficient for adhesion and growth of human articular chondrocytes (HAC), and whether it enhances their post expansion chondrogenic capacity. HAC/substrate interaction was restricted to RGD by modifying tissue culture treated polystyrene (TCPS) with a poly-(ethylene glycol) (*PEG*) based copolymer system that renders the surface resistant to protein adsorption while at the same time presenting the bioactive RGD-containing peptide GCRGYGRGDSPPG (*RGD*). As compared to TCPS, HAC cultured on *RGD* spread faster, better maintained their chondrogenic phenotype and had a lower spreading area. Attachment and proliferation, as well as type II collagen mRNA expression in the subsequent chondrogenic differentiation phase, were similar to those of HAC cultured on TCPS. In contrast, cartilaginous matrix deposition by HAC expanded on *RGD* was slightly but consistently higher. *RDG* (bioinactive peptide) and *PEG* (no peptide ligand) controls yielded drastically reduced attachment and proliferation, thus indicating specificity of *RGD*. The restriction of cell-substrate interactions to RGD could be implemented in materials for cartilage repair, whereby *in situ* recruited/infiltrated chondroprogenitor cells would proliferate while maintaining their ability to differentiate and generate new cartilage tissue.

INTRODUCTION

Human articular chondrocytes (HAC) have received great attention in the context of cell-based repair of cartilage, which *per se* has a very limited regeneration capacity (148). One of the current therapies to overcome this limitation is to restore the damage by autologous chondrocyte implantation (ACI) (169). In this procedure, HAC are enzymatically extracted from a small articular cartilage biopsy and subsequently expanded *in vitro* to obtain a sufficient number of cells for implantation. During expansion, HAC de-differentiate and their redifferentiation capacity is often limited (95;96). De-differentiation of chondrocytes manifests by cell morphological transition from round to fibroblast-like, the loss of large proteoglycans (e.g. aggrecan) and type II collagen production (97;98), and the switch to synthesis of type I collagen, fibronectin (FN), and small noncartilaginous proteoglycans (98;99). This raises the problem, that subsequent to monolayer culture the de-differentiated chondrocytes have the propensity to produce fibrocartilaginous tissue which is of inferior mechanical quality as compared to hyaline cartilage.

Tissue culture treated polystyrene (TCPS; gas plasma activated polystyrene) currently is the gold standard substrate for HAC monolayer expansion. It readily adsorbs proteins that are present in serum containing culture medium, which rapidly leads to the formation of a proteinaceous adlayer, determining the subsequent cell-surface interaction (170). The nature of such interfaces is highly complex with regard to composition and conformation of the adsorbed proteins (171). Since the biology of chondrocytes is highly influenced by interactions with specific extracellular matrix (ECM) molecules (172;173), controlled modification of cell culture substrates with biological motives has the potential to improve HAC expansion strategies.

A typical approach to investigate substrate effects on chondrocyte phenotype has been to coat TCPS with specific ECM-protein solutions. As compared to on plastic substrates, chicken epiphyseal chondrocytes longer retained their native morphology on type II collagen coatings (129), and rabbit articular chondrocytes better preserved their phenotype on type I collagen (128). In contrast, however, other studies showed that the expression of type I and II collagen by chondrocytes was not altered in response to substrates coated with either type I or II collagen or fibronectin (174;175). The controversial results could at least partially be due to the fact that simple application of natural protein layers lacks control over the presentation of active ligands to the cells (176). In fact, protein adsorption is generally governed by electrostatic interactions, van der Waals forces and short range repulsion forces and occurs randomly in various different orientations of the protein (177). Also, it has been demonstrated on a variety of surfaces including TCPS, that adsorption can induce conformational changes in several different proteins as for example in collagen and results in alteration of the native protein biological activity (for review see (178)). The uncertainties introduced by working with natural protein layers has driven the development and synthesis of materials which provide full control over the ligand-receptor interactions (179), not only for optimizing cell culture labware but also for the development of smart materials in regenerative medicine.

The peptide sequence RGD is present in several ECM-proteins like fibronectin, collagens and vitronectin and not only serves as the minimal requirement for integrin-mediated cell anchoring (180), but also provides signals which can modulate chondrocyte morphology, motility, proliferation and differentiation. Mice with a cartilage specific deletion of beta 1 integrins have abnormally shaped chondrocytes, that fail to arrange into columns within the growth plate and show a decreased proliferation rate (181). In the developing mouse

zegopod, it was even shown, that blocking $\alpha 5\beta 1$ integrin interaction with RGD from the ECM inhibits pre-hypertrophic chondrocyte differentiation and eventually leads to apoptosis (182). Although a great variety of materials has been modified with RGD, their *in vitro* biological effect has largely been tested on animal cell lines and often restricted to cell attachment, morphology and proliferation, mostly leaving unaddressed the impact on the cell phenotype and on the cell differentiation capacity (for review see (141)). No study has yet assessed primary human articular chondrocyte expansion on a fully controlled, RGD-restricted substrate.

In this work, we tested whether an RGD-restricted substrate interface is sufficient to allow for HAC adhesion, growth and maintenance of the chondrogenic capacity. In particular, HAC attachment, spreading kinetics, morphology, proliferation, gene expression and post-expansion cartilage formation were assessed on a poly-(ethylene glycol) (*PEG*) based copolymer system that renders the surface resistant to protein adsorption while at the same time presenting the bioactive, RGD-containing peptide GCRGYGRGDSPG (*RGD*) (183-185). HAC culture on *RGD* was compared to that on tissue culture treated polystyrene (TCPS, standard substrate) and on control *PEG* substrates, without or with the scrambled sequence *RDG*.

METHODS

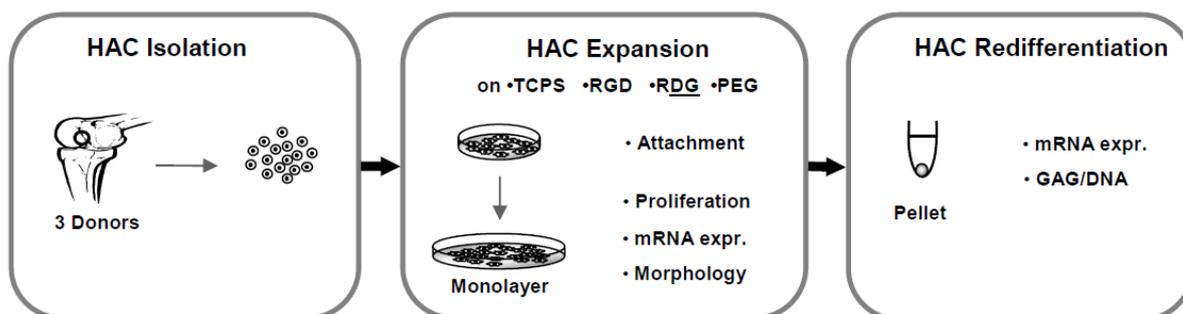


Fig. 1: Schematic view of the experimental design. Subsequent to isolation from three different donors (age 53-66years), human articular chondrocytes (HAC) were expanded either on RGD-functionalized PLL-g-PEG (RGD) or the standard substrate, tissue culture treated polystyrene (TCPS). The scrambled sequence RDG-functionalized PLL-g-PEG (RDG) and PLL-g-PEG served as negative controls. Subsequent to expansion, HAC were re-differentiated in pellet culture in presence of serum free chondrogenic medium.

Polymer Synthesis and Characterization

Peptide-functionalized and non-functionalized PLL-g-PEG polymers were synthesized and characterized as previously published (139;186). In brief, these polymers are based on a PLL backbone of approximately 120 L-lysine units (average value in view of the polydispersity of 1.4 of the polymer; Sigma-Aldrich, Buchs, CH), a PEG side chain of approximately 47 ethylene glycol units (PEG MW 2 kDa, polydispersity: 1.02; Nektar, Bradford, UK) and a grafting ratio (g) between 3.3 and 4.6, expressed as the number of lysine monomers per PEG side chain. A vinyl sulfone-modified PEG chain of 3.4 kDa molecular weight (polydispersity: 1.01; Nektar, Bradford, UK) was used to couple the peptide sequences with the PLL backbone. The following peptides were used for the

synthesis of functionalized PLL-*g*-PEG polymers: the bioactive RGD-containing N-acetyl-GCRGYGRGDSPG-amide and the scrambled (bio-inactive) N-acetyl-GCRGYGRRDGSPG-amide (both purchased from Jerini, Berlin, GER). Polymer architectures (grafting ratios and fractions of peptide-functionalization) were determined with nuclear magnetic resonance spectroscopy (NMR) whereas adsorbed polymer and serum masses were measured using optical waveguide lightmode spectroscopy (OWLS) (see Table 1 for details). All polymers used were proven to be highly resistant to non-specific serum adsorption (<5 ng/cm²).

Tab 1. Molecular weight, grafting ratio, peptide functionalization, polymer/protein adsorption and peptide surface density for all polymers used in this paper. ^aMeasured with NMR technique, ^bmeasured with OWLS technique. ^cSee Schuler, *et al.* 2006 (186) for details.

	<i>PEG</i>	<i>RGD</i>	<i>RDG</i>
Molecular weight PLL [kDa]	15.9	15.9	15.9
Molecular weight lysine unit [kDa]	0.128	0.128	0.128
Molecular weight peptide [kDa]	-	1.222	1.222
Molecular weight entire polymer [kDa]	91.1	52.8	56.8
Grafting ratio <i>g</i> [-] ^a	3.3	7.0	6.4
Peptide-functionalized PEG-chains [%] ^a	-	3.4	3.7
Polymer adsorption [ng/cm ²] ^b	150	143	135
Protein adsorption [ng/cm ²] ^b	< 5	< 5	< 5
Peptide surface density ρ_{ps} [pmol/cm ²] ^c	-	1.6	1.7

Surface Modification for Cell Culture

For modifying the surface of tissue culture treated polystyrene (TCPS; atmospheric gas plasma treated polystyrene), frozen samples of dehydrated PLL-*g*-PEG polymer powders were warmed up to room temperature, dissolved in a salt buffer solution (denoted hereafter as HEPES2) containing 10 mM HEPES and 150 mM NaCl at pH 7.4 (to reach a final concentration of 0.5 mg/ml) and filter sterilized (0.22 µm filter, Milian, Basel, CH). TCPS dishes/flasks (TPP, Tarasdingen, Switzerland) and Thermanox[®] lamellae (Nunc, USA, for CLSM, activated with a UVO-Cleaner (Model 42-220, Jetlight Company, USA)) were coated at room temperature for 45 min. with 100 µl/cm² of the above described polymer solutions while stirring on an orbital shaker. Supernatant polymer solution was aspirated and surfaces were washed twice with 200 µl/cm² HEPES2 buffer solution for 5 min. For convenience, PEGylated surfaces will be named hereafter according to their peptide sequences (PLL-*g*-PEG/PEG-RGD as *RGD* and PLL-*g*-PEG/PEG-RDG as *RDG*) whereas the non-functionalized PLL-*g*-PEG surface will be denoted as *PEG*.

Cell isolation and Expansion

Full thickness human articular cartilage samples were collected within 24 hours *post mortem* from the femoral lateral condyle of three different donors (age in years; A:53, B:62, C:66), with no history of joint disease, after obtained informed consent, following protocol approval by the local ethical committee (No. 78/07) (Fig. 1, HAC Isolation). HAC were isolated upon 22-hour incubation at 37 °C in 0.15% type II collagenase and resuspended with Dulbecco's modified Eagle's medium (DMEM) containing 4.5 mg/ml

D-glucose, 0.1 mM non-essential amino acids, 1 mM sodium pyruvate, 10 mM HEPES buffer, 100 U/ml penicillin, 100 µg/ml streptomycin, and 0.29 mg/ml L-glutamine, supplemented with 10% FBS (all from Gibco, UK) (DMEM complete). For the first expansion phase, HAC from each donor were seeded onto either TCPS, *RGD*, *RDG* or *PEG* substrates at a concentration of 10^4 cells/cm². HAC were cultured in CM supplemented with 1 ng/ml TGF-β1, 5 ng/ml FGF-2, 10 ng/ml PDGF-BB (expansion medium, all from R&D, UK) in a humidified 37°C/5% CO₂ incubator. These specific growth factors have previously been shown to enhance HAC proliferation and post-expansion redifferentiation capacity (Fig. 1, HAC Expansion) (102). HAC were detached at confluency (passage 1) by a treatment with 0.3% type II collagenase, followed by 0.05% trypsin/0.52 mM EDTA (Gibco, UK), re-plated on the corresponding surfaces at a density of 5×10^3 cells/cm² for the second expansion step, and cultured in expansion medium until they reached confluency again (passage 2).

Cell Attachment & Proliferation

To determine cell attachment 24 hours after inoculation (Fig. 1, HAC Expansion), supernatants containing non-adherent cells were collected, counted in a Neumann chamber and their viability was assessed using Trypan blue (Sigma Chemical, USA). The non-adherent HAC from *RDG* and *PEG* were returned to the corresponding dishes at each medium change. Cell proliferation rate was calculated as the ratio of $\log_2(N/N_0)$ to T, where N₀ and N are the numbers of cells respectively at the beginning and the end of the expansion phase, and T is the time required for the expansion (102).

Cell Morphology

HAC after the second confluency on TCPS or *RGD* were detached, reseeded onto a correspondingly coated lamellae at a density of 5×10^3 cells/cm² and cultured in expansion medium in a humidified 37°C/5% CO₂ incubator for three days. The lamellae were then rinsed with PBS (Gibco, UK). Rinsed HAC were fixed with 1% glutaraldehyde in PBS for 30 min. at room temperature. Substrates were rinsed with PBS before permeabilizing and further fixing with 2 % Octyl-polyethylene (Octyl-POE) and 0.125% glutaraldehyde for 5 min. Following a PBS wash, residual glutaraldehyde was reduced with a solution of 0.5 g/ml NaBH₄ in PBS at 0°C for 20 min. After washing with PBS again, HAC were labeled with TRITC-phalloidin 1:900 ($\lambda_{\text{Ex}}=488$ nm, Sigma Chemicals, USA) against actin filaments and DRAQ5 1:200 ($\lambda_{\text{Ex}}=647$ nm, Alexis Biochemicals) to label DNA in the nuclei (all dilutions in PBS). Finally, the lamella were mounted onto a glass slide using mowiol-1188 (Hoechst, Frankfurt, Germany) containing 0.75 % of the anti-fading agent N-propyl-gallate (Sigma Chemicals, USA) and stored at 4°C in the dark. Fluorescence images were acquired with a Leica TCS SP CLSM, using a 63x HC PL APO immersion objective. The number of stacks was fixed to 20, while each stack (1024x1024 pixel²) was scanned at medium speed and averaged four times.

To describe the HAC morphology and the degree of spreading, a cell shape factor ϕ (Eq. 1) was used (186;187).

$$\phi = \frac{4 \pi A}{p^2} \quad (1)$$

The area A and the perimeter p required for calculating the shape factor ϕ were determined from the CLSM images using Image J version 1.37 (188). A shape factor for a round cell can assume values near to one. Circles have the greatest area-to perimeter ratio

and their shape factor ϕ is 1, whereas a thin, thread-like object would have a shape factor ϕ near 0.

Initial Cell Spreading, Kinetic & Motility

Time lapse microscopy experiments were performed on an Olympus IX81 motorized, inverted microscope in phase contrast mode, using a 10x LCPFL objective combined with a 1.6x magnifying lens (to investigate initial spreading) or an UplanApo 4x objective (to investigate motility). The microscopes were equipped with a high resolution position controller to drive the motorized stage. HAC were seeded onto either TCPS or *RGD* in expansion medium at a density of 10^4 cells/cm² (for studies on initial spreading) or 7.5×10^3 cells/cm² (for studies on motility) and kept in a box at 37°C / 5% CO₂. The initial spreading kinetic of HAC was followed for 18 min. Starting 5 min. *post* seeding, every two min. an image was acquired from 15 randomly selected areas of each substrate. Using Image J, the spreading kinetic of 28 cells, which were at the onset of spreading, was determined on each surface based on the spreading area.

Chondrogenic Assay

The chondrogenic capacity of HAC expanded on either TCPS or *RGD* was investigated in pellet culture (Fig. 1, HAC Redifferentiation) using a chemically defined, serum-free medium (SFM), which consists of DMEM containing 4.5 mg/ml D-glucose, 0.1 mM non-essential amino acids, 1 mM sodium pyruvate, 10 mM HEPES buffer, 100 U/ml penicillin, 100 µg/ml streptomycin, and 0.29 mg/ml L-glutamine (all Gibco, UK) supplemented with ITS⁺¹ (10 µg/ml insulin, 5.5 mg/ml transferrin, 5 ng/ml selenium, 0.5

mg/ml bovine serum albumin, 4.7 mg/ml linoleic acid), 1.25 mg/ml human serum albumin, 0.1 mM ascorbic acid 2-phosphate and 10^{-7} M dexamethasone (all Sigma Chemical, USA) and 10 ng/ml TGF- β 1 (R&D, UK) (chondrogenic medium) (100;189). Aliquots of 5×10^5 HAC/0.5ml were centrifuged at 250 g for 5 min. in 1.5 ml polypropylene conical tubes (Saarstedt, Nümbrecht, Germany) to form spherical pellets, which were placed onto a 3D orbital shaker (Bioblock Scientific, Frenkenkdorf, Switzerland) at 30 rpm. Pellets were cultured for 2 weeks at 37°C / 5% CO₂, with medium changes twice per week, and subsequently processed for histological, immunohistochemical, biochemical and mRNA analysis.

Gene Expression Analysis

RNA was extracted from tissue constructs using 250 μ l Trizol (Life Technologies, Basel, CH) according to the manufacturer's instructions. Extracted RNA was treated with DNase following the instructions of the Rneasy Kit (Ambion, Austin TX). cDNA was generated from total RNA using reverse-transcriptase Stratascript (Stratagene) in the presence of dNTP and DTT. Real-time PCR reactions were performed and monitored using the ABI prism 7700 Sequence Detection System and the Sequence Detector V program (Perkin-Elmer Applied Biosystems). cDNA samples were analyzed for type I, II, X collagen and for the housekeeping gene (18S ribosomal RNA), using previously described sequences of primers and probes (100). Each cDNA sample was assessed in duplicate and the collagen mRNA expression levels were normalized to the corresponding 18S rRNA levels.

Biochemical Analysis

HAC pellets cultured in chondrogenic medium for two weeks were digested with protease K (0.5 ml of 1 mg/ml protease K in 50 mM Tris with 1 mM EDTA, 1 mM iodoacetamide, and 10 µg/ml pepstatin-A) for 15 hours at 56°C (157). The GAG content was measured spectrophotometrically using dimethylmethylene blue (158), with chondroitin sulfate as a standard, and normalized to the DNA amount, measured spectrofluorometrically using the CyQUANT Kit (Molecular Probes, Eugene, OR), with calf thymus DNA as a standard. GAG contents are reported as µg GAG / µg DNA.

Histological and Immunohistochemical Analysis

Cell pellets cultured in chondrogenic medium were fixed in 4% formalin for 24 h, embedded in paraffin, cross-sectioned (5 µm thick), and stained with Safranin O for sulphated glycosaminoglycan (GAG) (100). Sections were also processed for immunohistochemistry to visualize type II collagen (II-II6B3, Hybridoma Bank, University of Iowa, USA), as previously described (159).

Statistical Analysis

Statistical evaluation was performed using SPSS software (version 15.0, SPSS Schweiz AG, Zürich, Schweiz). All mean values are presented as standard error (\pm SE). Differences between the surfaces TCPS, *RGD* and *PEG* were assessed using complying statistical tests as indicated at each result. The level of significance was set to $p < 0.05$.

RESULTS

Substrate Characterization

The *RGD* modified surface was determined to have a PLL-*g*-PEG/PEG-*RGD*-polymer concentration of 143 ng/cm² (see Table 1). This concentration was sufficient to render the surface resistant to protein adsorption (< 5ng/cm²) and implies that the bio-ligand *RGD* was presented at a density of 1.6 pmol/cm² (Table 1). Similar results were obtained for the control peptide *RDG*.

HAC attachment, Spreading Kinetics & Proliferation

Phase contrast microscopy observation revealed that, as early as 10 min. after seeding, adult human articular chondrocytes (HAC) on *RGD* started to spread, while on TCPS they still showed a more round morphology. This impression was validated by following the spreading kinetic of HAC every 2 min., starting 5 min. after seeding onto the corresponding surface (see Fig. 2). On *RGD*, the maximal spreading speed (88±6 μm²/min.) was 1.9-fold higher as compared to that on TCPS (46±4 μm²/min.; $p < 10^{-5}$; U-test Mann-Whitney, two tailed). Despite this initial difference, HAC attachment (24h after seeding) on *RGD* did not significantly differ from that on TCPS, while it was lower on *PEG* (4.7-fold) and *RDG* (5.6-fold) (Tukey HSD test: $p < 0.009$; see Fig. 3A). Phase

contrast images confirmed attachment of HAC on TCPS and *RGD* and indicated a spread, fibroblastic cell morphology (Fig. 4). In contrast, on *PEG* and *RDG*, HAC attached to a very limited extent, and predominantly remained in suspension as clusters. The proliferation rate of HAC on *RGD* did not differ from that measured on TCPS, while it was lower on the bio-inactive surfaces *PEG* (2.9-fold) and *RDG* (3.1-fold) ($p < 0.004$; Tukey HSD test; see Fig. 3B).

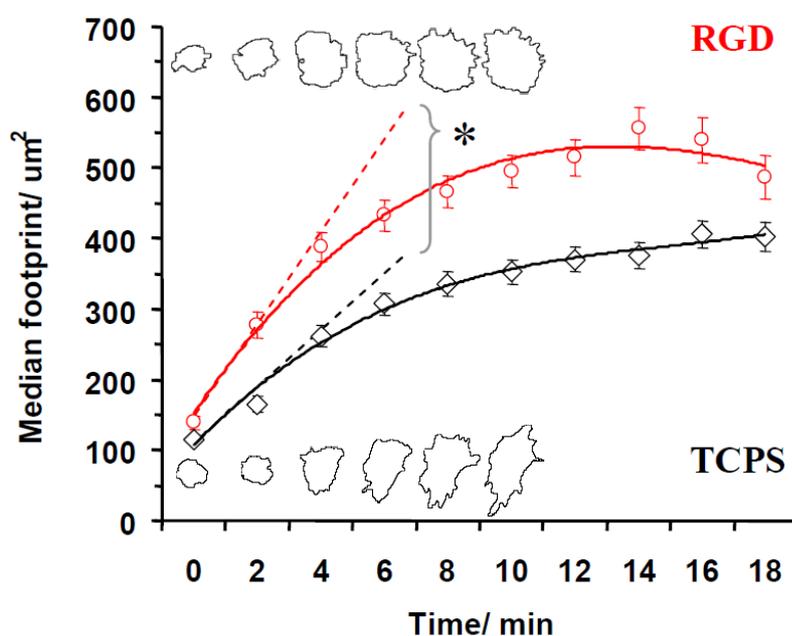


Fig. 2: Initial spreading of human articular chondrocytes (HAC) on tissue culture polystyrene (\diamond TCPS) and on RGD-functionalized PLL-g-PEG (\circ RGD). Immediately after seeding onto the corresponding surface, the spreading kinetic of HAC was followed by time lapse phase contrast microscopy every two min. during 18 min. Spreading was measured as footprint area ($n=28$ for each surface) and reported as median value in μm^2 . The dashed tangential lines indicate maximal the slope m_{max} which was significantly different on the two substrates (the asterisk indicates $p = 3.4 \times 10^{-5}$; U-test Mann-Whitney, two tailed). Cell outlines at each timepoint (up to min. 10) visualize an example HAC from each surface (**RGD**: upper row; **TCPS**: lower row) which matches with the indicated trend line (solid). Error bars represent the standard error.

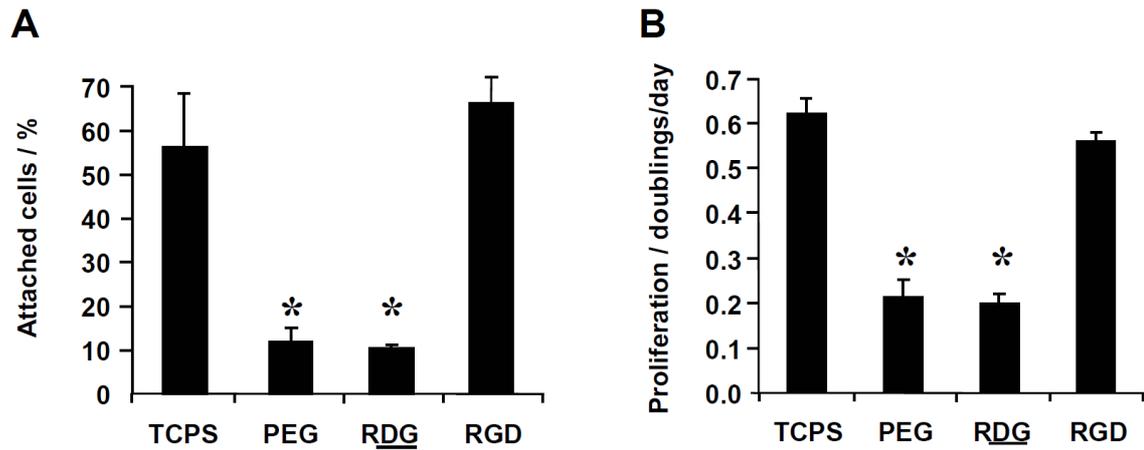


Fig. 3: Attachment and proliferation of adult human articular chondrocytes (HAC) on tissue culture polystyrene (TCPS), RGD-functionalized PLL-*g*-PEG (RGD) and non-functionalized PLL-*g*-PEG (PEG). RGD peptide surface density was 1.6 pmol/cm². **A** The number of attached cells was determined indirectly by counting the floating cells in the supernatant (alive and dead) and subtracting them from the number of inoculated cells. The attachment is expressed as percentage of the number of inoculated cells. **B** The proliferation rate of HAC is expressed as N doublings per day (during the two expansion steps). The asterisk indicates a significant difference vs. TCPS (n = 6 experimental replicates; p ≤ 0.009, Tukey HSD test).

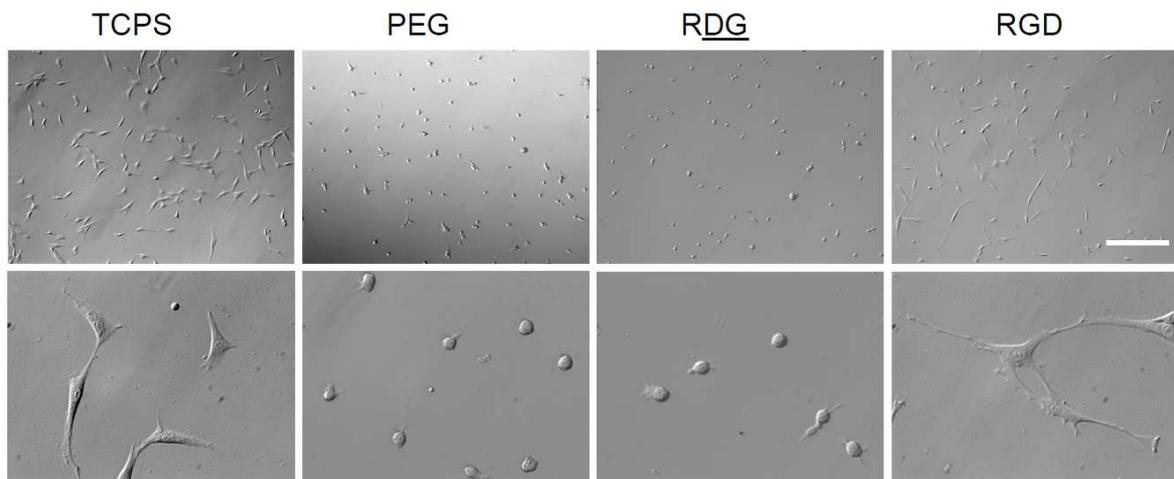


Fig. 4: Phase contrast images of adult human articular chondrocytes (HAC) during expansion on tissue culture polystyrene (TCPS), non-functionalized PLL-*g*-PEG (PEG), the scrambled sequence RDG-functionalized PLL-*g*-PEG (RDG) and the RGD-functionalized PLL-*g*-PEG (RGD). RGD and RDG peptide surface density was 1.6 and 1.7 pmol/cm² respectively. Scale bars correspond to 100 μm.

HAC Morphology & Motility During Cell Expansion

The average footprint area (see Fig. 5A) of HAC growing on TCPS was 19% higher than on *RGD* (Two-way Anova: $p = 0.014$), while the average perimeter of HAC on TCPS ($330 \pm 22 \mu\text{m}$) was consistently lower than on *RGD* ($424 \pm 27 \mu\text{m}$; Two-way Anova: $p < 10^{-7}$). As a consequence, the average shape factor ϕ_A on *RGD* (see Fig. 5A) was 2.0-fold lower (Two-way Anova: $p < 10^{-7}$) as compared to that of HAC expanded on TCPS. This morphological difference also became apparent by directly comparing the CLSM images (see Fig. 5 C&D). On both TCPS and *RGD*, a homogenous fluorescence signal could be seen throughout an entire HAC as actin appeared to be mostly organized into fine filamentous structures. Only rarely, thicker actin bundles, as they are typical for stress fibres, were evident. Regions of highest actin-signal intensities were located at the lamellipodia, as well as at the filopodia-like extensions. These extensions were the most distinctive morphological feature of HAC adherently growing on *RGD* as compared to TCPS.

Time-lapse phase contrast microscopy revealed that on *RGD* cell motility ($3.8 \pm 0.2 \text{nm/s}$, $n=230$) was approximately 20% lower than on TCPS ($4.7 \pm 0.2 \text{nm/s}$, $n = 209$; $p = 0.002$; Student's t-test, two tailed). The direction of HAC migration was judged by the distribution of centered cell trajectories and found to be isotropic on both *RGD* and TCPS (data not shown).

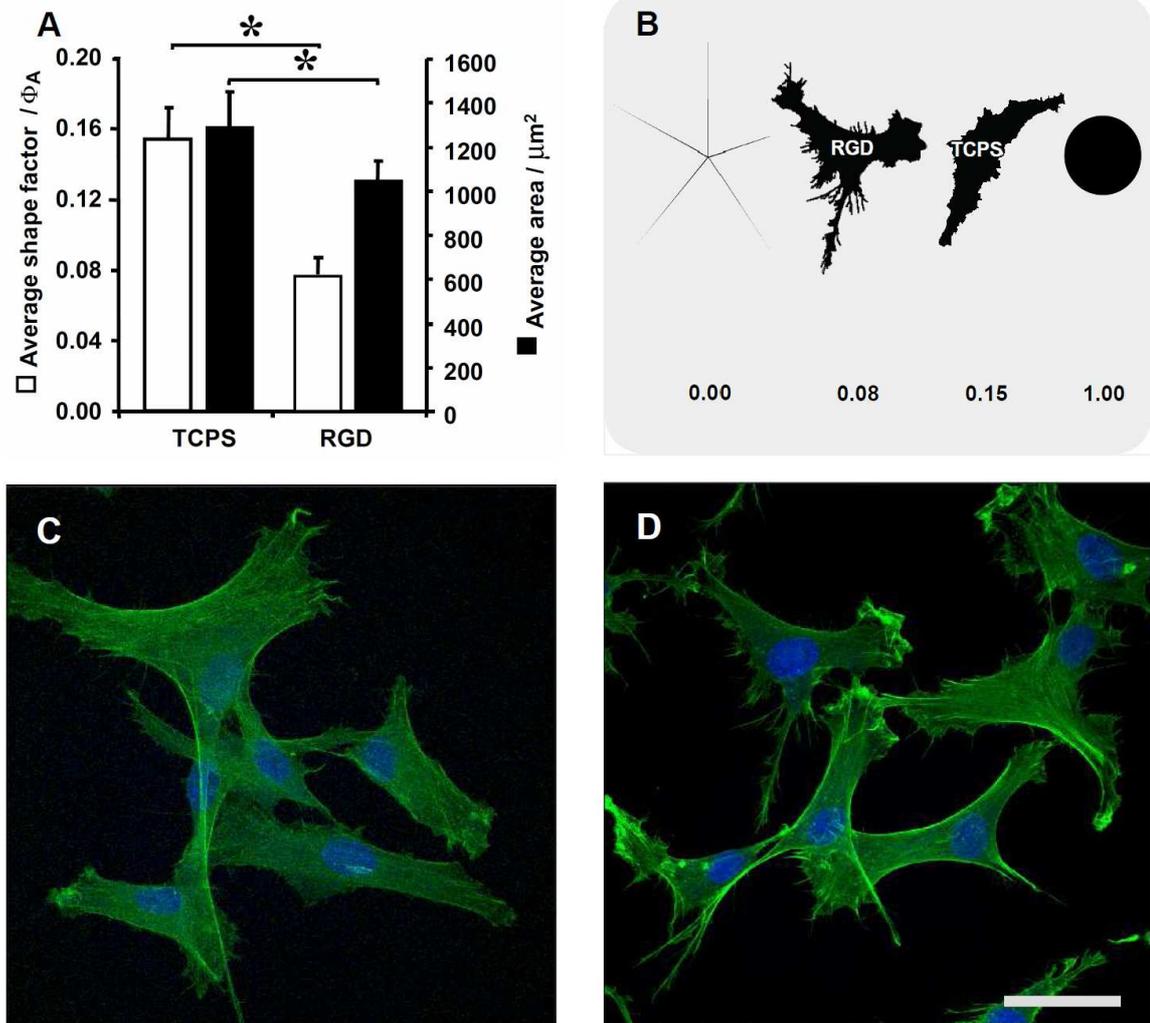


Fig. 5: Morphology of adult human articular chondrocytes (HAC) during expansion on tissue culture polystyrene (TCPS) and RGD-functionalized PLL-g-PEG (RGD). The graph in **A**) represents the average shape factor Φ_A (white bars) and the average footprint area in μm^2 (black bars) of HAC on the corresponding substrate. The asterisk indicates a significant difference ($n = 90$ per surface; $p < 0.0014$, two-way ANOVA). The cartoon in **B**) visualizes shape factor values which can range from zero for starfish-shaped cells to one for perfectly round shaped cells. Representative confocal laser scanning microscopy images of HAC on **C**) TCPS and **D**) RGD show actin stress fibres (green) and nuclei (blue). Note the filopodia-like structures, which appear more frequent on RGD. Scale bar corresponds to $20 \mu\text{m}$.

HAC De-Differentiation During Cell Expansion

During expansion in monolayer, type II collagen mRNA expression of HAC on *RGD* was 4.9-fold higher as compared to that on TCPS ($p < 0.04$; U-test Mann-Whitney, two tailed) while the level for type I collagen mRNA remained similar (see Fig. 6). Type X collagen was only upregulated in cells from Donor B (34-fold) and thus no significant difference was found on *RGD* vs. TCPS.

On *PEG*, type II collagen mRNA was up-regulated 46-fold ($p < 0.04$; U-test Mann-Whitney, two tailed). This up-regulation coincided with a 91-fold increase in type X collagen mRNA expression ($p < 0.03$; U-test Mann-Whitney, two tailed) while the expression level of type I collagen mRNA remained unaltered.

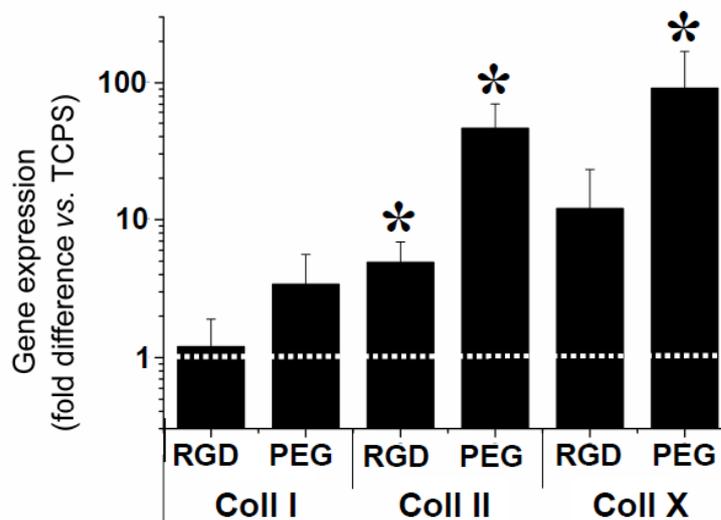


Fig. 6: Type I (Coll I), II (Coll II) and X (Coll X) collagen mRNA expression levels of adult human articular chondrocytes (HAC) during expansion on RGD-functionalized PLL-g-PEG (RGD) or non-functionalized PLL-g-PEG (PEG) normalized vs. tissue culture polystyrene (TCPS, indicated by white dashed line). RGD peptide surface density was 1.6 pmol/cm². Black bars represent m-RNA expression levels on of HAC after four weeks of culture on the corresponding substrate. Asterisks indicate a significant differences vs. TCPS (n = 6 experimental replicates; $p < 0.05$, U-test Mann-Whitney, two tailed).

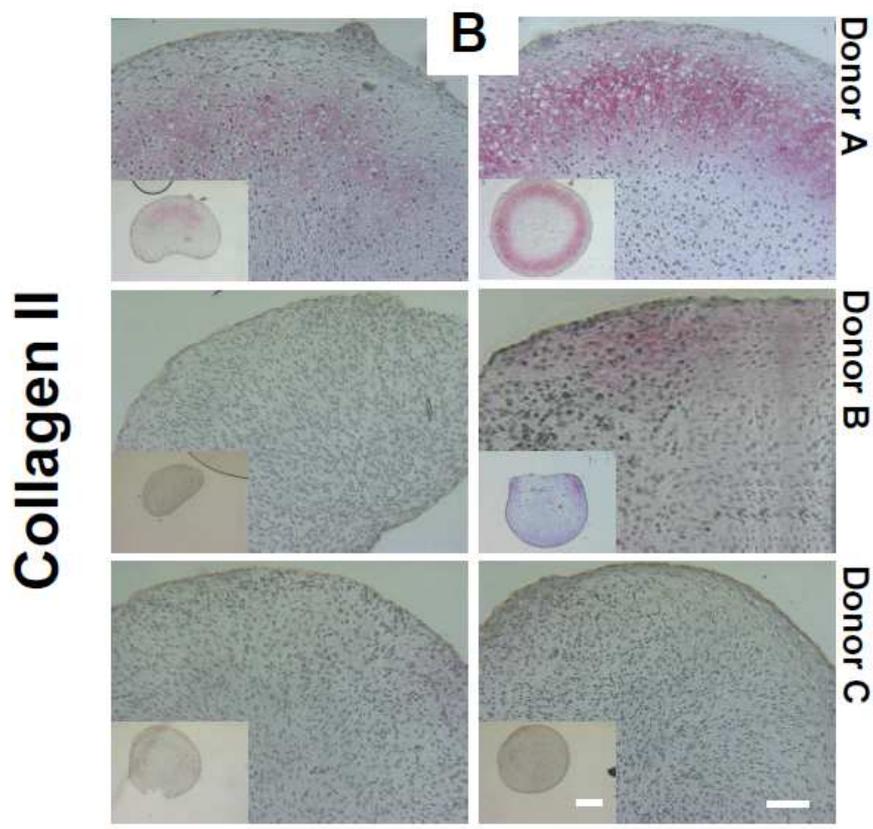
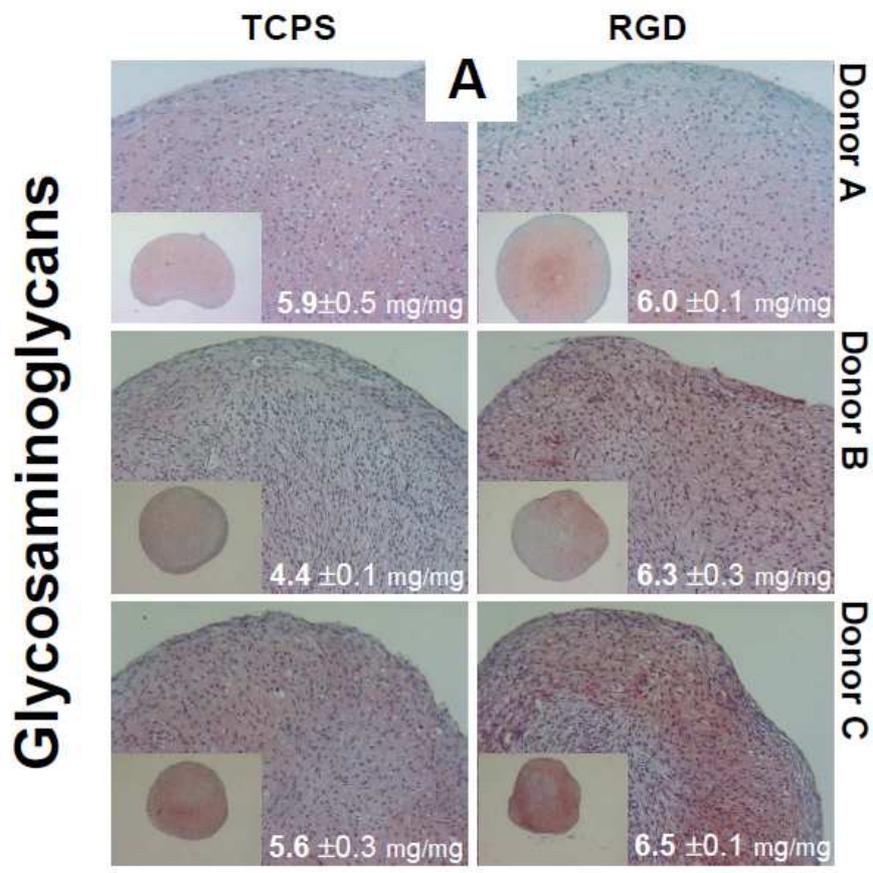
HAC Re-Differentiation in Pellet Culture

Pellets were generated with HAC expanded on TCPS or on *RGD* and cultured in chondrogenic medium for two weeks.

The up-regulation of type II collagen mRNA during the expansion of HAC on *RGD* was not maintained in the subsequent pellet culture. Only for type X collagen mRNA a statistically significant ($p < 0.004$; U-test Mann-Whitney, two tailed) but rather limited up-regulation (1.7-fold) was found.

HAC expanded on *RGD* generated pellets with 15% higher GAG content accumulation ($6.3 \pm 0.2 \mu\text{g}/\mu\text{g}$; $p = 0.1$, U-test Mann-Whitney, two tailed) than HAC expanded on TCPS ($5.3 \pm 0.5 \mu\text{g}/\mu\text{g}$). Additionally, sections of pellets from *RGD* expanded HAC stained slightly more intense for GAG (Safranin O staining) and type II collagen (Fig. 7).

Fig. 7 (following page) : Histology of pellets generated from adult human articular chondrocytes (HAC) which have been cultured for two passages on either tissue culture polystyrene (TCPS) or RGD-functionalized PLL-*g*-PEG (RGD). RGD peptide surface density was $1.6 \text{ pmol}/\text{cm}^2$. **A)** representative pellet sections stained red for glycosaminoglycans with Safranin O. The number at the lower right of each image shows the value for accumulated GAG/DNA in $\mu\text{g}/\mu\text{g}(\pm\text{SD}, n = 4)$. **B)** representative pellet sections immunohistochemically labelled red for collagen II. Representative sections are displayed for each donor and surface type. As an overview, the insets present entire pellet sections. Scale bars correspond to $50 \mu\text{m}$ for the pellet sections and $500 \mu\text{m}$ for insets.



DISCUSSION

In this *in vitro* study, we exploited the advantage of the PLL-*g*-PEG/PEG- RGD (*RGD*) model to restrict the interaction of human articular chondrocytes (HAC) with the culture substrate exclusively through the cell adhesion ligand RGD, even in the presence of serum. As compared to TCPS, *RGD* allowed for comparable attachment, proliferation and migration while supporting faster initial spreading but smaller final spreading area. The superior preservation of HAC chondrogenic phenotype in monolayer culture on *RGD* resulted in limited, yet consistent improvements in the post-expansion cartilage forming capacity in pellet cultures, although that was not reflected in the type II collagen gene expression.

The amount of serum proteins measured on the PLL-*g*-PEG modified substrates was very low and fell below the detection limit range reported for the optical waveguide lightmode spectroscopy technique. (190) This protein resistant effect can be attributed to the architecture of the PEG brush. (191) Indeed, on *PEG* and *RDG* (scrambled cell adhesion sequence), HAC attached to a very limited extent and mostly remained suspended in the culture medium as clusters. The fact that on these bio-inactive surfaces cell attachment was not completely abolished could be explained by small local defects in the PLL-*g*-PEG or PLL-*g*-PEG/PEG-*RDG*- layer, which likely permitted limited serum adsorption. These defects appeared to occur at a low frequency and merely allowed for cell anchoring but never for cell spreading. Only where PLL-*g*-PEG was modified with the cell adhesion ligand RGD, HAC attached and spread comparably to the way they do on TCPS. As *RDG* was not able to mediate the same effects, we assume that the effects observed in this study are specifically mediated by the bioligand RGD. Thus, the PLL-*g*-PEG/PEG-RGD culture

surface effectively allows for HAC/substrate interactions exclusively through RGD ligands, thereby circumventing the formation of a complex proteinaceous interface, even in presence of serum containing medium.

Early after seeding, HAC spreading always appeared more advanced on *RGD* than on TCPS. This observation was confirmed by measuring an almost two fold higher initial spreading rate on *RGD* as compared to that on TCPS. Since the spreading area was smaller on *RGD* than on TCPS, the higher spreading rate on *RGD* was likely not due to a higher cell adhesion ligand density, but rather to a sterically more direct mode of interaction of HAC integrins with the surface bound *RGD*. This is consistent with the fact that the RGD ligand is displayed in front of an otherwise inert environment (PEG brush border), as opposed to the various different orientations (177) of randomly adsorbed serum proteins, where ligands can remain encrypted (e.g., within the FnIII modules of folded fibronectin (192)). Although cells have the ability to access these cryptic domains by applying cytoskeletal tension, (193) this active remodeling process of the protein adlayer would require longer time. Whether the faster spreading on *RGD* is really due to a more direct mode of interaction, would however require further investigations, beyond the scope of this study.

HAC cultured on *RGD* and on TCPS attached and proliferated to an extent as previously reported for standard HAC culture (102;194). A drastically reduced attachment on the bio-inactive surfaces (*PEG* & *RDG*) coincided with a decreased proliferation rate, which is in line with findings for human dermal fibroblasts (186). Chondrocytes adhering to cartilage ECM-proteins highly express $\beta 1$ integrins and knocking out these integrins in a mouse model led to decreased chondrocyte proliferation due to impaired G1/S transition

and cytokinesis (181). RGD partially activates $\alpha 5 \beta 1$ (195;196) but primarily $\alpha v \beta 3$ integrin receptor (135) and thus seems likely to have stimulated proliferation through integrin activated signalling.

HAC cultured on *RGD* or TCPS assumed an elongated morphology (see Fig. 5), as confirmed by quantification of the shape factor (ϕ_A), which did not exceed the value of 0.2. The lower shape factor on *RGD* than on TCPS does not reflect further elongation but can be attributed to the protrusive extensions which mainly contributed to the increased perimeter. Such distinctive morphological features remind of filopodia which have been reported to occur at the leading edge of motile cells (197). However, HAC motility on TCPS was found to be in the same range as reported for rabbit chondrocytes (198), and lower on *RGD*, where filopodia-like structures were primarily observed.

Both the lower motility and the higher type II collagen mRNA expression of HAC expanded on *RGD*, as compared to TCPS, could be related to the reduced cell spreading area. In fact, cell spreading is associated with ROCK-mediated cytoskeletal tension (119) and is known to block chondrogenesis in mouse mesenchymal limb bud cells by inhibiting the expression of the transcription factor Sox9 (165). A reason for the reduced HAC spreading on *RGD* could be its lower bioactivity as compared to native ligands, where complementary or modulatory domains are present (135). In fact, FN, which readily adsorbs to TCPS (199), contains the synergistic binding site PHSRN on 9th type III repeat (FIII9) in addition to the RGD motif in the 10th type III repeat (FIII10). RGD is considered to be a poor FN mimic (135) as on its own it is not sufficient to fully activate $\alpha 5 \beta 1$ integrin but requires the synergy with PHSRN (111;200). Disturbing the

interdomain interaction of the FIII9-10 pair was reported to result in reduced spreading of baby hamster kidney cells and human endometrial stromal fibroblasts (137).

The better maintenance of HAC chondrogenic phenotype on *RGD* resulted in consistent but rather marginal improvements of chondrogenesis during pellet culture, as evidenced by the slightly higher accumulation of GAG/DNA, staining intensity for GAG and type II collagen expression in the formed tissues. It is possible that enzymatic disruption of HAC adhesion to *RGD* (for establishing pellet cultures) degraded important cell surface proteins (201) and partially reset the instructive signal to HAC. In this regard, future investigations should circumvent the need for such a harvesting step. As an example, HAC could be expanded on an RGD-ligand restricted scaffold that could be directly continued into differentiation culture. Still, the presentation of RGD might have to be transient (during expansion), since modifying alginate with an RGD-ligand was previously found to inhibit MSC chondrogenesis (136;202).

Beyond allowing control over the mode of cell interaction with a biomaterial interface, small ECM-fragments also offer to modify/tune the bioactivity of native proteins. The results of this study suggest that the limited bioactivity of *RGD* better supports the chondrogenic phenotype of proliferating HAC as compared to a complex proteinaceous adlayer containing native FN (TCPS). Thus, it would be intriguing to test whether tuning RGD-restricted HAC/substrate interactions could yield still higher type II collagen expression (as i.e. on *PEG*), while preserving its effect to promote proliferation (as i.e. on *RGD*). Approaches to tune HAC/RGD-restricted substrate interaction could involve changing the sequence of the peptide ligand (138), controlling its spatial array (112) or coupling it to substrates with different mechanical compliance than stiff TCPS (109).

CONCLUSION

In summary, forcing HAC-substrate interactions through *RGD* peptides not only mediated instantaneous cell attachment but also supported cell migration, proliferation and maintenance of the post-expansion cartilage forming capacity. Assisting these processes with inductive/instructive biomaterials may be essential for improving *in situ* cartilage regeneration, stimulated by microfracturing (152;203). In microfracturing, the subchondral bone plate is penetrated by small perforations which allow the recruitment/infiltration of mesenchymal stromal cells (MSC) from the bone marrow (204). MSC have the potential to chondrogenically differentiate (156), but due to their low numbers they first need to proliferate *in situ* in order to possibly improve the final outcome (152). Thus, an RGD-ligand restricted biomaterial interface could be a valuable tool to assist microfracture stimulated cartilage regeneration.

Chapter III

SUBSTRATE ELASTICITY
MODULATES
TGF BETA STIMULATED
RE-DIFFERENTIATION OF
EXPANDED HUMAN
ARTICULAR CHONDROCYTES

ABSTRACT

Culture of mesenchymal progenitor cells on substrates with different elasticity has been shown to modulate cell fate/commitment. We aimed this study at investigating, whether substrate elasticity modulates TGF β -3 (TGF) stimulated chondrogenic re-differentiation of expanded/de-differentiated human articular chondrocytes (HAC).

Expanded HAC from 4 donors (43-77 years) were seeded onto 2D substrates of different elasticity and induced to re-differentiate in a defined serum free medium containing or not TGF for 7 days. Type I collagen (CI) functionalized poly acrylamide (PA) films (100-150 thickness) with a Young's modulus of 0.26 ± 0.08 kPa (*soft*), 21.32 ± 0.79 kPa (*intermediately stiff*) and 74.88 ± 5.13 kPa (*stiff*) were employed. CI coated tissue culture treated plastic was considered as an *infinitely stiff* substrate and HAC aggregate cultures served as a standard re-differentiation control. HAC cultured on the corresponding substrate were assessed for attachment, proliferation, morphology, mRNA (type I & II collagen), and protein (type II collagen) expression.

Under re-differentiation conditions, HAC attached similarly on the different substrates and accomplished less than one total doubling within 7 days. On *intermediately stiff* to *infinitely stiff* substrates HAC assumed a fully spread fibroblastic morphology (shape factor $\phi_A = 0.23-0.27$), whereas on the *soft* substrate, they remained more spherical ($\phi_A = 0.35\pm 0.02$) and had a reduced spreading area (up to 3.2-fold). F-actin organization on the *soft* substrate was restricted cortically, while on the stiffer substrates, F-actin assembled into stress fibres.

Type II collagen mRNA expression on the *soft* substrate was similar to that in aggregate culture and 18.1-fold higher than on *infinitely stiff* substrates. However, in absence of TGF, type II collagen mRNA remained at levels expressed by expanded/de-differentiated HAC. Strikingly, type II collagen protein expression was only detectable on the *soft*

substrates. Substrate elasticity modulated the re-differentiation response of expanded/de-differentiated HAC to the chondrogenic stimulus TGF, and thus underscores mechanical compliance in combination with appropriate soluble signals to be an important parameter in designing biomaterials for cartilage repair.

INTRODUCTION

Current visions in cartilage repair aim at moving from fibrocartilaginous to a more hyaline like repair tissue by combining autologous cells of different origins (*in situ* recruited or *in vitro* pre-cultivated) with repair supporting biomaterials (151). Therein, the role of a chondro-supportive biomaterial within a cartilage defect is seen to enhance the onset of chondrogenic differentiation of the progenitor cells and to protect/modulate the newly formed tissue (152).

Apart from controlling ligand identity, density and presentation, which determine biomaterial/cell interaction(108), substrate elasticity has emerged as an important, insoluble, mechanical cue and has been shown to influence the phenotype of several members of the mesenchymal lineage, including fibroblasts (143;144), myoblasts (145;146) and osteoblasts (110). Moreover Mesenchymal stem cells (MSC) have been found to specify lineage and to commit to phenotypes with extreme sensitivity to tissue level elasticity. Soft substrates which mimic brain were neurogenic, stiffer substrates that mimic muscle were myogenic and comparatively stiffer substrates that mimic collagenous bone, proofed to be osteogenic. Moreover, the insoluble mechanical cue was shown to be additive to chemical/soluble induction of differentiation (109).

Chondrocytes are considered to have a primitive precursor termed “the mechanocyte” which suggests, that they have inherited the ability to respond to mechanical stimuli (205). Indeed, chondrocytes express several members of the integrin family which, apart from mediating adhesion, function as mechanoreceptors that transmit information from the extracellular matrix (ECM) into the cell, through the activation of cell signalling pathways(206). This integrin mediated perception of the ECM has been found to play a

crucial role in regulating chondrocyte morphology, motility, proliferation as well as differentiation (181;182).

Although depending on the type of cell, increased matrix stiffness generally leads to an increased protein phosphorylation, and stress fibre assembly (144;207). In line with this general rule, porcine chondrocytes flattened and spread on stiff substrates (100kPa) while they retained their typical round appearance on soft (4kPa), compliant matrices (208).

The importance of morphology on chondrocyte function started to be recognized around 30 years ago (209). Several findings reported the chondrocyte phenotype to be strongly depending on its cell shape, which changes from fibroblastoid to rounded/polygonal during cartilage development and is associated with a cortical actin filament organization, as well as the expression of extra cellular matrix proteins such as type II collagen and large proteoglycans (i.e. aggrecan) (210;211). Monolayer expansion of chondrocytes, isolated from adult cartilage, can revert this differentiation process and leads to de-differentiated chondrocytes which cease the production of large proteoglycans and type II collagen (97;98) and switch to the synthesis of type I collagen, fibronectin (FN), and small non-cartilaginous proteoglycans (98;99).

As a consequence considerable research efforts have focused on developing reliable procedures to maintain a round morphology in cultured chondrocytes. Conditions that support a round cell morphology and expression of the chondrocytic phenotype include culture in suspension (101;212), in agarose (96), in collagen gels (124), in alginate beads (213), and the disruption of the actin cytoskeleton by Cytochalasin D (214;215). Most recently, soft (4kPa) type I collagen coated polyacrylamide (PA) gels have also been demonstrated to induce a round morphology in porcine chondrocytes (208). However, in comparison to stiffer substrates, the better support of the chondrogenic phenotype by soft

PA gels was limited and paralleled by reduced proliferation. Proliferation is known to lead to rapid de-differentiation in chondrocytes (95) and thus, may have clouded the analysis of matrix elasticity as a direct influence on the maintenance of the chondrogenic phenotype.

The use of specific factors during monolayer expansion of HAC has been shown to accelerate the process of de-differentiation, and induces HAC to acquire a differentiation plasticity which is similar to that of mesenchymal progenitor stem cells (100). Culturing aggregates (suspension or pellet culture) of expanded/de-differentiated HAC in a medium containing the strong chondrogenic stimulus TGF β -3 (TGF), allows for re-induction of chondrogenic differentiation (101;102). Thus, expanded/de-differentiated HAC are not only of clinical relevance but, owing to their plasticity, also serve as a potent model to investigate processes involving fate commitment and the maintenance of mesenchymal progenitor cells.

Given the mechano-sensitivity of chondrocytes in general and the differentiation plasticity of expanded/de-differentiated HAC in specific, we hypothesized that matrix elasticity as an insoluble signal allows to control the morphology of expanded/de-differentiated HAC and thereby permits to modulate their re-differentiation stimulated by the soluble chondrogenic differentiation signal TGF.

Among different models for investigating the substrate elasticity influence on cell behaviour, polyacrylamide (PA) has emerged as an important tool since it can be easily adjusted in elasticity by varying the concentration of the monomer acrylamide (AA) and the crosslinker N,N'-methylenebisacrylamide (BIS). PA itself is almost completely inert

for cell adhesion, but can be functionalized by covalently grafting proteins to its surface (216). This offers the advantage to restrict cell/substrate interaction to a selected type of ligand. For the present study, type I collagen (CI) was chosen as it contains the cell adhesion peptide sequence Arg-Gly-Asp (RGD) (217), has been used to study the influence of matrix elasticity on the lineage specification of mesenchymal stem cells (109) and plays an important role during limb bud chondrogenesis (218).

To test our hypothesis, expanded/de-differentiated HAC were seeded onto 2D substrates of different elasticity and induced to re-differentiate in a defined serum free medium containing or not TGF β -3 for 7 days. CI functionalized PA films (100-150 μ m thickness) with a Young's modulus of 0.26 ± 0.08 kPa (soft), 212 ± 0.79 kPa (intermediately stiff) and 74.88 ± 5.13 kPa (stiff) were employed. CI coated tissue culture treated plastic was considered as an infinitely stiff substrate and HAC aggregate cultures served as a standard re-differentiation control. HAC cultured on the corresponding substrate were assessed for attachment, proliferation, morphology and expression of Sox-9 transcription factor, type I and II collagen mRNA and type II collagen protein.

METHODS

Substrate Preparation

Poly acrylamide (PA) gels of three different contrasting compositions, were cast onto 3-(trimethoxysilyl)-propyl methacrylate (Sigma-Aldrich, Buchs, CH) activated glass slides, and functionalized with type I collagen following a protocol adapted from Beningo *et al.* 2002 (219;220). Using coverglass (No. 1, Medite, CH) spacers, the gel thickness was set to a thickness ranging from 100 to 170 μm (confirmed by cryo SEM, data not shown). According to the time course measurements of the shear storage modulus G' , the polymerization was near complete 20 min. after initiation (see Fig. 1). Based on this finding, > 4 hours were considered to be safe for the polymerization to complete. Subsequently, the glass immobilized PA gels were washed with autoclaved MilliQ water followed by 50 mM HEPES pH 8.5 (Sigma-Aldrich, Buchs, CH). The PA gels were covered with 1 mM sulfo-SANPAH (heterobifunctional protein crosslinker, ProteoChem, USA) in 50 mM HEPES pH 8.5, UV activated (350 nm, 8 min., distance: 6 cm). This step was repeated once before thoroughly washing the substrates with PBS (Gibco, UK). Immediately after, the activated PA gels were functionalized with 0.2 mg/ml type I collagen (CI, rat tail, BD, UK) at 4°C over night. The density of surface-bound CI is independent of PA gel stiffness (221) and does not alter the elastic modulus of the substrate (145).

All substrates were UV light sterilized (30 min. at a sterile work bench). CI functionalized PA gels were washed and stored in PBS until further use.

Substrate Characterization by Rotational Rheometry

The polymerization time course (20 min, see Fig. 1) of three different mixtures consisting of acrylamide (AA, monomer) and N,N'-methylenebisacrylamide (BIS, crosslinker) was followed *in situ* in a rotational rheometer (Physica MCR 501, Anton Paar, Graz, Austria), fitted with a 50 mm diameter parallel plate (PP50). Shear storage modulus (G' , increases with the progressing degree of polymerization & crosslinking) measurements were conducted at room temperature (25°C), an oscillation frequency of 1 Hz and an amplitude of 1%. The volume for polymerization was 2 ml and initiated with 30 μ l of 10% ammonium persulfate (APS) and 30 μ l of 10% tetramethylethylenediamine (TEMED). The concentrations for AA_BIS were: 5%_0.003%, 10%_0.2%, 20%_0.3% as described above and the duplicates prepared independently. To prevent drying, polymerization was performed in a humidified atmosphere. All of the three distinct AA/BIS compositions displayed variable patterns during the lag phase in which G' was negligibly small (< 0.1 Pa). Following the lag phase, G' increased monotonically but ceased less than 5 min. after initiation of polymerization. After ~20 min. of polymerization, each of the three AA/BIS compositions reached its distinct plateau value (see Fig. 1 A). Degassing the AA/BIS solution prior to polymerization neither changed the polymerization pattern (G' time course), nor the final plateau levels for G' (data not shown).

To measure PA under conditions more representative of *in vitro* cell culture conditions, PA slabs of 4 mm thickness were polymerized for >4h and swelling equilibrated in PBS at room temperature > 24h. Shear storage and loss modulus (G' and G'') measurements were performed using the same rheometer settings as described above.

The elastic modulus describes the ability of a material to deform elastically (strain) when a force (stress) is applied to it, is quantified as a ratio of stress to strain and expressed in Pascals (Pa). Depending on the mode of measurement, the elastic modulus is commonly reported either as Young's modulus (E , uniaxial stress over the uniaxial strain, e.g. indentation) or shear storage modulus (G' , deformation of shape at constant volume, e.g. shearing), given the Hooke's law holds for the material described. Since PA hydrogels have a vanishingly low viscous component (shear loss modulus G'') (222) their elasticity can adequately be described by either E or G' . As a fact, the elastic component of PA (G') was always higher (6.9 to 161.4-fold) compared to its viscous component G'' . The shear storage modulus would be appropriate in the context of this work, since cells like i.e. fibroblasts are known to probe substrate mechanoproperties by shearing (223). However, the Young's modulus was preferred based on its wide spread use in the field of mechanobiology.

Tab.1: Rheology of polyacrylamide (PA) gels. The shear storage modulus (G') and the shear loss modulus (G'') of PA gels with three different acrylamide (AA, monomer)/N,N'-methylenebisacrylamide (BIS, crosslinker) compositions was measured by a rotational rheometer (Physica MCR 501, Anton Paar, Graz, Austria) fitted with a 50 mm diameter parallel plate (PP50). Measurements were conducted at an oscillation frequency of 1 Hz and an amplitude of 1% at 37°C in a humidified chamber. The PA gels were measured either 20 min. after initiation of polymerization directly in the rheometer ($n=2$) or after swelling equilibration (in PBS at room temperature over night, $n = 4$). The Young's modulus (E), which is widely spread to describe substrate elasticity, was computed from the dynamic modulus $G = G' + G''$ according to $E = 2G'(1+\nu)$. The Poisson ratio (ν) for PA is 0.464 (224) which is close to that of ideal rubber like materials (0.5). The values are reported as mean \pm standard deviation.

Composition	<i>In situ</i> polymerized			Swelling equilibrated		
	E (kPa)	G' (kPa)	G'' (Pa)	E (kPa)	G' (kPa)	G'' (Pa)
5/0.003	1.52 \pm 0.24	0.51 \pm 0.06	11.77 \pm 0.33	0.26 \pm 0.08	0.08 \pm 0.02	11.5 \pm 2.7
10/0.2	36.14 \pm 2.28	12.34 \pm 0.45	378.66 \pm 436.64	21.32 \pm 0.79	7.28 \pm 0.27	45.1 \pm 8.1
20/0.3	110.99 \pm 2.66	37.91 \pm 0.45	423.04 \pm 692.99	74.88 \pm 5.13	25.57 \pm 1.75	347.8 \pm 395.7

Cell Culture

Full thickness human articular cartilage samples were collected within 24 hours *post mortem* from the femoral lateral condyle of four donors (43 to 77 years), with no history of joint disease, after obtained informed consent, following protocol approval by the local ethical committee (No. 78/07). HAC were isolated upon 22-hour incubation at 37 °C in 0.15% type II collagenase and resuspended with Dulbecco's modified Eagle's medium (DMEM) containing 4.5 mg/ml D-glucose, 0.1 mM non-essential amino acids, 1 mM sodium pyruvate, 10 mM HEPES buffer, 100 U/ml penicillin, 100 µg/ml streptomycin, and 0.29 mg/ml L-glutamine, supplemented with 10% FBS (all from Gibco, UK) (complete medium, CM).

HAC were expanded in CM supplemented with 1 ng/ml TGF-β1, 5 ng/ml FGF-2, 10 ng/ml PDGF-BB (expansion medium, all from R&D, UK) in a humidified 37°C/5% CO₂ incubator. These specific growth factors have previously been shown to enhance HAC proliferation and post-expansion redifferentiation capacity (102). HAC were detached at confluency (passage 1) by a treatment with 0.3% type II collagenase, followed by 0.05% trypsin/0.52 mM EDTA (Gibco, UK) and re-plated at a density of 5 x10³ cells/cm² for the second expansion step. After passage 3, expanded HAC were taken into chondrogenic re-differentiation culture.

Chondrogenic Re-differentiation culture

The chondrogenic re-differentiation of expanded HAC was stimulated using a chemically defined, serum-free medium (SFM), which consists of DMEM containing 4.5 mg/ml D-glucose, 0.1 mM non-essential amino acids, 1 mM sodium pyruvate, 10 mM HEPES buffer, 100 U/ml penicillin, 100 µg/ml streptomycin, and 0.29 mg/ml L-glutamine (all

Gibco, UK) supplemented with ITS⁺ (10 µg/ml insulin, 5.5 mg/ml transferrin, 5 ng/ml selenium, 0.5 mg/ml bovine serum albumin, 4.7 mg/ml linoleic acid), 1.25 mg/ml human serum albumin, 0.1 mM ascorbic acid 2-phosphate and 10⁻⁷ M dexamethasone (all Sigma Chemical, USA) and 10 ng/ml TGF-β1 (R&D, UK) (chondrogenic medium) (100;189). To investigate the influence of substrate stiffness on HAC re-differentiation, expanded HAC were cultured for 7 days on type I collagen coated PA gels of different stiffness at density of 2 x 10⁴ cells/cm². Aggregate cultures were prepared by culturing HAC at the same density on bare (w/o CI) tissue culture plastic (TCPS). Due to the absence of serum proteins, HAC display moderate initial substrate adhesion and preferentially stick to each other rather than to the substrate. After one day of re-differentiation culture, nearly all HAC have detached from the substrates and float in suspension as cellular aggregates similarly as described previously by Wolf *et al.* (2008) (101).

Attachment & Proliferation

The number of adherent HAC (N₀) was determined from representative phase contrast light microscopy images and expressed as percentage of the number of theoretically seeded cells. After 7 days of re-differentiation culture, the number of adherent HAC (N₁) was counted again (as described above) to assess proliferation which was expressed by the total number of doublings: log₂ (N₁/N₀).

Cell morphology

HAC morphology and the degree of spreading were determined after 24hours of re-differentiation culture. The cell shape factor ϕ (Eq. 1) (186;187) was calculated according to:

$$\phi = \frac{4 \pi A}{p^2} \quad (1)$$

The area A and the perimeter p required for calculating the shape factor ϕ were determined from phase contrast images using Image J version 1.37 (188). Rounded cells with high area-to perimeter ratio assume shape factor ϕ values close to 1, whereas starfish-shaped cells have a shape factor ϕ near 0.

Fluorescence Labelling, Acquisition and Analysis

After fixation in 4% (w/w) formaldehyde in phosphate buffer pH 7.4 (Univerity Hospital Pharmacy Basel, Switzerland) at 4°C over night, HAC were rinsed with PBS three times prior to a 10 min. permeabilization on ice with a solution containing 0.02% (w/w) Triton X100 (Sigma-Aldrich, Switzerland). Immediately after aspiration of the permabilization solution, the specimen were blocked for 1 hour at room temperature in PBS containing 30 mg/ml BSA (Sigma-Aldrich, Switzerland). Then, the specimens were rinsed with labelling buffer (LB) containing 15 mg/ml BSA in PBS and incubated with the primary antibody for 1h at room temperature. Subsequently, the specimens were rinsed with LB four times for 5 min. each and incubated with the secondary antibody for 1h at room temperature. Finally, the slides were washed again with LB four times for 5min. each,

rinsed with autoclaved milliQ water, mounted with Aqueous Mounting Media (AbD SeroTec, Oxford, UK) and sealed with Klarlack (Lady Manhattan Cosmetics, Germany).

All antibodies/labelling agents were diluted in LB. Vinculin was labelled with a primary monoclonal mouse antibody (Sigma-Aldrich, Switzerland; clone: hVIN-1; dilution: 1:400) followed by a Cy3 conjugated IgG goat anti-mouse secondary antibody (Acris Antibodies, Herford Germany; dilution: 1:800).

F-actin was detected with Alexa488 conjugated phalloidin (Invitrogen, Oregon USA; dilution: 1:400) and nuclei stained with DAPI (Invitrogen, Oregon USA; 4',6-diamidino-2-phenylindole; dilution: 1:48'000).

Sox-9 transcription factor was labelled with a monoclonal mouse antibody (Lubio-Science, Switzerland, clone: 3F11; dilution: 1:200) followed by an Alexa546 conjugated IgG1 goat anti- mouse secondary antibody (Lubio-Science, Switzerland, dilution: 1:200).

Fluorescence images were acquired on a Zeiss LSM 710 TYPE (Zeiss, Wetzlar, Germany) confocal laser scanning microscope under constant conditions using either a 40x or a63x immersion objective. Eight bit z-stack images were recorded in three different, regions of each substrate.

To quantify type II collagen expression pixels with a fluorescence intensity higher than 20 (arbitrary units) were counted on each z-plane, using the Zen2008 software (version 5.0, Zeiss MicroImaging GmbH). The z-stack with the highest florescent counts was taken and normalized vs. the number of DAPI stained nuclei in the corresponding stack.

Gene Expression Analysis

After 7 days of re-differentiation culture, HAC were harvested (as described above; using collagenase and trypsin). RNA was extracted from the obtained cell pellets with 250 µl

Trizol (Life Technologies, Basel, CH) according to the manufacturer's instructions. Extracted RNA was treated with DNase following the instructions of the RNeasy Kit (Ambion, Austin TX). cDNA was generated from total RNA using reverse-transcriptase Stratascript (Stratagene) in the presence of dNTP and DTT. Real-time PCR reactions were performed and monitored using the ABI prism 7700 Sequence Detection System and the Sequence Detector V program (Perkin-Elmer Applied Biosystems). cDNA samples were analyzed for type I and II collagen and for the housekeeping gene (18S ribosomal RNA), using previously described sequences of primers and probes (100). Each cDNA sample was assessed in duplicate and the collagen mRNA expression levels were normalized to the corresponding 18S rRNA levels.

RESULTS

Substrate Characterization

The elasticity of swelling equilibrated polyacrylamide (PA) gels was determined by rotational rheometry, measuring the dynamic shear modulus (G) which consists of the shear storage modulus (G') and the shear loss modulus (G'' , see Fig. 1 and Tab. 1). The dynamic shear modulus ($G = G' + G''$) was converted into the Young's modulus ($E = 2G'(1+\nu)$), which is more widely spread to describe substrate elasticity and thus referred to hereafter (see Tab. 1). For the Poisson ratio (ν) a value of 0.464 was assumed as it has been reported for PA by others (224).

Based on the mechanical compliance of the corresponding type I collagen (CI) functionalized PA, the substrates employed in this work are referred to as *0.3kPa (soft)*, *21kPa (intermediately stiff)* and *75kPa (stiff)*. TCPS coated with CI (TCPS w/ CI) was considered to be an *infinitely stiff* substrate.

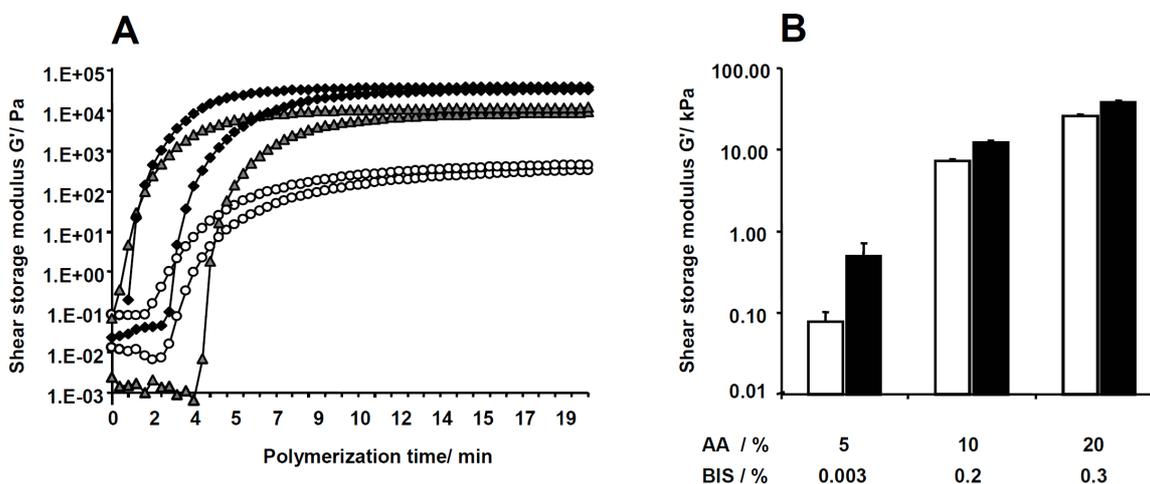


Fig. 1 Characterization of polyacrylamide substrate elasticity. (A) Time course of shear storage modulus (G' , Pa) in polymerizing acrylamide (PA) mixtures. The polymerization time course (20 min.) of three different mixtures consisting of acrylamide (AA, monomer) and N,N'-methylenebisacrylamide (BIS, crosslinker) was followed *in situ* in a rotational rheometer (Physica MCR 501, Anton Paar, Graz, Austria), fitted with a 50 mm diameter parallel plate (PP50). Measurements were conducted at an oscillation frequency of 1 Hz and an amplitude of 1% at 37°C in a humidified chamber. The volume for polymerization was 2 ml and initiated with 30 μ l 10% ammonium persulfate (APS) and 30 μ l 10% tetramethylethylenediamine (TEMED). The concentrations for AA_BIS were: 5%_0.003% (open circles), 10%_0.2% (grey triangles), 20%_0.3% (black diamonds) and the duplicates prepared independently. Following the lag phase, G' increased monotonically but ceased less than 5 min. after initiation of polymerization. After ~20 min. of polymerization, each of the three AA/BIS compositions reached its distinct plateau value. (B) G' comparison of *in situ* polymerized PA (20 min. after initiation, black bars; $n = 2$) and swelling equilibrated PA (in PBS at room temperature over night, white bars, $n = 4$). Swelling equilibrated PA displayed G' values which were 33 to 85% lower compared to the corresponding *in situ* polymerized PA. Error bars represent standard deviation.

HAC Attachment and Proliferation

Phase contrast images taken 24 hours after seeding expanded/de-differentiated HAC in chondrogenic medium revealed a homogenous cell distribution (see Fig. 2). HAC attachment was comparable on of the three different PA substrates, but 17 to 28% lower (see Fig. 3, Kruskal Wallis, Conover, $p \leq 0.05$) than on TCPS w/ CI. Throughout the 7 days of HAC cultivation in chondrogenic medium, proliferation remained below one total doubling and was similar on the *soft* (0.20 ± 0.17 total doublings) and the *infinitely stiff* substrate (0.25 ± 0.16 total doublings).

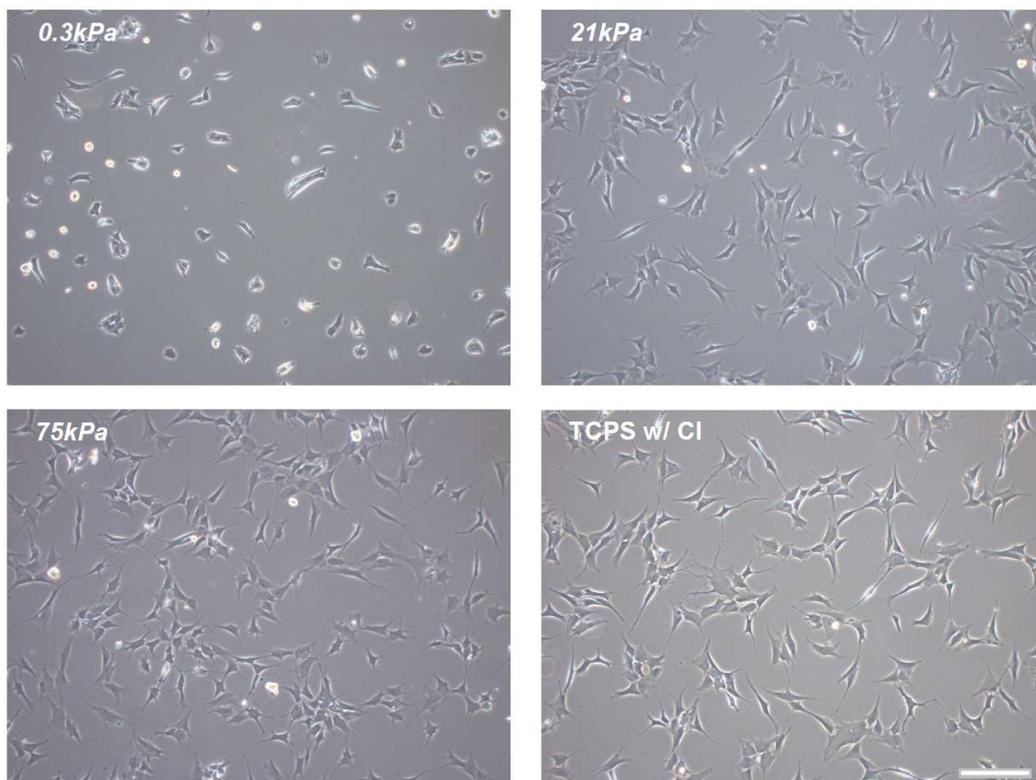


Fig. 2 Representative phase contrast images of expanded/de-differentiated adult human articular chondrocytes (HAC), 24 hours after seeding onto the corresponding substrate, in chondrogenic medium. *0.3*, *21* and *75kPa* indicate the substrate elasticity (Young's modulus) of the three contrasting, type I collagen functionalized polyacrylamide substrates. Tissue culture treated plastic coated with type I collagen (TCPS w/ Col I) served as an infinitely stiff control. Scale bar: 200 μm .

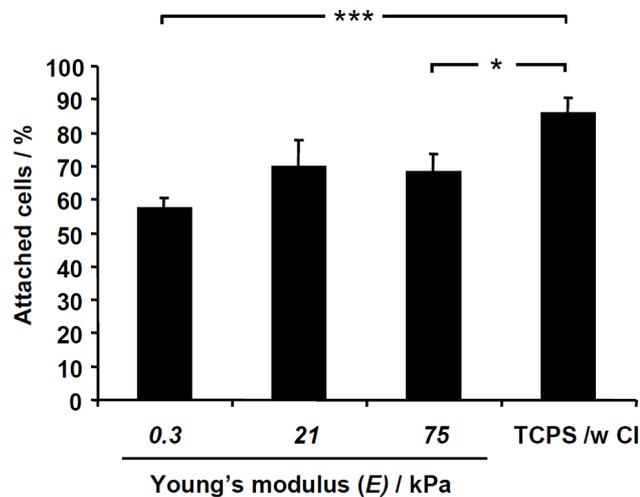


Fig. 3 Attachment of expanded/de-differentiated adult human articular chondrocytes (HAC) 24 hours after seeding onto the corresponding substrate, in chondrogenic medium. 0.3, 21 and 75kPa indicate the substrate elasticity (Young's modulus) of the three contrasting, type I collagen functionalized polyacrylamide substrates. Tissue culture treated plastic coated with type I collagen (TCPS w/ Col I) served as an infinitely stiff control. The number of adherent cells was determined from representative phase contrast light microscopy images and expressed as percentage of the number of initially seeded cells. The asterisks indicate significant differences (Kruskal-Wallis paired (Conover); $p = * < 0.05$ and $*** < 0.001$; $n = 6$).

HAC Morphology

In chondrogenic differentiation medium, a rounded morphology and a limited spreading were characteristic features of HAC, cultured on a *soft* substrate (see Fig. 2). Contrastingly, on *intermediately* to *infinitely stiff* substrates, HAC were fully spread and assumed an average spreading area which was more than 3.2-fold higher than on the *soft* substrate (see Fig. 4, One-Way ANOVA, Tukey HSD; $p < 0.001$). That on the *soft*

substrates, HAC tended to assume a round morphology was also reflected by the shapefactor Φ_A , which was 40 to 50% higher than on *intermediately* to *infinitely stiff* substrates (see Fig. 4, One-Way ANOVA, Tukey HSD; $p < 0.001$). Despite these differences, the average spreading area and shape factor of HAC on *intermediately stiff* to *infinitely stiff* substrates was found to be similar.

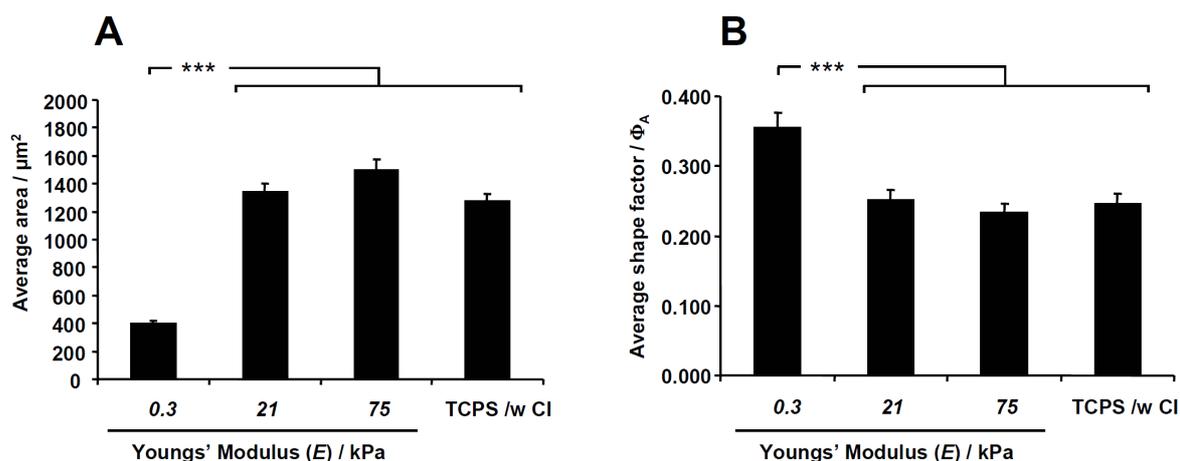


Fig. 4 Average area (A) and shape factor Φ_A (B) of expanded/de-differentiated adult human articular chondrocytes (HAC), 24 hours after seeding onto the corresponding substrate, in chondrogenic medium. *0.3I*, *21* and *75kPa* indicate the substrate elasticity (Youngs' modulus) range of the three contrasting, type I collagen functionalized polyacrylamide substrates. Tissue culture treated plastic coated with type I collagen (TCPS w/ Col I) served as an infinitely stiff control. The shape factor was computed from the cell area and perimeter and can range from zero for starfish-shaped cells to 1 for perfectly round shaped cells. Area and perimeter of adherent cells was measured on representative phase contrast light microscopy images. The asterisks indicate significant differences (One-Way ANOVA, Tukey HSD; $p = *** < 0.001$; $n \geq 55$).

HAC Actin Cytoskeleton and Focal Adhesions

Fluorescence microscopy of HAC labelled for F-actin and vinculin showed that the morphology observed by phase contrast microscopy (after 24 hours) was maintained after 7 days of re-differentiation culture (see Fig. 5). On the *soft* substrate, HAC remained spherical with F-actin mainly localized cortically. On *intermediately stiff* to *stiff* substrates however, HAC were spread, flattened and displayed a fibrillar F-actin organization into stress fibres. On all substrates, vinculin was dispersed throughout the entire cytoplasm but appeared most intense in the perinuclear region. Aggregations of vinculin into small clusters were detected in lamellipodial regions of HAC cultured on *intermediately stiff* to *stiff substrates*. On the latter, HAC in confluent spots displayed more actin stress fibres than cells which were more isolated. Moreover, actin stress fibres appeared more aligned and distinct on *stiff* as compared to *intermediately stiff* substrates, where F-actin was more diffuse throughout the cytoplasm (see Fig. 6).

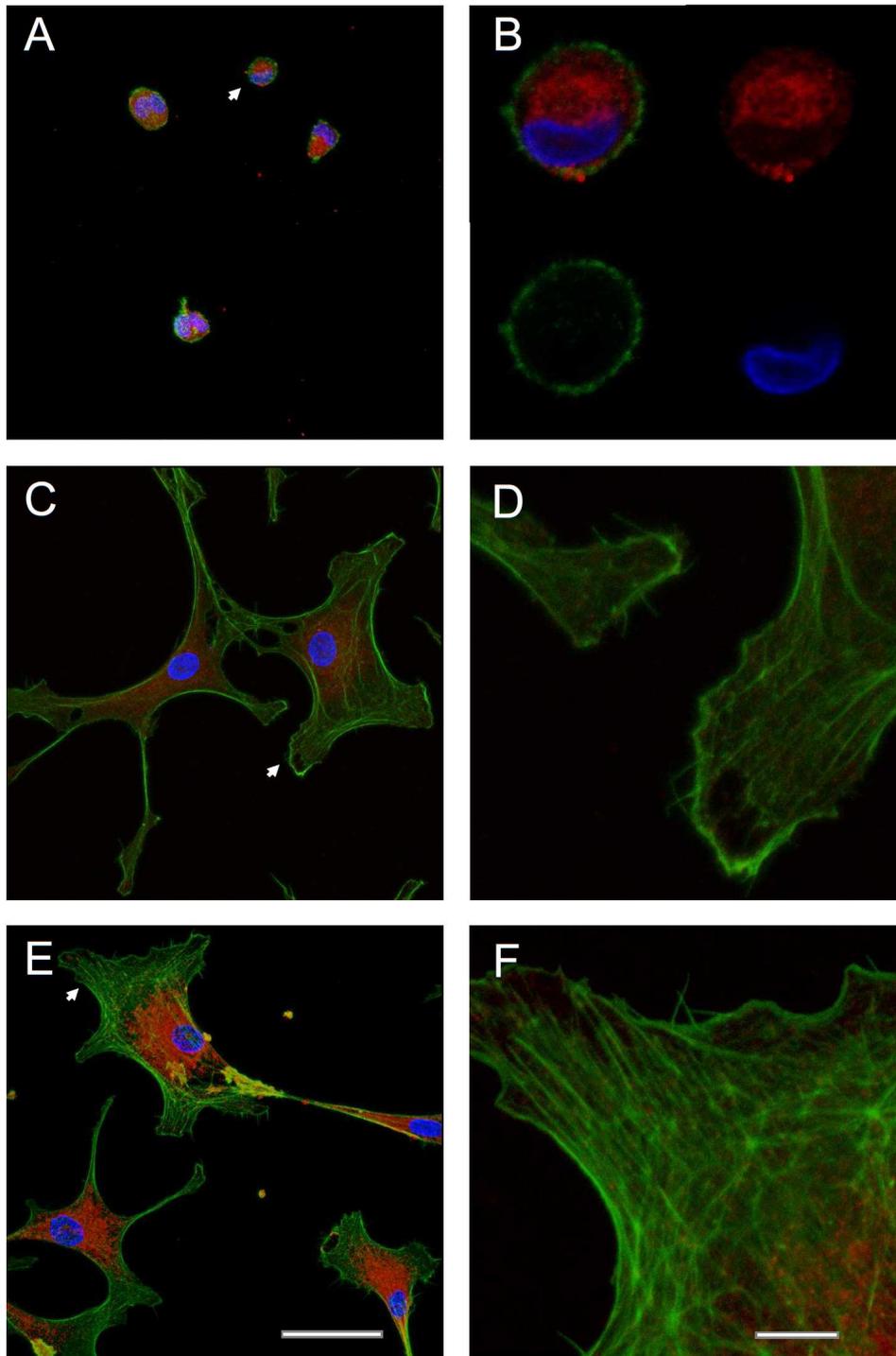


Fig. 5 Representative confocal laser scanning microscopy images (maximum projection) of expanded/de-differentiated adult human articular chondrocytes (HAC), labelled for F-actin (green), vinculin (red) and nuclei (blue). HAC were induced to re-differentiate for 7 days in chondrogenic medium, on substrates of contrasting elasticity (Young's modulus) which in (A, B) was $0.31kPa$, for (C, D) $21kPa$ and $75kPa$ in (E, F). Images in the right column show details (indicated by the white arrow) of the corresponding image to their left. (B) Shows a merge and the separate channels of a mid section through a single HAC with spherical morphology (as indicated by the arrow in image A). Scale bars are $50\mu m$ for the left column and $10\mu m$ for the right column

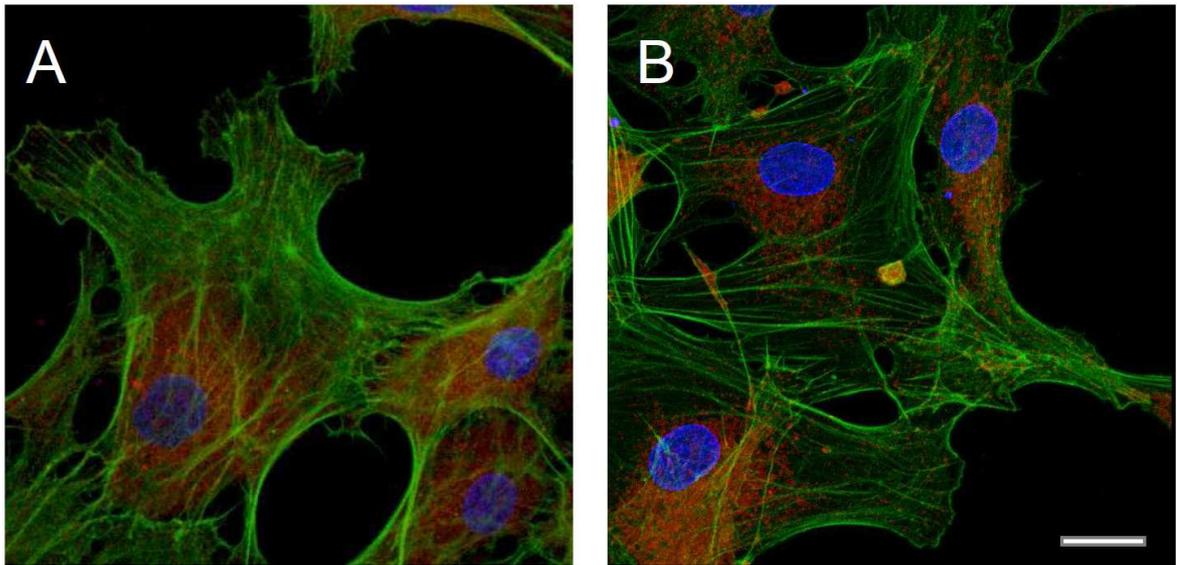


Fig. 6 Representative confocal laser scanning microscopy images (maximum projection) of expanded/de-differentiated adult human articular chondrocytes (HAC), labelled for F-actin (green), vinculin (red) and nuclei (blue). HAC were induced to re-differentiate for 7 days in chondrogenic medium, on substrates on intermediately stiff (A: 21kPa) and stiff (B: 75kPa) polyacrylamide substrates. HAC in more confluent regions formed more actin stress fibres than isolated cells. Moreover, actin stress fibres and aggregates of vinculin were more distinct on the stiffer than on the intermediately stiff substrate. Scale bar: 20µm.

Sox-9 Expression

After 7d of culture in chondrogenic medium on the corresponding substrates, HAC were immuno-labelled for transcription factor Sox-9 (see Fig. 8). Generally, frequency and intensity of nuclear Sox-9 localization was heterogeneous throughout the HAC population, but most frequent and intense in HAC cultured on the *soft* substrate. This also coincided with higher cytoplasmic concentrations as compared to in HAC cultured on *intermediately stiff* and the *stiff* PA substrate.

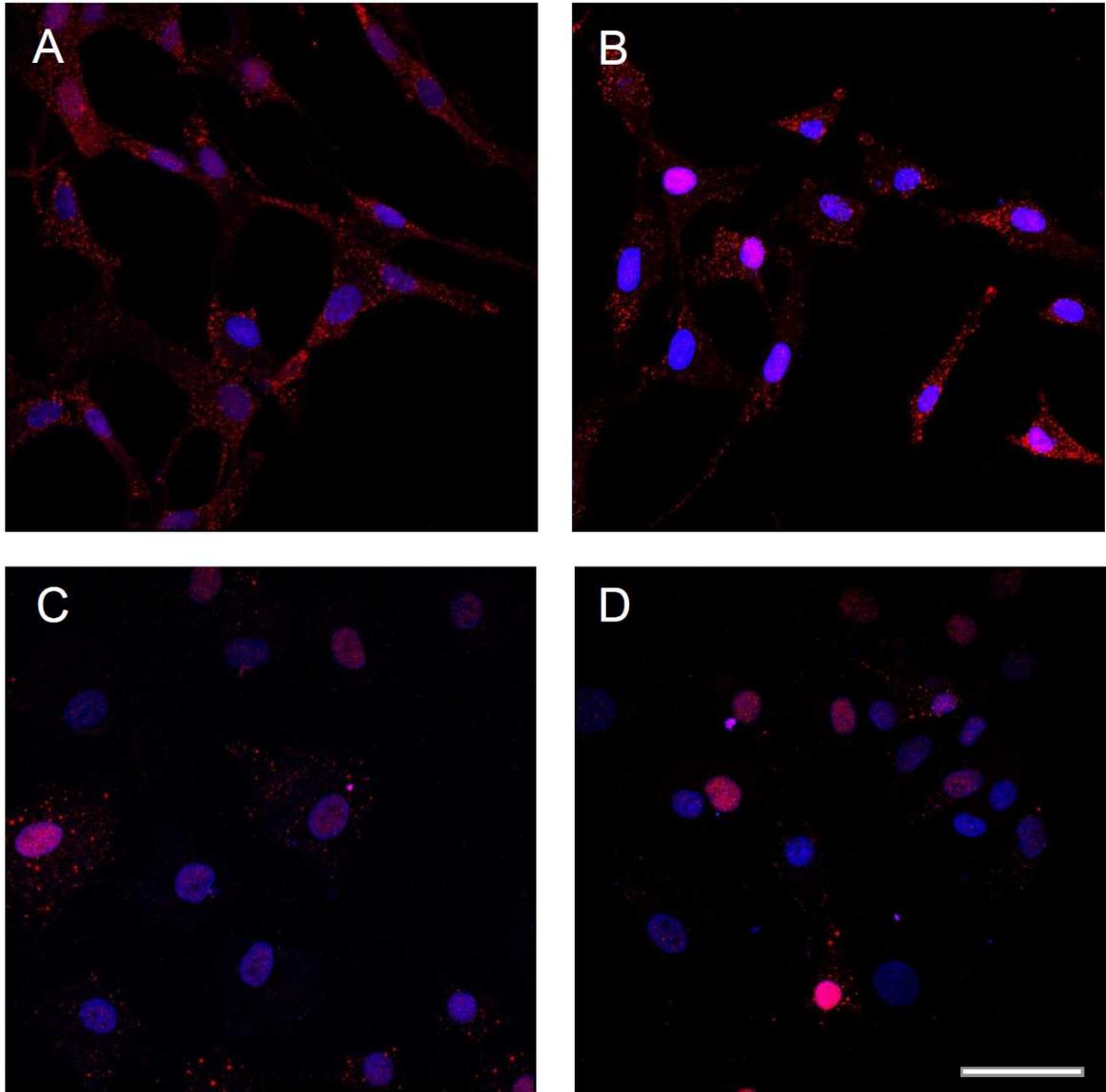


Fig. 7 Representative confocal laser scanning microscopy images of human articular chondrocytes (HAC) labelled for Sox-9 (red) and nuclei (blue). (A, B) HAC after expansion (passage 3) on infinitely stiff glass substrates. (C,D) Expanded/de-differentiated HAC after 7 days of re-differentiation culture in chondrogenic medium, on infinitely stiff glass substrates. Since Sox-9 expression was heterogeneous throughout the population, two images are shown representing lowest (left column) and highest Sox-9 expression (right column) for each condition. The presented images are midsections through the nucleus. Single planes were acquired at the z-level of highest Sox-9 intensity. Scale bar: 50 μ m.

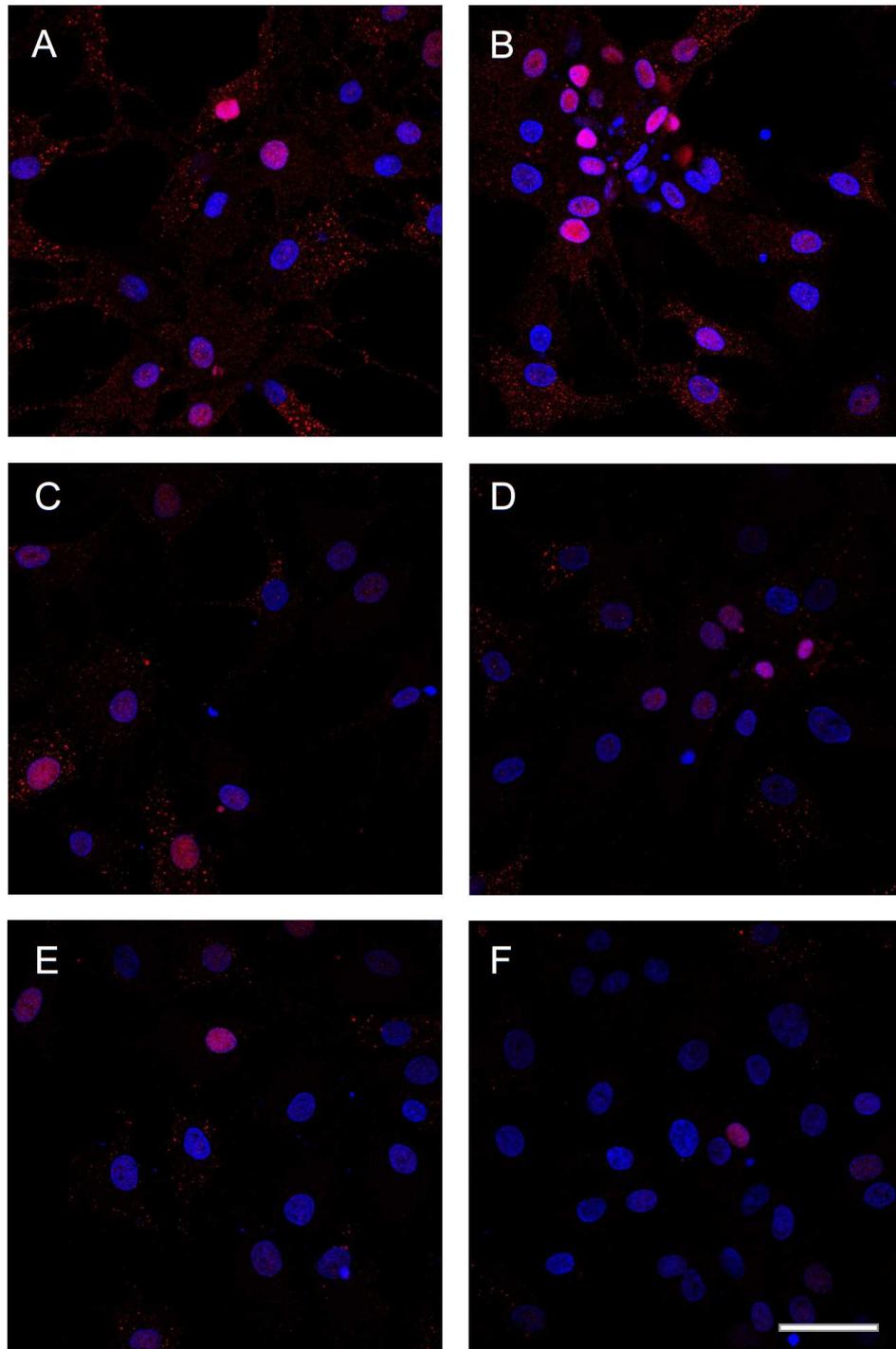


Fig. 8 Representative confocal laser scanning microscopy images of expanded/de-differentiated human articular chondrocytes (HAC), labelled for Sox-9 (red) and nuclei (blue). HAC were induced to re-differentiate for 7 days in chondrogenic medium, on substrates of contrasting elasticity (Young's modulus) which in (A, B) was $0.31kPa$, for (C, D) $21kPa$ and $75kPa$ in (E, F). Since Sox-9 expression was heterogeneous throughout the population, two images are shown representing lowest (left column) and highest Sox-9 expression (right column) for each condition. The presented images are midsections through the nucleus. Single planes were acquired at the z-level of highest Sox-9 intensity. Scale bar: $50\mu m$.

Gene Expression

Expanded/de-differentiated HAC cultured for 7 days on the corresponding substrate were analyzed for type I and II collagen mRNA expression (see Fig. 9). In control experiments, where TGF was omitted from the chondrogenic medium, type II collagen mRNA remained at levels comparable with that of expanded/de-differentiated HAC. Contrastingly, type I collagen mRNA was lower on the PA substrates and in aggregates (3.9 to 9.6-fold) but on TCPS w/CI also remained at levels comparable with that of expanded/de-differentiated HAC.

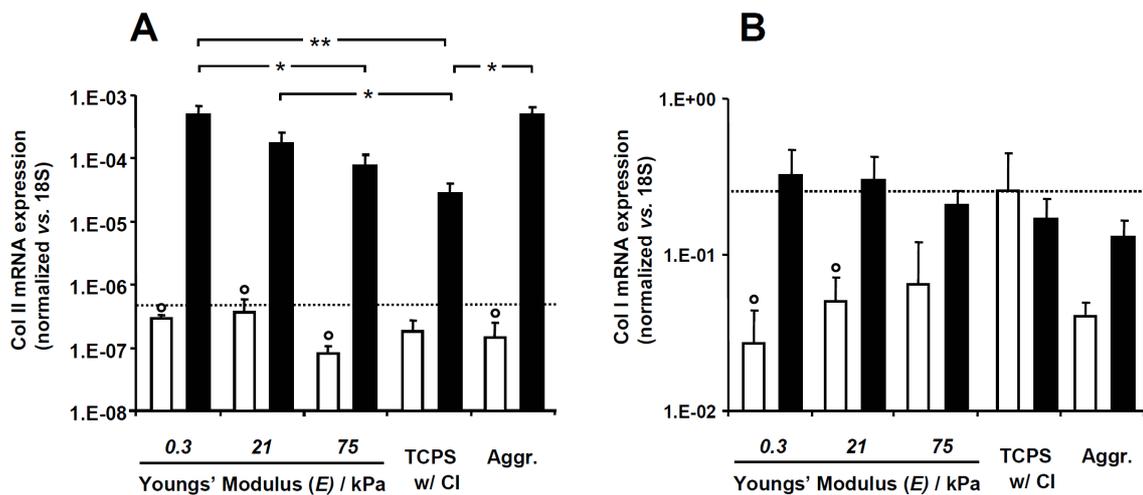


Fig. 9 Type II (A) and I (B) collagen mRNA expression levels of expanded/de-differentiated adult human articular chondrocytes (HAC) after 7 days of culture in chondrogenic medium without (white bars) or with (black bars) TGF. 0.31, 21 and 75kPa indicate the substrate elasticity (Youngs' modulus) range of the three contrasting, type I collagen functionalized polyacrylamide cell culture substrates. Tissue culture treated plastic coated with type I collagen (TCPS w/ Col I) served as an infinitely stiff and HAC aggregate cultures (Aggr.) as positive controls. All values are normalized vs. the housekeeping gene 18S and the dashed line represents the mRNA expression level in expanded/de-differentiated HAC. Asterisks above the brackets indicate a significant differences between two corresponding bars (Kruskal-Wallis paired (Conover); $p = * < 0.05$ and $** < 0.01$; $n = 15$, 4 donors). Open circles above the white bars indicate a significant difference vs. (+) TGF on the same substrate (Mann-Whitney, U-test, two tailed; $n = 4$, $p < 0.05$).

Inclusion of TGF in the chondrogenic medium (standard) had a strong general effect on type II collagen mRNA expression in HAC (Mann-Whitney, U-test, two tailed; $p = 6.0 \times 10^{-6}$) and despite for the *infinitely stiff* substrate, it induced an up-regulation ranging from 459-fold on *intermediately stiff* substrates to 3642-fold in HAC aggregates (Kruskal-Wallis paired (Conover); $p < 0.05$). Although less dramatic, TGF also had a general effect on type I collagen mRNA expression (Mann-Whitney, U-test, two tailed; $p = 1.5 \times 10^{-4}$) and induced an up-regulation in HAC cultured on *soft* (12.2-fold) and *intermediately stiff* substrates (6.2-fold; Kruskal-Wallis paired (Conover); $p < 0.05$).

Type II collagen mRNA expression by HAC after 7d of culture in chondrogenic medium on the *soft* substrate was similar to that in aggregate culture and 6.4 to 18.1-fold higher than on *stiff* and *infinitely stiff* substrates (Kruskal-Wallis paired (Conover); $p < 0.05$). While *intermediately stiff* substrates still allowed for a 6.2-fold higher type II collagen mRNA expression (Kruskal-Wallis paired (Conover); $p < 0.05$), no difference was found between the *stiff* PA substrate and the *infinitely stiff* TCPS w/ CI. Type I collagen mRNA expression was not altered by substrate stiffness and remained at levels comparable to that in expanded/de-differentiated HAC. However the absolute mRNA expression level of type I collagen was more than 514-fold higher than that of type II collagen.

Type II Collagen Protein Expression

Expanded/de-differentiated HAC cultured for either 7 or 14 days on the corresponding substrate were analyzed for type II collagen protein expression (see Fig. 10 & 11, data adapted from master thesis Andreas Trüssel 2010 (225)). Fluorescent staining in the form of intracellular granules could only be detected in HAC cultured on *soft* substrates. Surprisingly, after 14 days of culture the fluorescent intensity (see Fig. 11, data adapted

from master thesis Andreas Trüssel 2010 (225)) tended to be lower as compared to after 7 days. On the *intermediately to infinitely stiff substrates*, the fluorescence signal remained on levels comparable to that in negative control staining (secondary antibody only).

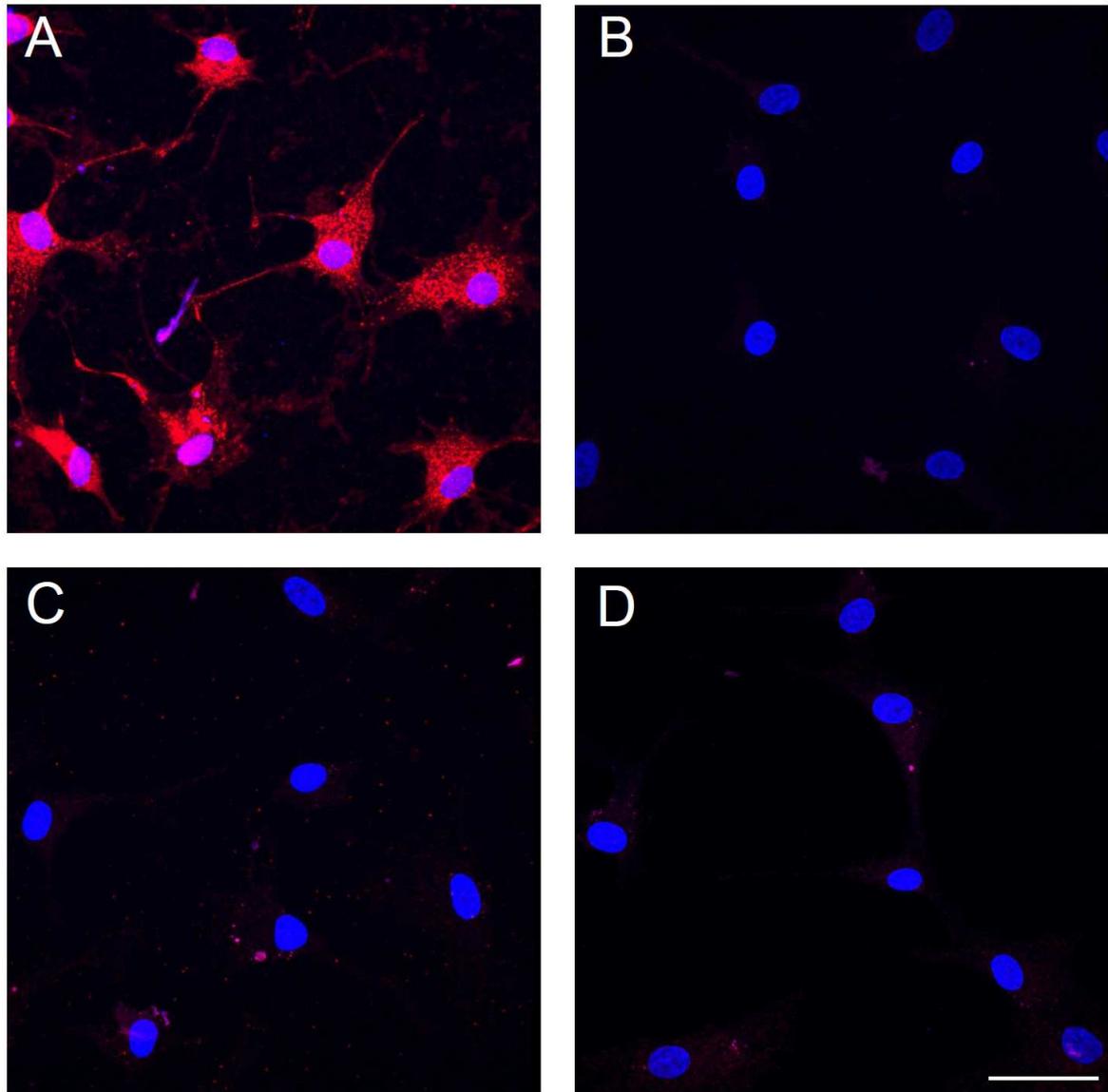


Fig. 10 Representative confocal laser scanning microscopy images (maximum projection) of expanded/de-differentiated adult human articular chondrocytes (HAC), labelled for type II collagen (red) and nuclei (blue). HAC were induced to re-differentiate for 7 days in chondrogenic medium, on substrates of contrasting elasticity. The substrate elasticity (Young's modulus) in (A) is 0.3kPa , for (B) 21kPa , 75kPa in (E) and *infinitely stiff* in (C; glass coated with type I collagen). Scale bar: $50\mu\text{m}$. Data adapted from master thesis A. Trüssel 2010 (225).

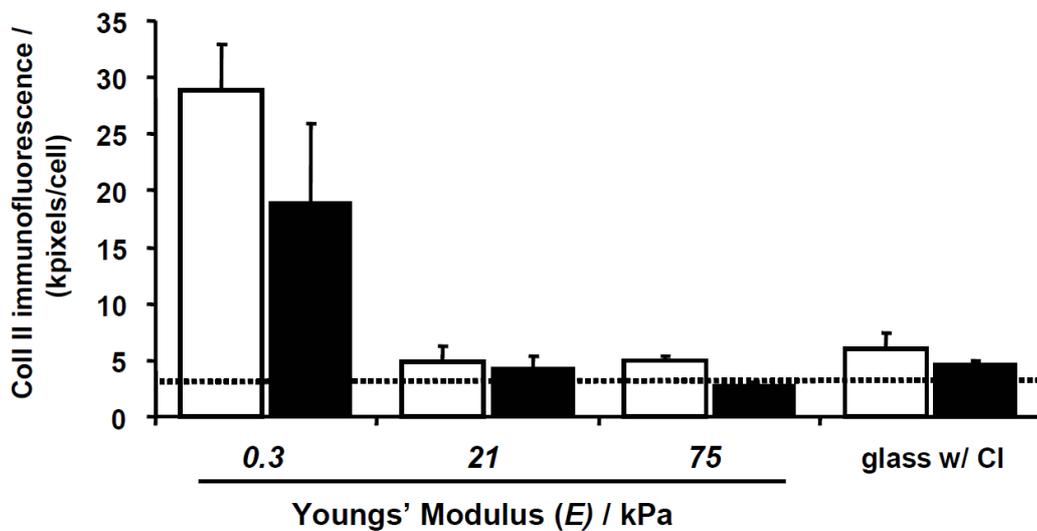


Fig. 11 Type II collagen expression of expanded/de-differentiated adult human articular chondrocytes (HAC). HAC were induced to re-differentiate for 7 days in chondrogenic medium, on substrates of contrasting elasticity. The substrate elasticity (Young's modulus) in (A) is 0.3kPa , for (B) 21kPa , 75kPa in (E) and *infinitely stiff* in (C; glass coated with type I collagen). The dashed line represents the fluorescence signal in HAC that were stained with the secondary antibody only (negative control; background fluorescence). After thresholding, the number of pixels were counted from confocal laser scanning microscopy images (maximum projection) of type II collagen labelled HAC, and expressed as kilopixels normalized vs. the number of nuclei. Scale bar: $50\mu\text{m}$. Data adapted from master thesis A. Trüssel 2010 (225).

DISCUSSION

Using type I collagen coated PA substrates of contrasting stiffness, (*0.3kPa: soft, 21kPa: intermediately* and: *75kPa stiff*), we investigated the influence of substrate elasticity on the re-differentiation of expanded/de-differentiated HAC. The *soft* substrates allowed for attachment comparably to the *intermediately* to *infinitely stiff* substrates, but supported a spherical morphology, from which actin stress fibres and focal complexes were absent. Moreover, HAC on *soft* substrates displayed highest Sox-9 nuclear translocation and type II collagen expression (mRNA and protein).

Attachment & Proliferation

The comparability of the PA substrates with regard to adhesive ligand presentation was reflected by the similar degree of HAC attachment thereon. That in contrast to PA, HAC attachment on TCPS w/ CI was higher, could be associated with the different modes of protein immobilization on the two substrates. While PA was functionalized with CI by chemisorption (sulfo-SANPAH crosslinker), TCPS was coated with CI by physisorption. Both approaches are known to influence native biological protein activity and likely do so in a distinct but unpredictable manner (for review see (178)) and thus prompts for carefully comparing TCPS and PA in this regard. However, considering substrate elasticity to be the key parameter, protein coated TCPS as well as glass have previously been employed as infinitely stiff substrates (in the order of MPa) and allow to extrapolate the maximal stiffness of PA (~80kPa) (226;227).

While on all substrates HAC attachment in chondrogenic medium roughly matched which with values previously found under expansion conditions (140), proliferation of re-differentiating HAC was very low on both *soft* and *infinitely stiff* substrates. This allowed to bypass proliferation inherent de-differentiation (95), which may have clouded the analysis of matrix elasticity as a direct differentiation cue in previous studies (208).

Morphology & Sox9 Expression

The *soft* substrates were demonstrated to permit for similar HAC morphology as can be achieved by well established culture conditions, which have been described to support a round cell morphology (96;101;124;212-215). In fact, HAC cultured on *soft* PA substrates in chondrogenic medium displayed characteristic aspects of chondrocytes *in situ* (228;229), including a round/spherical morphology, cortical actin filament organization and the lack of focal adhesions. Moreover, the morphological observations in the present work were in good agreement with a complementary study, which assessed the maintenance of porcine and bovine chondrocytes in response to matrix elasticity (208;230).

Contrastingly, *Intermediately stiff* to *infinitely stiff* substrates, allowed for cell spreading, actin stress fibre formation, and focal adhesion assembly which coincided with reduced Sox9 transcription factor expression/nuclear-translocation and type II collagen (mRNA and protein) expression. This coincidence suggests for the involvement of Rho GTPases, which are well characterized upstream regulators of the actin cytoskeleton (231;232) and have been found to influence chondrocyte differentiation and function. More specifically, RhoA and its effector ROCK suppress cortical actin organization, lead to stress fibre formation, the maturation of focal adhesions and inhibits chondrogenesis through the

suppression of Sox9 expression (165;233). To date, Sox9 is known to be the only transcription factor absolutely necessary for chondrogenesis (234-236) and directly regulates the transcription of the collagen II gene (236-238).

That Sox-9 expression was heterogeneous throughout the cell population may reflect the different zonal origins of HAC harvested from whole articular cartilage. This complicates the analysis of the fluorescence images and prompts for a quantitative assessment of nuclear Sox-9 translocation (normalized to cytoplasmic levels) to more precisely estimate its promoter activating levels (in progress).

Chondrodifferentiation

Matrix elasticity *per se* has been demonstrated to be sufficient for directing lineage specification of MSC (109), but it did not induce re-differentiation of HAC. This suggests, that although HAC expanded in presence of specific growth factors assume MSC-like traits (100), they might not fully acquire the degree of plasticity of their progenitors. Although not additional, substrate elasticity was able to modulate the soluble chondro-inductive stimulus provided by TGF. This suggests for a cross talk between soluble and insoluble signals and implies that depending on the mechanical compliance of their environment, cells might respond differently to the same soluble signal. This has first been demonstrated for contractile fibroblasts, which only were able to maintain/generate TGF induced α smooth muscle actin (α SMA), when cultured on stiff (20kPa) but not on soft (8kPa) collagen gels (239).

The strong up-regulation of type II collagen mRNA in HAC on *soft* substrates is in agreement with findings of a previous study using porcine chondrocytes (208). However,

the differences in type II collagen mRNA expression between the softest and the stiffest substrate were found to be more pronounced as than those reported by Schuh *et al.* (2010). This could be due to the difference in cell type and/or to the aforementioned proliferation associated de-differentiation. Another reason could be, that the softest substrate (4kPa) used by Schuh et al. (2010) was more than 10-fold stiffer as compared to the *soft* substrates (0.3kPa) employed in the present study.

The reason why type II collagen was mainly found intracellularly but not extracellularly is unclear but could possibly be due to blocked release from HAC or low retention on the inert PA substrates. Interestingly, the staining was not continuous but localized into small granular features which were scattered throughout the entire cytoplasm. Similar, staining has been observed in chick chondrocytes and attributed to type II pro-collagen (209). Although, the type II collagen expression looks promising, these are primary results, which need further confirmation.

Interestingly, the E modulus of the *soft* substrates matches well with values reported for mesenchymal stem cells (240). Since in the developing limb bud, mesenchymal stem cells aggregate to form mesenchymal condensations (205) this implies that they might greatly determine the mechanical properties thus suggests, that the *soft* substrates could have mimicked the mechanobiological environment present at the onset of chondrogenesis.

In chondrogenic medium, Type I collagen mRNA expression by HAC was rather high in both aggregates and on soft substrates. This could be due to the fact, that 7 days of re-differentiation is still quite short. Actually, it is known, that in the developing limb, Collagen I plays an important role during mesenchymal condensation but is down-regulated as chondrogenesis progresses (218).

Mechanisms of Mechanotransduction

The precise mechanisms by which substrate elasticity influences cell behaviour are still elusive (241). Still, the number of studies which provide mechanistic insight on the topic of mechanotransduction is increasing and has led to the proposal of different models.

An extracellular model describes that if cell generated tension meets resistance from the ECM, it allows to free/activate latency associated protein (LAP) bound growth factors (i.e. TGF) which are sequestered in their inactive form throughout the ECM (207). However, it seems unlikely, that matrix elasticity modulated the effect of TGF by this mechanism, since the chondrogenic medium was supplemented with free/active TGF and since type I collagen (immobilized on the PA substrates) is not known to possess a TGF or a LAP interaction site.

Other models focus on intracellular effects of matrix elasticity. The strain within a cell is manifested as protein extension, domain unfolding, and or protein-dissociation that relieves stress and/or creates sites for new binding partners, which elicits a chemical diffusion based signalling (241). Alternatively, external forces are thought to propagate into the cell nucleus through cell surface transmembrane receptors, that couple the ECM to cytoskeletal networks, which in turn link to nuclear scaffolds, nucleoli, chromatin and DNA. This channelling of forces across discrete load-bearing cytoskeletal filaments might promote changes in the shape, folding or kinetics of specific, load-bearing molecules or might modify higher-order chromatin organization and thereby alter nuclear protein-self-assembly, gene transcription, DNA replication or RNA processing. Moreover, this model suggests, that tissue elasticity as an insoluble cue could specify genome organization and nuclear matrix composition, which could prime cells to react differently to the same

soluble signal through differential tethering of genes to load-bearing nuclear scaffolds (242). Likely, both the chemical diffusion based, and the direct nuclear mechanotransduction work in a complementary/integral fashion.

OUTLOOK

The adhesive ligand employed in this work was restricted to type I collagen, but could be extended to other ECM proteins as i.e. type II collagen, which has been shown to support the native morphology of chicken epiphyseal chondrocytes (129). This suggestion also finds support by the fact that myogenic and osteogenic differentiation of human MSC can be directed by the interplay of substrate stiffness and type of adhesive ligand presented (243).

Instead of using native proteins like type I collagen, engineered proteins (i.e. modified FN-fragments) or truncated proteins (i.e. RGD-containing peptides) could also be used as cell-ligands and have previously been demonstrated to modulate the behavior of human fibroblasts and HAC respectively (137;140).

Although the two dimensional (2D) PA gels employed in the present work proved to be a valuable tool, future experiments to investigate the effects of substrate elasticity on cell behavior should be performed in a three dimensional environment (3D). 3D culture systems possess fundamental advantages over 2D models as they allow cells to adopt their native morphology, increase cell-cell interactions and facilitate contacts with the ECM (244;245). Moreover, a 3D environment would be more representative of i.e. an *in situ* situation and thereby be clinically more relevant. Unfortunately, PA polymerization is

not compatible with living cells, and thus does not allow for cell encapsulation. A simple approach to bypass this technical obstacle could be culturing cells in aggregates mixed with PA micro particles. Together, the 2D and the 3D PA model could allow to investigate cell responses to the influence of substrate elasticity & architecture in combination with other parameters such as soluble factors and/or the type of immobilized cell adhesion ligand.

A more sophisticated alternative would be i.e. PEG-based hydrogels which allow for cell encapsulation under physiological conditions and also can be tuned in their elasticity. Furthermore, PEG-based hydrogels can be doped with biological functionalities as i.e. matrix metalloproteinase-sensitive motifs and thus allow for enabling and controlling their biodegradability (246). This stands in strong contrast to most other synthetic materials which cannot be remodeled by cells, are limited in their degradation (hydrolysis) and thus may not be compatible with the *de novo* formation of matrix by cells (247). Still, PA-gels can easily be prepared in a biology lab since all the required ingredients are commercially available and simple to assemble. PEG-gels are not more complicated to assemble, yet, their building blocks cannot be bought off the shelf, but first have to be synthesized and characterized.

Taken together, 2D PA gels and 3D PA microparticles could be further exploited as simple but potent model tools in basic biology, while for rather clinically oriented investigations more sophisticated materials should be considered, which not only are biocompatible but also can be remodeled by cells.

Based on their chondroprogenitor like plasticity (100), expanded/de-differentiated HAC may provide a prediction on the behaviour of bone marrow derived mesenchymal stem cells, which are receiving increasing interest in association with *in situ* cartilage repair

approaches(152). These repair procedures involve the penetration of the subchondral bone plate by small perforations (microfracturing) which allow the recruitment/infiltration of mesenchymal stromal cells (MSC) from the bone marrow (204). MSC have the potential to undergo chondrogenic differentiation (156), but are thought to require the support of inductive/instructive biomaterials to improve microfracturing stimulated *in situ* cartilage regeneration (152;203). In this light, it appears promising to also investigate the effect of matrix elasticity on the chondrogenic differentiation of human MSC.

CONCLUSION

Substrate elasticity modulated the re-differentiation response of expanded/de-differentiated HAC to the chondrogenic stimulus TGF β -3, and thus underscores mechanical compliance in combination with appropriate soluble signals to be important parameter in designing biomaterials for cartilage repair.

Main Conclusion

By modifying specific substrate characteristics, CPC behaviour could be modulated under conditions which were either permissive for proliferation or differentiation. In chapter I for example, substrate composition & architecture were found to modulate the chondrogenic differentiation of MSC. That the di block copolymer model substrate (Polyactive®) with a more hydrophobic composition better supported MSC chondrogenesis, is likely associated with differential protein adsorption (from serum containing medium). However such proteinaceous interfaces are rather complex with regard to protein composition and conformation thereon. As this conceals the specific cues responsible for mediating the observed effects, it consequently prompted for reducing substrate interface complexity in subsequent investigations (chapter II & III).

A 3DF architecture with more highly interconnected pores and a pore size that allowed for the formation of larger MSC aggregates than the CM scaffolds was found to considerably better support MSC chondrogenesis. Taken together, the findings in chapter I underscore the importance to control substrate composition & architecture and point to their potential to modulate CPC cartilaginous matrix formation from fibrous towards more hyaline like.

Chapter II proofed, that restricting cell/substrate interaction to a specific ligand type (RGD-containing peptide) modulates de-differentiation of proliferating HAC and their subsequent capacity to form cartilaginous matrix. This demonstrated the advantage of small ECM fragments in combination with protein resistant materials to control cell/surface interaction. An important finding was the better maintenance of the HAC chondrocytic phenotype during expansion. It suggests, that an RGD-restricted substrate has the potential to improve the outcome of matrix assisted *in situ* cartilage repair, which initially requires recruited/infiltrated CPC to proliferate, while keeping/inducing their capacity to form cartilaginous matrix.

In chapter III, substrate elasticity allowed to modulate the chondrogenic commitment of HAC. The finding, that a soft substrate (0.3kPa) better supported the chondrogenic phenotype of HAC than i.e. a stiffer substrate (75kPa) suggests this parameter to be promising for modulating the outcome of matrix assisted cartilage repair.

All chapters clearly demonstrated the potential of substrate properties to modulate CPC behaviour. Yet, although differentially supporting CPC chondrogenesis, none of the substrates was *per se* chondro-inductive (see chapter I and III) but required for additional, exogenic stimuli as for e.g. TGF. Thus, substrate modifications hold considerable potential for improving matrix assisted cartilage repair but likely have to be combined with additional soluble stimuli to exploit their full potential.

Main Outlook

For reasons of feasibility, the sequences following micro fracturing stimulated cartilage repair have been grouped into two main phases consisting of i) proliferation and ii) differentiation. From these phases *in vitro* conditions were inferred for testing the response of chondrogenitor cells (CPC) to specifically modified substrate interfaces. However, aiming at *in situ* repair, these two phases would have to be linked. Thus, the supportive properties found in this thesis would have to be provided by one and the same material. This could be accomplished by a dynamic, clock-like material that adapts to the specific needs during the two different phases. As an example, such a hypothetical material could be an RGD-restricted, relatively stiff substrate ($\geq 20\text{kPa}$). After a duration long enough to allow for proliferation, the material would need to soften ($\sim 1\text{kPa}$) for supporting chondrogenic differentiation of the augmented CPC pool. The architecture of the envisioned ideal material initially should allow for efficient CPC infiltration and distribution but also should permit the formation of cellular aggregation during chondrogenic differentiation. These requirements could possibly be met by a single architecture like the 3DF.

As mentioned above, such a supportive material should be combined with appropriate soluble factors to stimulate either proliferation or induce differentiation. The release of these factors should be in concert with the corresponding phase of cartilage repair and

could be preceded by a burst of suitable cytokines to enhance CPC recruitment/infiltration.

Combining supportive substrate properties with inductive soluble stimuli, it should ultimately be possible to move from biomaterials which support cartilaginous repair to active medical devices which mediate cartilage repair.

References

Reference List

- (1) Buckwalter JA, Mankin HJ. Articular cartilage: tissue design and chondrocyte-matrix interactions
278. *Instr Course Lect* 1998;47:477-86.:477-86.
- (2) Bayliss MT, Venn M, Maroudas A, Ali SY. Structure of proteoglycans from different layers of human articular cartilage. *Biochem J* 1983 Feb 1;209(2):387-400.
- (3) Takada N, Wada I, Sugimura I, Sakuma E, Maruyama H, Matsui N. A possible barrier function of the articular surface. *Kaibogaku Zasshi* 1999 Dec;74(6):631-7.
- (4) Flannery CR, Hughes CE, Schumacher BL, Tudor D, Aydelotte MB, Kuettner KE, et al. Articular cartilage superficial zone protein (SZP) is homologous to megakaryocyte stimulating factor precursor and is a multifunctional proteoglycan with potential growth-promoting, cytoprotective, and lubricating properties in cartilage metabolism. *Biochem Biophys Res Commun* 1999 Jan 27;254(3):535-41.
- (5) Schumacher BL, Hughes CE, Kuettner KE, Caterson B, Aydelotte MB. Immunodetection and partial cDNA sequence of the proteoglycan, superficial zone protein, synthesized by cells lining synovial joints. *J Orthop Res* 1999 Jan;17(1):110-20.
- (6) Kempson GE, Muir H, Pollard C, Tuke M. The tensile properties of the cartilage of human femoral condyles related to the content of collagen and glycosaminoglycans. *Biochim Biophys Acta* 1973 Feb 28;297(2):456-72.
- (7) Akizuki S, Mow VC, Muller F, Pita JC, Howell DS, Manicourt DH. Tensile properties of human knee joint cartilage: I. Influence of ionic conditions, weight bearing, and fibrillation on the tensile modulus. *J Orthop Res* 1986;4(4):379-92.
- (8) Kempson GE, Muir H, Pollard C, Tuke M. The tensile properties of the cartilage of human femoral condyles related to the content of collagen and glycosaminoglycans. *Biochim Biophys Acta* 1973 Feb 28;297(2):456-72.

- (9) Roth V, Mow VC. The intrinsic tensile behavior of the matrix of bovine articular cartilage and its variation with age. *J Bone Joint Surg Am* 1980 Oct;62(7):1102-17.
- (10) Dallek M, Jungbluth KH, Holstein AF. Studies on the arrangement of the collagenous fibers in infant epiphyseal plates using polarized light and the scanning electron microscope. *Arch Orthop Trauma Surg* 1983;101(4):239-45.
- (11) Hagiwara H, Schroter-Kermani C, Merker HJ. Localization of collagen type VI in articular cartilage of young and adult mice
71. *Cell Tissue Res* 1993 Apr;272(1):155-60.
- (12) Keene DR, Engvall E, Glanville RW. Ultrastructure of type VI collagen in human skin and cartilage suggests an anchoring function for this filamentous network
80. *J Cell Biol* 1988 Nov;107(5):1995-2006.
- (13) Poole AR, Pidoux I, Reiner A, Rosenberg L. An immunoelectron microscope study of the organization of proteoglycan monomer, link protein, and collagen in the matrix of articular cartilage
99. *J Cell Biol* 1982 Jun;93(3):921-37.
- (14) Poole CA, Flint MH, Beaumont BW. Morphological and functional interrelationships of articular cartilage matrices. *J Anat* 1984 Jan;138(Pt 1):113-38.
- (15) STOCKWELL RA. Structural and histochemical aspects of the pericellular environment in cartilage. *Philos Trans R Soc Lond B Biol Sci* 1975 Jul 17;271(912):243-5.
- (16) Poole AR, Pidoux I, Reiner A, Rosenberg L. An immunoelectron microscope study of the organization of proteoglycan monomer, link protein, and collagen in the matrix of articular cartilage
99. *J Cell Biol* 1982 Jun;93(3):921-37.
- (17) Poole AR, Kojima T, Yasuda T, Mwale F, Kobayashi M, Lavery S. Composition and structure of articular cartilage - A template for tissue repair. *Clinical Orthopaedics and Related Research* 2001;(391):S26-S33.
- (18) de Bont LG, Liem RS, Havinga P, Boering G, van der KJ. Collagenous network in cartilage of human femoral condyles. A light microscopic and scanning electron microscopic study. *Acta Anat (Basel)* 1986;126(1):41-7.
- (19) Jeffery AK, Blunn GW, Archer CW, Bentley G. Three-dimensional collagen architecture in bovine articular cartilage. *J Bone Joint Surg Br* 1991 Sep;73(5):795-801.
- (20) Lai WM, Hou JS, Mow VC. A triphasic theory for the swelling and deformation behaviors of articular cartilage. *J Biomech Eng* 1991 Aug;113(3):245-58.

- (21) Mow VC, Wang CC, Hung CT. The extracellular matrix, interstitial fluid and ions as a mechanical signal transducer in articular cartilage. *Osteoarthritis Cartilage* 1999 Jan;7(1):41-58.
- (22) Maroudas AI. Balance between swelling pressure and collagen tension in normal and degenerate cartilage. *Nature* 1976 Apr 29;260(5554):808-9.
- (23) LINN FC, SOKOLOFF L. MOVEMENT AND COMPOSITION OF INTERSTITIAL FLUID OF CARTILAGE. *Arthritis Rheum* 1965 Aug;8:481-94.:481-94.
- (24) Yoshikawa T, Nishida K, Doi T, Inoue H, Ohtsuka A, Taguchi T, et al. Negative charges bound to collagen fibrils in the rabbit articular cartilage: a light and electron microscopic study using cationic colloidal iron. *Arch Histol Cytol* 1997 Dec;60(5):435-43.
- (25) Cancedda R, Descalzi CF, Castagnola P. Chondrocyte differentiation. *Int Rev Cytol* 1995;159:265-358.:265-358.
- (26) Cancedda R, Castagnola P, Cancedda FD, Dozin B, Quarto R. Developmental control of chondrogenesis and osteogenesis. *Int J Dev Biol* 2000;44(6):707-14.
- (27) Olsen BR, Reginato AM, Wang W. Bone development. *Annu Rev Cell Dev Biol* 2000;16:191-220.:191-220.
- (28) Ganan Y, Macias D, Duterque-Coquillaud M, Ros MA, Hurlle JM. Role of TGF beta s and BMPs as signals controlling the position of the digits and the areas of interdigital cell death in the developing chick limb autopod. *Development* 1996 Aug;122(8):2349-57.
- (29) Vogel A, Rodriguez C, Izpisua-Belmonte JC. Involvement of FGF-8 in initiation, outgrowth and patterning of the vertebrate limb. *Development* 1996 Jun;122(6):1737-50.
- (30) Heegaard JH, Beaupre GS, Carter DR. Mechanically modulated cartilage growth may regulate joint surface morphogenesis. *J Orthop Res* 1999 Jul;17(4):509-17.
- (31) Hall BK, Miyake T. All for one and one for all: condensations and the initiation of skeletal development. *Bioessays* 2000 Feb;22(2):138-47.
- (32) Thorogood PV, Hinchliffe JR. An analysis of the condensation process during chondrogenesis in the embryonic chick hind limb. *J Embryol Exp Morphol* 1975 Jun;33(3):581-606.
- (33) Coelho CN, Kosher RA. Gap junctional communication during limb cartilage differentiation. *Dev Biol* 1991 Mar;144(1):47-53.
- (34) Ahrens PB, Solursh M, Reiter RS. Stage-related capacity for limb chondrogenesis in cell culture. *Dev Biol* 1977 Oct 1;60(1):69-82.

- (35) DeLise AM, Fischer L, Tuan RS. Cellular interactions and signaling in cartilage development. *Osteoarthritis Cartilage* 2000 Sep;8(5):309-34.
- (36) San Antonio JD, Tuan RS. Chondrogenesis of limb bud mesenchyme in vitro: stimulation by cations. *Dev Biol* 1986 Jun;115(2):313-24.
- (37) Dessau W, von der MH, von der MK, Fischer S. Changes in the patterns of collagens and fibronectin during limb-bud chondrogenesis. *J Embryol Exp Morphol* 1980 Jun;57:51-60.:51-60.
- (38) Cao L, Lee V, Adams ME, Kiani C, Zhang Y, Hu W, et al. beta-Integrin-collagen interaction reduces chondrocyte apoptosis 58. *Matrix Biol* 1999 Aug;18(4):343-55.
- (39) Lee JW, Kim YH, Kim SH, Han SH, Hahn SB. Chondrogenic differentiation of mesenchymal stem cells and its clinical applications 35. *Yonsei Med J* 2004 Jun 30;45 Suppl:41-7.:41-7.
- (40) Horton WA, Machado MM. Extracellular matrix alterations during endochondral ossification in humans. *J Orthop Res* 1988;6(6):793-803.
- (41) Mackie EJ, Ahmed YA, Tatarczuch L, Chen KS, Mirams M. Endochondral ossification: how cartilage is converted into bone in the developing skeleton. *Int J Biochem Cell Biol* 2008;40(1):46-62.
- (42) Shimizu H, Yokoyama S, Asahara H. Growth and differentiation of the developing limb bud from the perspective of chondrogenesis. *Development Growth & Differentiation* 2007;49(6):449-54.
- (43) Castagnola P, Moro G, scalzi-Cancedda F, Cancedda R. Type X collagen synthesis during in vitro development of chick embryo tibial chondrocytes 4. *J Cell Biol* 1986 Jun;102(6):2310-7.
- (44) Delise AM, Fischer L, Tuan RS. Cellular interactions and signaling in cartilage development. *Osteoarthritis Cartilage* 2000 Sep;8(5):309-34.
- (45) Thorp BH, Anderson I, Jakowlew SB. Transforming growth factor-beta 1, -beta 2 and -beta 3 in cartilage and bone cells during endochondral ossification in the chick. *Development* 1992 Apr;114(4):907-11.
- (46) Chen D, Zhao M, Mundy GR. Bone morphogenetic proteins. *Growth Factors* 2004 Dec;22(4):233-41.
- (47) Oh CD, Chun JS. Signaling mechanisms leading to the regulation of differentiation and apoptosis of articular chondrocytes by insulin-like growth factor-1. *J Biol Chem* 2003 Sep;278(38):36563-71.
- (48) Phornphutkul C, Wu KY, Yang X, Chen Q, Gruppuso PA. Insulin-like growth factor-I signaling is modified during chondrocyte differentiation. *J Endocrinol* 2004 Dec;183(3):477-86.

- (49) Martel-Pelletier J, Di Battista JA, Lajeunesse D, Pelletier JP. IGF/IGFBP axis in cartilage and bone in osteoarthritis pathogenesis. *Inflamm Res* 1998 Mar;47(3):90-100.
- (50) Oh CD, Chun JS. Signaling mechanisms leading to the regulation of differentiation and apoptosis of articular chondrocytes by insulin-like growth factor-1. *J Biol Chem* 2003 Sep;278(38):36563-71.
- (51) Olney RC, Wang J, Sylvester JE, Mougey EB. Growth factor regulation of human growth plate chondrocyte proliferation in vitro. *Biochem Biophys Res Commun* 2004 May 14;317(4):1171-82.
- (52) Bauer M, Jackson RW. Chondral lesions of the femoral condyles: a system of arthroscopic classification. *Arthroscopy* 1988;4(2):97-102.
- (53) Brittberg M, Winalski CS. Evaluation of cartilage injuries and repair. *J Bone Joint Surg Am* 2003;85-A Suppl 2:58-69.:58-69.
- (54) Redman SN, Oldfield SF, Archer CW. Current strategies for articular cartilage repair. *Eur Cell Mater* 2005 Apr 14;9:23-32; discussion 23-32.:23-32.
- (55) Hunziker EB. Articular cartilage repair: are the intrinsic biological constraints undermining this process insuperable? *Osteoarthritis Cartilage* 1999 Jan;7(1):15-28.
- (56) Caplan AI, Elyaderani M, Mochizuki Y, Wakitani S, Goldberg VM. Principles of cartilage repair and regeneration. *Clin Orthop Relat Res* 1997 Sep;(342):254-69.
- (57) Shapiro F, Koide S, Glimcher MJ. Cell origin and differentiation in the repair of full-thickness defects of articular cartilage. *J Bone Joint Surg Am* 1993 Apr;75(4):532-53.
- (58) Buckwalter JA, Mankin HJ, Grodzinsky AJ. Articular cartilage and osteoarthritis. *Instr Course Lect* 2005;54:465-80.:465-80.
- (59) Almarza AJ, Athanasiou KA. Design characteristics for the tissue engineering of cartilaginous tissues. *Ann Biomed Eng* 2004 Jan;32(1):2-17.
- (60) Chang RW, Falconer J, Stulberg SD, Arnold WJ, Manheim LM, Dyer AR. A randomized, controlled trial of arthroscopic surgery versus closed-needle joint lavage for patients with osteoarthritis of the knee. *Arthritis Rheum* 1993 Mar;36(3):289-96.
- (61) Hubbard MJ. Articular debridement versus washout for degeneration of the medial femoral condyle. A five-year study. *J Bone Joint Surg Br* 1996 Mar;78(2):217-9.
- (62) Beaver RJ, Mahomed M, Backstein D, Davis A, Zukor DJ, Gross AE. Fresh osteochondral allografts for post-traumatic defects in the knee. A survivorship analysis. *J Bone Joint Surg Br* 1992 Jan;74(1):105-10.

- (63) Hangody L, Vasarhelyi G, Hangody LR, Sukosd Z, Tibay G, Bartha L, et al. Autologous osteochondral grafting--technique and long-term results. *Injury* 2008 Apr;39 Suppl 1:S32-9.:S32-S39.
- (64) Hangody L, Kish G, Karpati Z, Szerb I, Udvarhelyi I. Arthroscopic autogenous osteochondral mosaicplasty for the treatment of femoral condylar articular defects. A preliminary report. *Knee Surg Sports Traumatol Arthrosc* 1997;5(4):262-7.
- (65) Temenoff JS, Mikos AG. Review: tissue engineering for regeneration of articular cartilage. *Biomaterials* 2000 Mar;21(5):431-40.
- (66) Jakob M, Demarteau O, Schafer D, Hintermann B, Dick W, Heberer M, et al. Specific growth factors during the expansion and redifferentiation of adult human articular chondrocytes enhance chondrogenesis and cartilaginous tissue formation in vitro. *J Cell Biochem* 2001 Mar 26;81(2):368-77.
- (67) Benya PD, Shaffer JD. Dedifferentiated chondrocytes reexpress the differentiated collagen phenotype when cultured in agarose gels. *Cell* 1982 Aug;30(1):215-24.
- (68) Benya PD, Shaffer JD. Dedifferentiated chondrocytes reexpress the differentiated collagen phenotype when cultured in agarose gels. *Cell* 1982 Aug;30(1):215-24.
- (69) Binette F, McQuaid DP, Haudenschild DR, Yaeger PC, McPherson JM, Tubo R. Expression of a stable articular cartilage phenotype without evidence of hypertrophy by adult human articular chondrocytes in vitro. *J Orthop Res* 1998 Mar;16(2):207-16.
- (70) Benya PD, Shaffer JD. Dedifferentiated chondrocytes reexpress the differentiated collagen phenotype when cultured in agarose gels. *Cell* 1982 Aug;30(1):215-24.
- (71) Bonaventure J, Kadhom N, Cohen-Solal L, Ng KH, Bourguignon J, Lasselin C, et al. Reexpression of cartilage-specific genes by dedifferentiated human articular chondrocytes cultured in alginate beads. *Exp Cell Res* 1994 May;212(1):97-104.
- (72) Benya PD, Shaffer JD. Dedifferentiated chondrocytes reexpress the differentiated collagen phenotype when cultured in agarose gels. *Cell* 1982 Aug;30(1):215-24.
- (73) Grigolo B, Lisignoli G, Piacentini A, Fiorini M, Gobbi P, Mazzotti G, et al. Evidence for redifferentiation of human chondrocytes grown on a hyaluronan-based biomaterial (HYAff 11): molecular, immunohistochemical and ultrastructural analysis. *Biomaterials* 2002 Feb;23(4):1187-95.
- (74) Martin I, Shastri VP, Padera RF, Yang J, Mackay AJ, Langer R, et al. Selective differentiation of mammalian bone marrow stromal cells cultured on three-dimensional polymer foams. *J Biomed Mater Res* 2001 May;55(2):229-35.
- (75) Grigolo B, Lisignoli G, Piacentini A, Fiorini M, Gobbi P, Mazzotti G, et al. Evidence for redifferentiation of human chondrocytes grown on a hyaluronan-based biomaterial (HYAff 11): molecular, immunohistochemical and ultrastructural analysis. *Biomaterials* 2002 Feb;23(4):1187-95.

- (76) Caplan AI. Mesenchymal stem cells. *J Orthop Res* 1991 Sep;9(5):641-50.
- (77) Prockop DJ. Marrow stromal cells as stem cells for nonhematopoietic tissues. *Science* 1997 Apr 4;276(5309):71-4.
- (78) Caplan AI. Mesenchymal stem cells. *J Orthop Res* 1991 Sep;9(5):641-50.
- (79) Pittenger MF, Mackay AM, Beck SC, Jaiswal RK, Douglas R, Mosca JD, et al. Multilineage potential of adult human mesenchymal stem cells. *Science* 1999 Apr 2;284(5411):143-7.
- (80) Johnstone B, Hering TM, Caplan AI, Goldberg VM, Yoo JU. In vitro chondrogenesis of bone marrow-derived mesenchymal progenitor cells. *Exp Cell Res* 1998 Jan 10;238(1):265-72.
- (81) Yoo JU, Barthel TS, Nishimura K, Solchaga L, Caplan AI, Goldberg VM, et al. The chondrogenic potential of human bone-marrow-derived mesenchymal progenitor cells. *J Bone Joint Surg Am* 1998 Dec;80(12):1745-57.
- (82) Johnstone B, Hering TM, Caplan AI, Goldberg VM, Yoo JU. In vitro chondrogenesis of bone marrow-derived mesenchymal progenitor cells. *Exp Cell Res* 1998 Jan 10;238(1):265-72.
- (83) Martin I, Shastri VP, Padera RF, Yang J, Mackay AJ, Langer R, et al. Selective differentiation of mammalian bone marrow stromal cells cultured on three-dimensional polymer foams. *J Biomed Mater Res* 2001 May;55(2):229-35.
- (84) Steadman JR, Rodkey WG, Rodrigo JJ. Microfracture: surgical technique and rehabilitation to treat chondral defects. *Clin Orthop Relat Res* 2001 Oct;(391 Suppl):S362-S369.
- (85) Frisbie DD, Oxford JT, Southwood L, Trotter GW, Rodkey WG, Steadman JR, et al. Early events in cartilage repair after subchondral bone microfracture. *Clin Orthop Relat Res* 2003 Feb;(407):215-27.
- (86) Kramer J, Bohrsen F, Lindner U, Behrens P, Schlenke P, Rohwedel J. In vivo matrix-guided human mesenchymal stem cells. *Cell Mol Life Sci* 2006 Feb 16;.
- (87) Breinan HA, Martin SD, Hsu HP, Spector M. Healing of canine articular cartilage defects treated with microfracture, a type-II collagen matrix, or cultured autologous chondrocytes. *J Orthop Res* 2000 Sep;18(5):781-9.
- (88) Dorotka R, Windberger U, Macfelda K, Bindreiter U, Toma C, Nehrer S. Repair of articular cartilage defects treated by microfracture and a three-dimensional collagen matrix. *Biomaterials* 2005 Jun;26(17):3617-29.
- (89) Breinan HA, Martin SD, Hsu HP, Spector M. Healing of canine articular cartilage defects treated with microfracture, a type-II collagen matrix, or cultured autologous chondrocytes. *J Orthop Res* 2000 Sep;18(5):781-9.

- (90) Dorotka R, Windberger U, Macfelda K, Bindreiter U, Toma C, Nehrer S. Repair of articular cartilage defects treated by microfracture and a three-dimensional collagen matrix. *Biomaterials* 2005 Jun;26(17):3617-29.
- (91) Dorotka R, Bindreiter U, Macfelda K, Windberger U, Nehrer S. Marrow stimulation and chondrocyte transplantation using a collagen matrix for cartilage repair. *Osteoarthritis Cartilage* 2005 Aug;13(8):655-64.
- (92) Breinan HA, Martin SD, Hsu HP, Spector M. Healing of canine articular cartilage defects treated with microfracture, a type-II collagen matrix, or cultured autologous chondrocytes. *J Orthop Res* 2000 Sep;18(5):781-9.
- (93) Pittenger MF, Mackay AM, Beck SC, Jaiswal RK, Douglas R, Mosca JD, et al. Multilineage potential of adult human mesenchymal stem cells. *Science* 1999;284(5411):143-7.
- (94) Johnstone B, Hering TM, Caplan AI, Goldberg VM, Yoo JU. In vitro chondrogenesis of bone marrow-derived mesenchymal progenitor cells. *Experimental Cell Research* 1998;238(1):265-72.
- (95) Darling EM, Athanasiou KA. Rapid phenotypic changes in passaged articular chondrocyte subpopulations. *Journal of Orthopaedic Research* 2005 Mar;23(2):425-32.
- (96) Benya PD, Shaffer JD. Dedifferentiated chondrocytes reexpress the differentiated collagen phenotype when cultured in agarose gels. *Cell* 1982 Aug;30(1):215-24.
- (97) Stockdale FE, Abbott J, Holtzer S, Holtzer H. The loss of phenotypic traits by differentiated cells : II. Behavior of chondrocytes and their progeny in vitro. *Developmental Biology* 1963;7:293-302.
- (98) Marlovits S, Hombauer M, Truppe M, Vecsei V, Schlegel W. Changes in the ratio of type-I and type-II collagen expression during monolayer culture of human chondrocytes. *J Bone Joint Surg Br* 2004 Mar 1;86-B(2):286-95.
- (99) Aulthouse A, Beck M, Griffey E, Sanford J, Arden K, Machado M, et al. Expression of the human chondrocyte phenotype in vitro. *In Vitro Cellular & Developmental Biology - Plant* 1989 Jul 1;25(7):659-68.
- (100) Barbero A, Ploegert S, Heberer M, Martin I. Plasticity of Clonal Populations of Dedifferentiated Adult Human Articular Chondrocytes. *Arthritis & Rheumatism* 2003;48(5):1315-25.
- (101) Wolf F, Candrian C, Wendt D, Farhadi J, Heberer M, Martin I, et al. Cartilage Tissue Engineering Using Pre-Aggregated Human Articular Chondrocytes. *European Cells & Materials* 2008;16:92-9.
- (102) Barbero A, Grogan S.P., Schafer D, Heberer M, Mainil-Varlet P. Age Related Changes in Human Articular Chondrocyte Yield, Proliferation and Post-expansion chondrogenic capacity. *Osteoarthritis and Cartilage* 2004;12:476-84.

- (103) Soen Y, Mori A, Palmer TD, Brown PO. Exploring the Regulation of Human Neural Precursor Cell Differentiation Using Arrays of Signalling Microenvironments. *Mol Syst Biol* 2006;2:37.
- (104) Battista S, Guarnieri D, Borselli C, Zeppetelli S, Borzacciello A, Mayol L, et al. The Effect of Matrix Composition of 3D Constructs on Embryonic Stem Cell Differentiation. *Biomaterials* 2005;26:6194-207.
- (105) Xu.C., He JQ, Kamp TJ, Police S, Hao X, O'Sullivan C, et al. Human Embryonic Stem Cell-Derived Cardiomyocytes can be Maintained in Defined Medium Without Serum. *Stem Cells Dev* 2006;15:931-41.
- (106) Mallon BS, Park K-J, Chen KG, Hamilton RS, McKay RDG. Toward Xeno-Free Culture of Human Embryonic Stem Cells. *Biochem Cell Biol* 2006;38:1063-75.
- (107) Martin MJ, Muotori A, Gage F, Varki A. Human Embryonic Stem Cells Express an Immunogenic Nonhuman Sialic Acid. *Nat Med* 2005;11:228-32.
- (108) Saha K, Pollok J, Schaffer DV, Healy K. Designing synthetic materials to control stem cell phenotype. *Current Opinion in Chemical Biology* 2007;11:381-7.
- (109) Engler AJ, Sen S, Sweeney HL, Discher DE. Matrix elasticity directs stem cell lineage specification. *Cell* 2006;126(4):677-89.
- (110) Kong HJ, Polte TR, Alsberg E, Mooney DJ. Fret Measurements of Cell-traction Forces and Nano-scale Clustering of Adhesion Ligands Varied by Substrate Stiffness. *Procl Nat Acad Sci USA* 2005;102:4300-5.
- (111) Kreiner M, Li Z, Beattie J, Kelly SM, Mardon HJ, van der Walle CF. Self-assembling multimeric integrin alpha 5 beta 1 ligands for cell attachment and spreading. *Protein Engineering Design & Selection* 2008;21(9):553-60.
- (112) Maheshwari G, Brown G, Lauffenburger DA, Wells A, Griffith LG. Cell adhesion and motility depend on nanoscale RGD clustering. *Journal of Cell Science* 2000;113(10):1677-86.
- (113) Mahmood TA, Miot S, Frank O, Martin I, Riesle J, Langer R, et al. Modulation of chondrocyte phenotype for tissue engineering by designing the biologic-polymer carrier interface. *Biomacromolecules* 2006;7(11):3012-8.
- (114) Tziampazis E, Kohn J, Moghe P.V. PEG-variant Biomaterials as Selectively Adhesive Proteins Templates: Model Surfaces for Controlled Cell Adhesion and Migration. *Biomaterials* 2000;21:511-20.
- (115) Malda J, Woodfield TBF, van der Vloodt F, Kooy FK, Martens DE, Tramper J, et al. The effect of PEGT/PBT scaffold architecture on oxygen gradients in tissue engineered cartilaginous constructs. *Biomaterials* 2004;25(26):5773-80.

- (116) Malda J, Woodfield TBF, van der Vloodt F, Wilson C, Martens DE, Tramper J, et al. The effect of PEGT/PBT scaffold architecture on the composition of tissue engineered cartilage. *Biomaterials* 2005;26(1):63-72.
- (117) Miot S, Woodfield T, Daniels AU, Suetterlin R, Peterschmitt I, Heberer M, et al. Effects of scaffold composition and architecture on human nasal chondrocyte redifferentiation and cartilaginous matrix deposition. *Biomaterials* 2005;26(15):2479-89.
- (118) Woodfield TBF, Malda J, de Wijn J, Peters F, Riesle J, van Blitterswijk CA. Design of porous scaffolds for cartilage tissue engineering using a three-dimensional fiber-deposition technique. *Biomaterials* 2004;25(18):4149-61.
- (119) McBeath R, Pirone DM, Nelson CM, Bhadriraju K, Chen CS. Cell Shape, Cytoskeletal Tension, and RhoA Regulate Stem Cell Lineage Commitment. *Developmental Cell* 2004 Apr;6(4):483-95.
- (120) Du C, Meijer GJ, van de Valk C, Haan RE, Bezemer JM, Hesseling SC, et al. Bone growth in biomimetic apatite coated porous Polyactive((R)) 1000PEGT70PBT30 implants. *Biomaterials* 2002;23(23):4649-56.
- (121) Ghosh S, Laha M, Mondal S, Sengupta S, Kaplan DL. In vitro model of mesenchymal condensation during chondrogenic development. *Biomaterials* 2009;30(33):6530-40.
- (122) Ji Y, Ghosh K, Shu XZ, Li BQ, Sokolov JC, Prestwich GD, et al. Electrospun three-dimensional hyaluronic acid nanofibrous scaffolds. *Biomaterials* 2006;27(20):3782-92.
- (123) Moroni L, Licht R, de Boer J, de Wijn JR, van Blitterswijk CA. Fiber diameter and texture of electrospun PEOT/PBT scaffolds influence human mesenchymal stem cell proliferation and morphology, and the release of incorporated compounds. *Biomaterials* 2006;27(28):4911-22.
- (124) Yasui N, Osawa S, Ochi T, Nakashima H, Ono K. Primary Culture of Chondrocytes Embedded in Collagen Gels. *Exp Cell Biol* 1982;50:92-100.
- (125) Watt F, Dudhia J. Prolonged Expression of Differentiated Phenotype by Chondrocytes Cultured at Low Density on a Composite Substrate of Collagen and Agarose that Restricts Cell Spreading. *Differentiation* 1988;38:140-7.
- (126) Park Y, Lutolf MP, Hubbell JA, Hunziker EB, Wong M. Bovine primary chondrocyte culture in synthetic matrix metalloproteinase-sensitive poly(ethylene glycol)-based hydrogels as a scaffold for cartilage repair. *Tissue Engineering* 2004;10(3-4):515-22.
- (127) Erickson IE, Huang AH, Chung C, Li RT, Burdick JA, Mauck RL. Differential Maturation and Structure–Function Relationships in Mesenchymal Stem Cell- and Chondrocyte-Seeded Hydrogels. *Tissue Engineering Part A* 2009 May 1;15(5):1041-52.

- (128) Kino-Oka M, Yashiki S, Ota Y, Mushiaki Y, Sugawara K, Yamamoto T, et al. Subculture of Chondrocytes on a Collagen Type I-Coated Substrate with Suppressed Cellular Dedifferentiation. *Tissue Engineering* 2005;11(3-4):597-608.
- (129) Shakibei M, DE SOUZA P, MERKER H-J. Integrin Expression and Collagen Type II Implicated in Maintenance of Chondrocyte Shape in Monolayer Culture: An Immunomorphological Study. *Cell Biology International* 1997 Feb;21(2):115-25.
- (130) Rowlands AS, George PA, Cooper-White JJ. Directing osteogenic and myogenic differentiation of MSCs: interplay of stiffness and adhesive ligand presentation. *American Journal of Physiology-Cell Physiology* 2008;295(4):C1037-C1044.
- (131) Chastain SR, Kundu AK, Dhar S, Calvert JW, Putnam AJ. Adhesion of mesenchymal stem cells to polymer scaffolds occurs via distinct ECM ligands and controls their osteogenic differentiation. *Journal of Biomedical Materials Research Part A* 2006;78A(1):73-85.
- (132) Engler A, Bacakova L, Newman C, Hategan A, Griffin M, Discher D. Substrate compliance versus ligand density in cell on gel responses. *Biophysical Journal* 2004;86(1):617-28.
- (133) Xia N, Thodeti CK, Hunt TP, Xu QB, Ho M, Whitesides GM, et al. Directional control of cell motility through focal adhesion positioning and spatial control of Rac activation. *Faseb Journal* 2008;22(6):1649-59.
- (134) Lehnert D, Wehrle-Haller B, David C, Weiland U, Ballestrem C, Imhof BA, et al. Cell behaviour on micropatterned substrata: limits of extracellular matrix geometry for spreading and adhesion. *Journal of Cell Science* 2004;117(1):41-52.
- (135) Petrie TA, Capadona JR, Reyes CD, Garcia AJ. Integrin specificity and enhanced cellular activities associated with surfaces presenting a recombinant fibronectin fragment compared to RGD supports. *Biomaterials* 2006;27(31):5459-70.
- (136) Connelly JT, Garcia AJ, Levenston ME. Interactions between integrin ligand density and cytoskeletal integrity regulate BMSC chondrogenesis. *Journal of Cellular Physiology* 2008;217(1):145-54.
- (137) Grant RP, Spitzfaden C, Altroff H, Campbell ID, Mardon HJ. Structural Requirements for Biological Activity of the Ninth and Tenth FIII Domains of Human Fibronectin. *Journal of Biological Chemistry* 1997 Mar 7;272(10):6159-66.
- (138) Kato R, Kaga C, Kunimatsu M, Kobayashi T, Honda H. Peptide array-based interaction assay of solid-bound peptides and anchorage-dependant cells and its effectiveness in cell-adhesive peptide design. *Journal of Bioscience and Bioengineering* 2006;101(6):485-95.
- (139) Schuler M, Hamilton DW, Kunzler TP, Sprecher CM, de Wild M, Brunette DM, et al. Comparison of the Response of Cultured Osteoblasts and Osteoblasts

Outgrown From Rat Calvarial Bone Chips to Nonfouling KRSR and FHRIKA-Peptide Modified Rough Titanium Surfaces. *Journal of Biomedical Materials Research Part B-Applied Biomaterials* 2009;91B(2):517-27.

- (140) Vonwil D, Schuler M, Barbero A, Ströbel S, Wendt D, Textor M, et al. RGD-Peptide Restricted Interactions with a Protein Resistant Substrate are Sufficient for Human Articular Chondrocyte Adhesion, Growth and Maintenance of Cartilage Forming Capacity. Submitted to *Softmatter* 2010.
- (141) Hersel U, Dahmen C, Kessler H. RGD Modified Polymers: Biomaterials for Stimulated Cell Adhesion and Beyond. *Biomaterials* 2003;24:4385-415.
- (142) Saha K, Pollock JF, Schaffer DV, Healy KE. Designing synthetic materials to control stem cell phenotype. *Current Opinion in Chemical Biology* 2007;11(4):381-7.
- (143) Goffin JM, Pittet P, Csucs G, Lussi JW, Meister J.J., Hinz B. Focal Adhesion Size Controls Tension-dependent Recruitment of α -Smooth Muscle Actin to Stress Fibers. *Journal of Cell Biology* 2006;172(2):259-68.
- (144) Pelham Jr. RJ, Wang J. Cell Locomotion and Focal Adhesions are Regulated by Substrate Flexibility. *Proc Nat Acad Sci USA* 1997;94:3661-5.
- (145) Engler AJ, Griffin MA, Sen S, Bonnetmann CG, Sweeney HL, Discher DE. Myotubes differentiate optimally on substrates with tissue-like stiffness: pathological implications for soft or stiff microenvironments. *Journal of Cell Biology* 2004;166(6):877-87.
- (146) Peyton SR, Putnam A.J. Extracellular Matrix Rigidity Governs Smooth Muscle Motility in a Biphasic Fashion. *Journal of Cell Physiology* 2004;204:198-209.
- (147) Saha K, Pollock JF, Schaffer DV, Healy KE. Designing Synthetic Materials to Control Stem Cell Phenotype. *Curr Op Chem Biol* 2007;11:381-7.
- (148) Sittinger M, Perka C, Schultz O, Haupl T, Burmester GR. Joint Cartilage Regeneration by Tissue Engineering. *Z Rheumatol* 1999;58:130-5.
- (149) Hunziker EB. Articular cartilage repair: basic science and clinical progress. A review of the current status and prospects. *Osteoarthritis Cartilage* 2002 Jun;10(6):432-63.
- (150) Redman SN, Oldfield SF, Archer CW. Current strategies for articular cartilage repair. *Eur Cell Mater* 2005 Apr 14;9:23-32; discussion 23-32.:23-32.
- (151) Vinatier C, Mrugala D, Jorgensen C, Guicheux J, Noel D. Cartilage engineering: a crucial combination of cells, biomaterials and biofactors. *Trends in Biotechnology* 2009;27(5):307-14.
- (152) Richter W. Mesenchymal stem cells and cartilage in situ regeneration. *Journal of Internal Medicine* 2009;266(4):390-405.

- (153) Endo T, Bryant SV, Gardiner DM. A Stepwise Model System for Limb Regeneration. *Developmental Biology* 2004;270:135-45.
- (154) Frank O, Heim M, Jakob M, Barbero A, Schafer D, Bendik I, et al. Real-time quantitative RT-PCR analysis of human bone marrow stromal cells during osteogenic differentiation *in vitro*. *Journal of Cellular Biochemistry* 2002;85(4):737-46.
- (155) Bianchi G, Banfi A, Mastrogiacomo M, Notaro R, Luzzatto L, Cancedda R, et al. Ex vivo enrichment of mesenchymal cell progenitors by fibroblast growth factor 2. *Experimental Cell Research* 2003 Jul 1;287(1):98-105.
- (156) Yoo JU, Barthel TS, Nishimura K, Solchaga L, Caplan AI, Goldberg VM, et al. The chondrogenic potential of human bone-marrow-derived mesenchymal progenitor cells. *Journal of Bone and Joint Surgery-American Volume* 1998;80A(12):1745-57.
- (157) Hollander AP, Heathfield TF, Webber C, Iwata YBR, Rorabeck A. Increased Damage to Type II Collagen in Osteoarthritic Articular Cartilage Detected by a New Immunoassay. *J Clin Invest* 1994;93:1722-32.
- (158) Farndale R.W., Buttle DJ, Barrett A.J. Improved Quantitation and Discrimination of Sulfphated Glycosaminoglycans by use of Dimethylene Blue. *Biochim Biophys Acta* 1986;883:173-7.
- (159) Grogan S.P., Rieser F., Winkelmann V., Berardi S., Mainil-Varlet P. Static, Closed and Scaffold-Free Bioreactor System that Permits Chondrogenesis *in vitro*. *Osteoarthritis Cart* 2003;11:403-11.
- (160) Lee JH, Kopecek J, Andrade JD. Protein-Resistant Surfaces Prepared by PEO-Containing Block Copolymer Surfactants. *Journal of Biomedical Materials Research* 1989;23(3):351-68.
- (161) Grassel S, Ahmed N. Influence of cellular microenvironment and paracrine signals on chondrogenic differentiation. *Frontiers in Bioscience* 2007;12:4946-56.
- (162) Schueller G, Tichy B, Jagersberger T, Van Griensven M, Marlovits S, Redl H. Human cartilage regeneration in an in-vivo mouse model. *Tissue Engineering* 2007;13(7):216.
- (163) Bang OS, Kim EJ, Chung JG, Lee SR, Park TK, Kang SS. Association of Focal Adhesion Kinase with Fibronectin and Paxillin Is Required for Precartilage Condensation of Chick Mesenchymal Cells. *Biochemical and Biophysical Research Communications* 2000 Nov 30;278(3):522-9.
- (164) Kang SS. Regulation of early steps of chondrogenesis in the developing limb. *Animal Cells and Systems* 2008;12(1):1-9.

- (165) Woods A, Wang GY, Beier F. RhoA/ROCK signaling regulates Sox9 expression and actin organization during chondrogenesis. *Journal of Biological Chemistry* 2005;280(12):11626-34.
- (166) Bilgen B, Orsini E, Aaron RK, Ciombor DM. FBS suppresses TGF-beta 1-induced chondrogenesis in synoviocyte pellet cultures while dexamethasone and dynamic stimuli are beneficial. *Journal of Tissue Engineering and Regenerative Medicine* 2007;1(6):436-42.
- (167) Homminga GN, Buma P, Koot HWJ, Vanderkraan PM, Vandenberg WB. Chondrocyte Behavior in Fibrin Glue In-Vitro. *Acta Orthopaedica Scandinavica* 1993;64(4):441-5.
- (168) Neuss S, Schneider RKM, Tietze L, Knuchel R, Jahnen-Dechent W. Secretion of Fibrinolytic Enzymes Facilitates Human Mesenchymal Stem Cell Invasion into Fibrin Clots. *Cells Tissues Organs* 2010;191(1):36-46.
- (169) Brittberg M. Autologous chondrocyte implantation--Technique and long-term follow-up. *Injury* 2008 Apr;39(1, Supplement 1):40-9.
- (170) Horbett TA. Techniques for protein adsorption studies. In: D.F. Williams, editor. *In Techniques of Biocompatibility Testing II*. CRC Press Boca Raton; 1986. p. 183-213.
- (171) Koenig AL, Gambillara V, Grainger DW. Correlating Fibronectin Adsorption with Endothelial Cell Adhesion and Signalling on Polymer Substrates. *J Biomed Mater Res* 2003;64:20-37.
- (172) Scully SP, Lee JW, Ghert MA, i W. The Role of the Extracellular Matrix in Articular Chondrocyte Regulation. *Clinical Orthopaedics and Related Research* 2001;391:S72-S89.
- (173) van der Kraan PM, Buma P, van Kuppevelt T, van Den Berg WB. Interaction of chondrocytes, extracellular matrix and growth factors: relevance for articular cartilage tissue engineering. *Osteoarthritis and Cartilage* 2002 Aug;10(8):631-7.
- (174) Brodtkin KR, Garcia AJ, Levenston ME. Chondrocyte phenotypes on different extracellular matrix monolayers. *Biomaterials* 2004 Dec;25(28):5929-38.
- (175) Barbero A, Grogan SP, Mainil-Varlet P, Martin I. Expansion on Specific Substrates Regulates the Phenotype and Differentiation Capacity of Human Articular Chondrocytes. *Journal of Cellular Biochemistry* 2006;98:1140-9.
- (176) Mrksich M. What can surface chemistry do for cell biology? *Current Opinion in Chemical Biology* 2002 Dec 1;6(6):794-7.
- (177) Talbot J, Tarjus G, Van Tassel PR, Viot P. From car parking to protein adsorption: an overview of sequential adsorption processes. *Colloids and Surfaces A: Physicochemical and Engineering Aspects* 2000 May 30;165(1-3):287-324.

- (178) Nakanishi K, Sakiyama T, Imamura K. On the adsorption of proteins on solid surfaces, a common but very complicated phenomenon. *Journal of Bioscience and Bioengineering* 2001;91(3):233-44.
- (179) Hubbell JA. Bioactive biomaterials. *Current Opinion in Biotechnology* 1999 Apr 1;10(2):123-9.
- (180) Ruoslahti E. RGD and other Recognition Sequences for Integrins. *Annual Review of Cell and Developmental Biology* 1996 Nov 1;12(1):697-715.
- (181) Aszodi A, Hunziker EB, Brakebusch C, Fässler R. β 1 integrins regulate chondrocyte rotation, G1 progression, and cytokinesis. *Genes & Development* 2003 Oct 1;17(19):2465-79.
- (182) Garciadiego-Cázares D, Rosales C, Hatoh M, Chimal-Monroy J. Coordination of chondrocyte differentiation and joint formation by α 5 β 1 integrin in the developing appendicular skeleton. *Development* 2004;131:4735-42.
- (183) Pasche S, Voros J, Griesser HJ, Spencer ND, Textor M. Effects of Ionic Strength and Surface Charge on Protein Adsorption at PEGylated Surfaces. *The Journal of Physical Chemistry B* 2005 Aug 24;109(37):17545-52.
- (184) VandeVondele S, Vörös J, Hubbell JA. RGD-Grafted Poly-L-lysine-graft-(polyethylene glycol) Copolymers Block Non-specific Protein Adsorption While Promoting Cell Adhesion. *Biotechnology and Bioengineering* 2003;82, No. 7:784-90.
- (185) Schuler M, Trentin D, Textor M, Tosatti SGP. Biomedical interfaces: titanium surface technology for implants and cell carriers. *Nanomedicine* 2006;1(4):449-63.
- (186) Schuler M, Owen GR, Hamilton DW, De Wilde M, Textor M, Brunette DM, et al. Biomimetic Modification of Titanium Dental Implant Model Surfaces Using the RGDSP-Peptide Sequence: A Cell Morphology Study. *Biomaterials* 2006;27(21):4003-15.
- (187) Schuler M, Kunzler TP, de Wild M, Sprecher CM, Trentin D, Brunette DM, et al. Fabrication of TiO₂-coated epoxy replicas with identical dual-type surface topographies used in cell culture assays. *Journal of Biomedical Materials Research Part A* 2009;88A(1):12-22.
- (188) Image J [computer program]. Version 1.37v. U. S. National Institutes of Health, Bethesda, Maryland, USA: 2009.
- (189) Jakob M, Demartean O, Schafer D, Hintermann B, Dick W, Heberer M. Specific Growth Factors During the Expansion and Redifferentiation of Adult Human Articular Chondrocytes Enhance Chondrogenesis and Cartilaginous Tissue Formation *in vitro*. *J Cell Biochem* 2001;81:368-77.

- (190) Pasche S, De Paul SM, Voros J, Spencer ND, Textor M. Poly(l-lysine)-graft-poly(ethylene glycol) Assembled Monolayers on Niobium Oxide Surfaces: A Quantitative Study of the Influence of Polymer Interfacial Architecture on Resistance to Protein Adsorption by ToF-SIMS and in Situ OWLS. *Langmuir* 2003 Sep 13;19(22):9216-25.
- (191) Heuberger M, Drobek T, Spencer N.D. Interaction Forces and Morphology of a Protein-Resistant Poly(ethylene glycol) Layer. *Biophys J* 2005;88:495-504.
- (192) Vogel V. Mechanotransduction Involving Multimodular Proteins: Converting Force into Biochemical Signals. *Annual Review of Biophysics and Biomolecular Structure* 2006 Jun 1;35(1):459-88.
- (193) Baneyx G, Baugh L, Vogel V. Fibronectin extension and unfolding within cell matrix fibrils controlled by cytoskeletal tension. *Proceedings of the National Academy of Sciences of the United States of America* 2002 Apr 16;99(8):5139-43.
- (194) Cui YL, Qi AD, Liu WG, Wang XH, Wang H, Ma DM, et al. Biomimetic surface modification of poly(-lactic acid) with chitosan and its effects on articular chondrocytes in vitro. *Biomaterials* 2003 Sep;24(21):3859-68.
- (195) Redick SD, Settles DL, Briscoe G, Erickson HP. Defining fibronectin's cell adhesion synergy site by site-directed mutagenesis. *Journal of Cell Biology* 2000;149(2):521-7.
- (196) Ochsenhirt SE, Kokkoli E, McCarthy JB, Tirrell M. Effect of RGD secondary structure and the synergy site PHSRN on cell adhesion, spreading and specific integrin engagement. *Biomaterials* 2006;27(20):3863-74.
- (197) Mitchison TJ, Cramer LP. Actin-Based Cell Motility and Cell Locomotion. *Cell* 1996;84:371-9.
- (198) Maniwa S, Ochi M, Motomura T, Nishikori T, Chen J, Naora H. Effects of hyaluronic acid and basic fibroblast growth factor on motility of chondrocytes and synovial cells in culture. *Acta Orthopaedica Scandinavica* 2001;72(3):299-303.
- (199) Kowalczyńska HM, Kolos R, Nowak-Wyrzykowska M, Dobkowski J, Elbaum D, Szczepankiewicz A, et al. Atomic force microscopy evidence for conformational changes of fibronectin adsorbed on unmodified and sulfonated polystyrene surfaces. *Journal of Biomedical Materials Research Part A* 2009;91A(4):1239-51.
- (200) Mardon HJ, Grant KE. The Role of the 9Th and 10Th Type-Iii Domains of Human Fibronectin in Cell-Adhesion. *Febs Letters* 1994;340(3):197-201.
- (201) Majd H, Wipff PJ, Buscemi L, Bueno M, Vonwil D, Quinn TM, et al. A Novel Method of Dynamic Culture Surface Expansion Improves Mesenchymal Stem Cell Proliferation and Phenotype. *Stem Cells* 2009;27(1):200-9.

- (202) Connelly JT, Garcia AJ, Levenston ME. Inhibition of *in vitro* chondrogenesis in RGD-modified three-dimensional alginate gels. *Biomaterials* 2007;28(6):1071-83.
- (203) McNickle AG, Provencher MT, Cole BJ. Overview of Existing Cartilage Repair Technology. *Sports Medicine and Arthroscopy Review* 2008;16(4):196-201.
- (204) Kramer J, Bohrsen F, Lindner U, Behrens P, Schlenke P, Rohwedel J. *In vivo* matrix-guided human mesenchymal stem cells. *Cellular and Molecular Life Sciences* 2006;63(5):616-26.
- (205) Hall BK, Miyake T. All for one and one for all: condensations and the initiation of skeletal development. *Bioessays* 2000;22(2):138-47.
- (206) Millward-Sadler SJ, SALTER DM. Integrin Dependent Signal Cascades in Chondrocyte Mechanotransduction. *Annals of Biomedical Engineering* 2004;32:435-46.
- (207) Wells RG, Discher DE. Matrix Elasticity, Cytoskeletal Tension, and TGF- β : The Insoluble and Soluble Meet. *Science Signalling* 2008;1(10):pe13.
- (208) Schuh H, Kramer JK, Rohwedel J, Notbohm H, Müller R, Gutschmann T, et al. Effect of Matrix Elasticity on the Maintenance of the Chondrogenic Phenotype. *Tissue Engineering* 2010; ahead of print.
- (209) von der Mark H, Gauss V, von der Mark H, Müller P. Relationship Between Cell Shape and Type of Collagen Synthesised as Chondrocytes Lose their Cartilage Phenotype in Culture. *J* 1977;531-2.
- (210) Sandell LJ, Adler P. Developmental Patterns of Cartilage. *Frontiers in Bioscience* 1999;4:731-2.
- (211) Iwamoto M, Higuchi Y, Enomoto-Iwamoto M, Kurisu K, Koyama E, Yeh H, et al. The role of ERG (ets related gene) in cartilage development. *Osteoarthritis and Cartilage* 2001;9:S41-S47.
- (212) Pacifici M, Oettinger HF. Stable Phenotypic Expression by Chick Chondroblasts in Long-term Suspension Cultures as Determined by Proteoglycans Analysis. *Experimental Cell Research* 1985;161:381-92.
- (213) Häuselmann HJ, Aydelotte MB, Shumacher BL, Kuettner KE, Gitelis SH, Tonar EJMA. Synthesis and Turnover of Proteoglycans by Human and Bovine Adult Articular Chondrocytes Cultured in Alginate Beads. *Matrix* 1992;12:116-29.
- (214) Loty S, Forest N, Boulekbache H, Sautier JM. Cytochalasin D induces Changes in Cell Shape and Promotes *in vitro* Chondrogenesis: A Morphological Study. *J* 1995.
- (215) Zanetti NC, Solursh M. Induction of Chondrogenesis in Limb Mesenchymal Cultures by Disruption of the Actin Cytoskeleton. *Journal of Cell Biology* 1984;99:115-23.

- (216) Georges PC, Janmey PA. Cell type-specific response to growth on soft materials. *Journal of Applied Physiology* 2005;98(4):1547-53.
- (217) Pierschbacher E, Ruoslahti E. Cell Attachment Activity of Fibronectin can be Duplicated by Small Synthetic Fragments of the Molecule. *Nature* 1984;309:30-3.
- (218) Dessau W, Mark HVD, Mark KVD, Fischer S. Changes in the patterns of collagens and fibronectin during limb-bud chondrogenesis. *Journal of Embryology and Experimental Morphology* 1980 Jun;57(1):51-60.
- (219) Beningo KA, Lo CM, Wang YL. Flexible polyacrylamide substrata for the analysis of mechanical interactions at cell-substratum adhesions. SAN DIEGO: ACADEMIC PRESS INC; 2002.
- (220) Beningo KA, Wang YL. Flexible substrata for the detection of cellular traction forces. *Trends in Cell Biology* 2002;12(2):79-84.
- (221) Flanagan LA, Ju YE, Marg B, Osterfield M, Janmey PA. Neurite branching on deformable substrates. *Neuroreport* 2002;13(18):2411-5.
- (222) Calvet D, Wong JY, Giasson S. Rheological monitoring of polyacrylamide gelation: Importance of cross-link density and temperature. *Macromolecules* 2004;37(20):7762-71.
- (223) Harris AK, Wild P, Stopak D. Silicone rubber substrata: a new wrinkle in the study of cell locomotion. *Science* 1980 Apr 11;208(4440):177-9.
- (224) Takigawa T, Morino Y, Urayama K, Masuda T. Poisson's ratio of polyacrylamide (PAAm) gels. *Polymer Gels and Networks* 1996;4(1):1-5.
- (225) Trüssel A. The Influence of Substrate Elasticity on the Adhesion Force of Re-differentiation Human Articular Chondrocytes University of Basel; 2010.
- (226) Engler AJ, Richert L, Wong JY, Picart C, Discher DE. Surface probe measurements of the elasticity of sectioned tissue, thin gels and polyelectrolyte multilayer films: Correlations between substrate stiffness and cell adhesion. *Surface Science* 2004;570(1-2):142-54.
- (227) Solon J, Levental I, Sengupta K, Georges PC, Janmey PA. Fibroblast adaptation and stiffness matching to soft elastic substrates. *Biophysical Journal* 2007;93(12):4453-61.
- (228) Durrant LA, Archer CW, Benjamin M, Ralphs JR. Articular Chondrocytes Reorganize their Cytoskeleton in Response to Changing Mechanical Conditions in Organ Culture. *J Anat* 1999;194:343-53.
- (229) Benjamin M, Archer CW, Ralphs JR. Cytoskeleton of Cartilage Cells. *Micro Res Tec* 1994;28:372-7.

- (230) Genes GG, Rowley JA, Mooney DJ, Bonassar LJ. Effect of Substrate Mechanics on Chondrocyte Adhesion to Modified Alginate Surfaces. *Archives of Biochemistry and Biophysics* 2004;422:161-7.
- (231) Hall A, Nobes CD. *Philos Trans R Soc* 2000;355:965-70.
- (232) Aspenstrom P. *Experimental Cell Research* 1999;246:20-5.
- (233) Burridge. *Cell* 2004;167-79.
- (234) Akiyama H, Chaboissier M-C, Martin JF, Schedl A, de Crombrughe B. *Genes & Development* 2002;16:2813-28.
- (235) Bi W, Huang W, Whithworth DJ, Deng JM, Zhang Z, Behringer RR, et al. *Procl Nat Acad Sci USA* 2001;98:6698-703.
- (236) Bi W, Deng JM, Zhang Z, Behringer RR, de Crombrughe B. *Nat Genet* 1999;22:85-9.
- (237) Lefebvre V, Li P, de Crombrughe B. *EMBO Journal* 1998;17:5718-33.
- (238) Lefebvre V, Huang W, Harley VR, Goodfellow PN, de Crombrughe B. *Molecular and Cellular Biology* 1997;17:2336-46.
- (239) Arora PD, Narani N, McCulloch CA. The Compliance of Collagen Gels Regulates Transforming Growth Factor-beta Induction of Alpha-Smooth Muscle Actin in Fibroblasts. *Am J Path* 1999;154:871-82.
- (240) Tan S, Pan W, Ma G, Cai N, Leong K, Liao K. Viscoelastic behaviour of human mesenchymal stem cells. *BMC Cell Biology* 2008;9(1):40.
- (241) Zajac AL, Discher DE. Cell differentiation through tissue elasticity-coupled, myosin-driven remodeling. *Current Opinion in Cell Biology* 2008;20(6):609-15.
- (242) Wang N, Tytell JD, Ingber D. Mechanotransduction at a Distance: Mechanically Coupling the Extracellular Matrix with the Nucleus. *Nature Reviews* 10, 75-82. 2009.
Ref Type: Journal (Full)
- (243) Rowlands AS, George PA, Cooper-White JJ. Directing Osteogenic and Myogenic Differentiation of MSCs: Interplay of Stiffness and Adhesive Ligand Presentation. *Am J Physiol Cell Physiol* 2008;295:C1037-C1044.
- (244) Abott A. Cell Culture: Biologi's New Dimension. *Nature* 2003;424:870-2.
- (245) Cukierman E, Pankov R, Stevens DR, Yamada KM. Taking Cell-matrix Adhesions to the Third Dimension. *Science* 2001;294:1708-12.
- (246) Park Y, Lutolf MP, Hubbell JA, Hunziker EB, Wong M. Bovine Primary Chondrocyte Culture in Synthetic Matrix Metalloproteinase-Sensitive

Poly(ethylene glycol)-Based Hydrogels as Scaffold for Cartilage Repair. *Tissue Engineering* 2004;10:515-22.

- (247) Freed LE, Vunjak-Novakovic G, Biron R, Eagles DB, Lesnoy DC, Barlow SK, et al. Biodegradable Polymer Scaffolds for Tissue Engineering. *Biotechnology* 1994;12:689.

Curriculum Vitae

Daniel Vonwil

Personal Data

Address Kaltbrunnenstrasse 3 (resident)
4054 Basel Switzerland
Phone +41 76 527 81 41 (mobile)
+41 61 328 73 75 (office)
e-mail vonwild@uhbs.ch
Date of birth 09/02/1977
Nationality Swiss



Education

02/06 - now **PhD Thesis**, University Hospital Basel, Departments of Surgery and Biomedicine. Title: *Chondroprogenitor Cell Response to Specifically Modified Substrate Interfaces*
Prof. Dr. U. Aebi
Prof. Dr. I. Martin

04/04 - 02/06 **Master in Nanosciences**, University of Basel. Final Grade: 5.9¹

04/05 - 02/06 **Master Thesis**, Departments of Surgery and Biomedicine, University Hospital of Basel in collaboration with Laboratory for Surface Science and Technology, ETH Zürich. Title: *Response of Human Adult Articular Chondrocytes to a Non-Fouling RGD-Peptide Modified Surface*. Final Grade: 6.0¹
Prof. Dr. U. Aebi
Prof. Dr. I. Martin
Prof. Dr. M. Textor

10/00 - 02/04 **Diploma in Chemistry (FH)**, Fachhochschule Nordwestschweiz (FHNW), Basel. Final Grade: 5.2¹
Roche Prize for 2nd Rank

09/03 - 02/04 **Diploma Thesis**, Departments of Surgery and Biomedicine, University Hospital of Basel. Title: *rhTGFβ 3 Bioactivity-Stability in Tissue Engineering Application*. Final Grade: 5.7¹
Prof. Dr. I. Martin
Prof. Dr. D. Gyax

¹ According to the grading system: A or 5.8-6.0 = excellent, 5.3-5.8 = very good, 4.6-5.2 = good

10/00 - 02/04	University of Applied Sciences in Chemistry (FH), Fachhochschule Nordwestschweiz (FHNW), Basel
07/00 - 10/00	Military Service (Swiss Army), training in & earning of the rank of a sergeant, Ecoles hôp 41 (VD)
07/98 - 10/98	Recruit School (Swiss Army), Ecoles hôp 41 (VD)
08/97 - 06/98	Exchange Year , Rochester Community and Technical College (MN, USA). Roche Scholarship. Focus on Anatomy and Physiology. Final Grade: A ¹ Dr. D. Carish
06/94 - 06/97	Professional Maturity of technical type (certified by the Swiss Federal Authorities). Final Grade 5.1 ¹
06/94 - 06/97	Chemistry Laboratory Assistant Apprenticeship , F. Hoffmann-La Roche AG, Basel. Final Grade 5.3 ¹
06/93 - 06/94	4 th year Secondary School , Kriens (LU)
06/90 - 06/93	1 st - 3 rd year Secondary School , Horw (LU)
06/85 - 06/90	1 st - 6 th year Primary School , Horw (LU)

Employment

10/98 - 07/00	Chemistry Laboratory Assistant , F. Hoffmann-La Roche AG, Basel, Switzerland. GMP small scale production plant.
---------------	--

Publications in Peer-Reviewed Scientific Journals

1. **Vonwil D**, Barbero A, Trüssel A, Haupt O, Martin I, Substrate Elasticity Modulates TGF beta Stimulated Redifferentiation of Expanded Human Articular Chondrocytes, manuscript in preparation
2. **Vonwil D**, Schuler M, Barbero A, Ströbel S, Wendt D, Textor M, Aebi U, Martin I. RGD-Peptide Restricted interactions with a Protein Resistant Substrate are Sufficient for Human Articular Chondrocyte Adhesion, Growth and Maintenance of Cartilage Forming Capacity, Manuscript submitted to *Soft Matter*
3. Candrian C, Bonacina E, Früh JA, **Vonwil D**, Dickinson S, Wirz D, Heberer M, Jakob M, Martin I, Barbero A. Intra-individual comparison of human ankle and knee chondrocytes in vitro: relevance for talar cartilage repair. *Osteoarthritis Cartilage* 17: 489-496 (2009)

¹ According to the grading system: A or 5.8-6.0 = excellent, 5.3-5.8 = very good, 4.6-5.2 = good

4. **Vonwil D**, Wendt D, Stroebel S, Wallny HJ, Gygax D, Heberer M, Martin I. Assessment of TGF- β 3 bioactivity for potential bioreactor applications. *Biochem Eng J* 39:586-589 (2008)
5. Candrian C, **Vonwil D**, Barbero A, Bonacina E, Miot S, Farhadi J, Wirz D, Dickinson S, Hollander A, Jakob M, Li Z, Alini M, Heberer M, Martin I. Engineered cartilage generated by nasal chondrocytes is responsive to physical forces resembling joint loading. *Arthritis Rheum* 58:197-208 (2008)

Congresses/Workshops/Summerschools

- 1st International Nanoscience Student Conference (INASCON) 2007, oral.
- 13th SSB Conference Neuchâtel 2007, poster presentation
- 12th Swiss Society of Biomaterials (SSB) Grenchen 2006, oral presentation
- Gemeinsame Jahrestagung der Deutschen, Österreichischen und Schweizerischen Gesellschaften für Biomedizinische Technik in Zürich 2006, poster presentation
- International Tissue Engineering Workshop in Belgrade 2006, oral presentation
- International Summer School in Belgrade 2006, participation

Tutorial and other Professional Activities

- Direct supervision/training of students during their master thesis in Nanosciences:
 - Andreas Trüssel 2009-2010
 - Olivia Haupt 2008-2009
 - Géraldine Guex 2007-2008
- Co-founding and managing the Regenerative Medicine Journal Club 2008-2009
- Managing administration and collaboration of scientific co-operation with eastern european (SCOPEs, SNF Project 111016) partner in Belgrade 2006-2009